

**THE EFFECT OF OPERATING PARAMETERS
AND MATRIX PROPERTIES ON THE
PRODUCTIVITY OF AN EXPANDED BED
ADSORPTION COLUMN**

A thesis submitted for the degree of ENGINEERING DOCTORATE

by

Philippa Jola Gardner

September 2005

The Advanced Centre for Biochemical Engineering

Department of Biochemical Engineering

University College London

Torrington Place

London WC1E 7JE

UMI Number: U592018

All rights reserved

INFORMATION TO ALL USERS

The quality of this reproduction is dependent upon the quality of the copy submitted.

In the unlikely event that the author did not send a complete manuscript and there are missing pages, these will be noted. Also, if material had to be removed, a note will indicate the deletion.



UMI U592018

Published by ProQuest LLC 2013. Copyright in the Dissertation held by the Author.
Microform Edition © ProQuest LLC.

All rights reserved. This work is protected against
unauthorized copying under Title 17, United States Code.



ProQuest LLC
789 East Eisenhower Parkway
P.O. Box 1346
Ann Arbor, MI 48106-1346

ABSTRACT

Expanded bed adsorption (EBA) combines clarification, concentration and purification into a single processing step reducing processing time and increasing productivity. Much work has been conducted on model proteins but little attention has been paid to the emerging issues of tailoring the operational variables of matrix size, operating flowrate and ligand type so as to maximise process outputs. The aims of this study were to investigate the effects of matrix properties and operating parameters on breakthrough behaviour and productivity. Second generation matrices designed to operate at high flowrates were also examined.

Operating at low velocities, beds formed from smaller particles had a shallower breakthrough than beds formed from large particles but the latter were more productive. At the higher velocities typically utilised in EBA, the behaviour of beds formed from either small or large particles was comparable in terms of breakthrough with the beds made up of small particles being slightly more productive than those containing large particles.

A prototype 2nd generation EBA matrix consisting of a multi-modal ligand that could operate at high conductivity levels typical of fermentation broths was also examined. It was found that the productivity could be increased 5-fold as compared with commercially available matrices, with no loss of yield or purity.

Conventional breakthrough curve analysis is not applicable in situations of variable particle size and operating velocity. Results using a novel dimensionless group to facilitate comparison between unlike systems is presented.

The thesis presents an analysis of the relative productivity of a range of systems and highlights the gains in terms of productivity to be achieved with the development of 2nd generation EBA multi-modal adsorbents. The thesis concludes with an analysis of the commercial and regulatory aspects of EBA.

ACKNOWLEDGEMENTS

Firstly, I would like to thank my supervisor Prof. Nigel Titchener-Hooker for all of his support, enthusiasm, advice and encouragement that made this work possible. I also owe a great deal of thanks to Dr Nik Willoughby for his technical expertise and help over the course of my studies.

This project would not have been possible without the support from Amersham Biosciences and their generous provision of equipment and matrices. In particular I would like to thank Rolf Hjorth for providing me with the opportunity to visit and work with them in Sweden, but also for his continued advice and guidance throughout this project.

The work and support of the technical and pilot plant staff within the Biochemical Engineering department at University College is gratefully acknowledged.

Finally, to my friends, colleagues and family that have helped me through this whole experience - I couldn't have done it without you.

CONTENTS

ABSTRACT	2
ACKNOWLEDGEMENTS.....	4
CONTENTS.....	5
LIST OF TABLES	11
LIST OF FIGURES	13
ABBREVIATIONS	18
1 INTRODUCTION	21
1.1 Introduction to the Engineering Doctorate	21
1.2 Introduction to Expanded Bed Adsorption.....	22
1.3 Traditional Processing Steps.....	22
1.4 General Chromatographic Theory.....	23
1.4.1 Ion Exchange Chromatography	24
1.4.2 Hydrophobic Interaction Chromatography	25
1.5 Expanded Bed Adsorption	27
1.5.1 STREAMLINE Expanded Bed Products.....	29
1.5.1.1 STREAMLINE Adsorbents	30
1.5.1.2 STREAMLINE Hardware	32
1.5.2 Operation.....	34
1.5.2.1 Matrix Preparation.....	34
1.5.2.2 Bed Expansion and Equilibration	34
1.5.2.3 Adsorption of Sample.....	35
1.5.2.4 Washing.....	36
1.5.2.5 Elution.....	36
1.5.2.6 Regeneration	37
1.6 Recent Developments - STREAMLINE Direct Expanded Bed Products.....	37
1.6.1 STREAMLINE Direct Adsorbents	38
1.6.2 STREAMLINE Direct Hardware.....	38
1.7 Conclusions	39

2	MATERIALS AND METHODS	40
2.1	Bacterial Cell Growth.....	40
2.1.1	Cell Culture Media.....	40
2.1.1.1	Nutrient Broth No.2.....	40
2.1.1.2	Terrific Broth.....	40
2.1.1.3	High Cell Density Media.....	41
2.1.2	Glycerol stock preparation and maintenance	42
2.1.3	Shake Flask Fermentation	42
2.1.4	5L Fermentation	42
2.2	Downstream Processing.....	44
2.2.1	Cell Disruption	44
2.2.1.1	Sonication	44
2.2.1.2	Homogenisation	44
2.2.2	Clarification.....	44
2.2.2.1	Bench top centrifugation.....	44
2.2.2.2	Lab scale centrifugation.....	44
2.3	Biological Systems.....	45
2.3.1	Alcohol Dehydrogenase/Yeast.....	45
2.3.1.1	Feedstock Preparation	45
2.3.1.2	Chromatography Details.....	45
2.3.1.3	Clean-in-Place Procedure.....	46
2.3.1.4	Residence Time Determination.....	46
2.3.2	Glutathione S-Transferase/ <i>E. coli</i>	46
2.3.2.1	Feedstock Preparation	46
2.3.2.2	Chromatography Details.....	47
2.3.2.3	Clean-in-Place Procedure.....	48
2.3.2.4	Residence Time Determination.....	48
2.3.3	Bovine Serum Albumin/Buffer.....	48
2.3.3.1	Feedstock Preparation	48
2.3.3.2	Chromatography Details.....	48
2.3.3.3	Clean-in-Place Procedure.....	48
2.4	Expanded Bed Chromatography	49
2.4.1	STREAMLINE 50.....	49

2.4.1.1	System Details.....	49
2.4.1.2	Mode of Operation.....	50
2.4.1.3	Matrix Elutriation and Segregation.....	50
2.4.2	STREAMLINE 25.....	51
2.4.2.1	System Details.....	51
2.4.2.2	Mode of Operation.....	51
2.5	Packed Bed Chromatography	52
2.6	Monitoring and Analysis	52
2.6.1	Optical Density	52
2.6.2	Dry Cell Weight.....	52
2.6.3	GST Assay	53
2.6.4	Total Protein (Bradford) Assay	53
2.6.5	SDS-PAGE Gels	54
2.6.5.1	Protein Preparation.....	54
2.6.5.2	Gel Preparation, Running and Staining.....	54
2.6.6	ADH Assay	54
2.6.7	Residence Time Determination.....	55
2.6.7.1	Packed Bed Operation.....	56
2.6.7.2	Expanded Bed Operation.....	56
2.6.8	Matrix Particle sizing.....	57
2.6.9	Number of Matrix Particles	58
2.6.10	Total Binding Capacity Measurements.....	58
3	THE PRODUCTION AND ANALYSIS OF GST FROM <i>E. COLI</i>.....	60
3.1	Introduction	60
3.2	Fermentation Development.....	61
3.2.1	Effect of culture media on <i>E. coli</i> growth.....	61
3.2.2	Effect of culture media on GST expression	63
3.3	GST Assay Development	68
3.4	GST Release.....	69
3.5	Discussion.....	71
3.6	Conclusions	73

4 THE EFFECT OF MATRIX PARTICLE SIZE DISTRIBUTION AND OPERATING VELOCITY ON THE PURIFICATION OF ALCOHOL DEHYDROGENASE FROM YEAST.....	74
4.1 Introduction	74
4.2 Matrix Segregation and Characterisation.....	75
4.3 Velocity and Particle Size Effects on Breakthrough.....	77
4.4 Impact of Residence Time on Breakthrough Profiles	81
4.5 Discussion.....	81
4.6 Conclusions.....	88
5 THE EFFECT OF MATRIX PARTICLE SIZE DISTRIBUTION AND OPERATING VELOCITY ON THE PURIFICATION OF GLUTATHIONE S-TRANSFERASE PRODUCED IN <i>E. COLI</i>	89
5.1 Introduction	89
5.2 Matrix Segregation and Characterisation.....	90
5.3 Velocity and Particle Size Effects on Breakthrough.....	91
5.4 Impact of Residence Time.....	94
5.5 Discussion.....	95
5.6 Conclusions.....	99
6 PROTOTYPE HIGH SALT TOLERANT ANION EXCHANGE LIGAND EVALUATION.....	101
6.1 Introduction	101
6.2 Adsorbent Characteristics.....	101
6.3 Purification of Bovine Serum Albumin.....	103
6.3.1 Without the addition of NaCl.....	103
6.3.2 With the addition of NaCl.....	104
6.4 Purification of Glutathione S-Transferase	105
6.4.1 Without the addition of NaCl.....	105
6.4.2 With the addition of NaCl.....	106
6.5 Discussion.....	107
6.6 Conclusions.....	110
7 INVESTIGATION INTO THE EFFECT OF CONDUCTIVITY ON THE BINDING OF GLUTATHIONE S-TRANSFERASE	111
7.1 Introduction	111
7.2 Adsorbent Verification and Characterisation	112

7.2.1	Purification of Bovine Serum Albumin.....	112
7.2.2	Adsorption Isotherm for GST.....	113
7.2.3	Determination of Feed Volume for Conductivity Investigations.....	113
7.3	Conductivity Studies	117
7.4	Discussion.....	119
7.5	Conclusions.....	124
8	THE PRODUCTIVITY IMPLICATIONS OF VARYING OPERATING PARAMETERS AND MATRIX PROPERTIES.....	125
8.1	Introduction	125
8.2	Productivity Definition Evaluation	126
8.3	Productivity Evaluation of the ADH Process	130
8.4	Productivity Evaluation of the GST Process	131
8.4.1	Velocity and Particle Size Distribution Effects	132
8.4.2	Conductivity Effects.....	132
8.5	Discussion.....	133
8.6	Conclusions.....	139
9	OVERVIEW AND CONCLUSIONS	141
10	FURTHER WORK.....	144
11	BIOPROCESS PROJECT MANAGEMENT.....	146
11.1	Introduction	146
11.2	Project Phase Definition	146
11.2.1	Phase 0: Objectives	147
11.2.2	Phase 1: Definition	147
11.2.3	Phase 2: Detailed Planning	147
11.2.4	Phase 3 Development	148
11.2.5	Phase 4: Market Readiness Preparation.....	148
11.2.6	Phase 5: Launch	149
11.3	Discussion.....	150
12	VALIDATION	151
12.1	Introduction	151
12.2	General considerations.....	151

12.3	Expanded Bed Adsorption Validation.....	152
12.3.1	Equipment Qualification.....	152
12.3.2	Raw Materials.....	153
12.3.3	Process Qualification.....	154
12.3.4	Cleaning, Sanitization and Storage.....	154
12.4	Conclusions.....	155
	REFERENCES	156
	APPENDIX I - FLUIDISATION THEORY	164
	Introduction	164
	Fluidisation theory for liquid-solid systems	164
	Minimum fluidisation velocity	167
	Models for describing bed expansion	169
	Effect of particle size distribution on fluidisation velocity	171
	Effect of particle size distribution on voidage	172
	APPENDIX II - PUBLICATIONS	174

LIST OF TABLES

Table 1.1: Illustration of densities and particle sizes for various types of STREAMLINE expanded bed adsorption matrices (Amersham Biosciences, 1997).

Table 3.1: Levels of GST (mg/mL) detected in sonicated *E. coli* samples taken each hour post induction with 1mM IPTG in three media grown in 2L shake flasks with a 250mL working volume at 200rpm and 30°C.

Table 3.2: Total protein and GST levels (mg/mL) detected in sonicated *E. coli* cell culture, resuspended pellet and supernatant taken 3 hours post induction with 1mM IPTG.

Table 4.1: Particle size range variations as shown by d_{10} , d_{50} and d_{90} measurements on a number basis for different sections of segregated STREAMLINE Phenyl matrix.

Table 4.2: Characterisation of segregated STREAMLINE Phenyl detailing the Total Binding Capacity for ADH when applied at a concentration of 100U/mL and the number of matrix particles per mL of settled matrix.

Table 4.3: Variation in residence time (sec) with bed arrangement.

Table 5.1: Particle size range variations as shown by d_{10} , d_{50} and d_{90} measurements on a number basis for different sections of segregated STREAMLINE DEAE matrix.

Table 5.2: Variation in residence time (sec) with bed arrangement.

Table 6.1: Total BSA and GST (mg/mL) captured on each prototype high salt ligand both with and without the presence of salt to adjust the conductivity. Numbers in bold highlight the highest capacity achieved for each product and conductivity level.

Table 6.2: Total GST (mg) in each collected fraction for all three of the prototype ligands both with and without the presence of salt to adjust the conductivity. Numbers in bold highlight the quantity of GST that was lost in the process.

Table 7.1: The total GST (mg) eluted at each conductivity level (20, 10 and 2.5 mS/cm) and from 100mL of each adsorbent (STREAMLINE Direct DAB, STREAMLINE DEAE and STREAMLINE Direct DEAE).

Table 8.1: The productivity defined as the total ADH recovered (Units) in the elution fraction per minute of processing time for each of the Yeast/ADH processes.

Table 8.2: The productivity defined as the total ADH bound (Units) based on breakthrough curve integration per minute of processing time for each of the Yeast/ADH processes.

Table 8.3: The productivity defined as the total ADH bound at 5% product breakthrough (Units) per minute of processing time for each of the Yeast/ADH processes.

Table 8.4: The productivity defined as the total GST recovered (mg) per minute of processing time for each of the *E. coli*/GST processes where the effect of operating velocity and particle size distribution was investigated.

Table 8.5: The productivity defined as the total GST recovered (mg) per minute of processing time for each of the *E. coli*/GST processes investigated in terms of conductivity effects.

LIST OF FIGURES

Figure 1.1: The Hofmeister Series on the effect of some anions and cations on hydrophobic interactions.

Figure 3.1: Growth of *E. coli* DH5 α within 3 different media. Cultures were grown in 2L shake flasks with a 250mL working volume at 200rpm and 30°C.

Figure 3.2: Relationship between optical density measurements (OD_{600nm}) and dry cell weight of *E. coli* DH5 α grown in High Density Media.

Figure 3.3: SDS-PAGE gels of proteins detected in *E. coli* samples taken each hour post induction in three media grown in 2L shake flasks with a 250mL working volume at 200rpm and 30°C:

- a) Nutrient Broth
- b) Terrific Broth
- c) High Density Media

Figure 3.4: Growth and expression of *E. coli* DH5 α producing GST within a 5L fermenter using High Cell Density culture media.

Figure 3.5: Effect of assay sample volume and reaction time on the measured concentration of GST produced in *E. coli* DH5 α . The highlighted points are those where the absorbance readings fell within the linear range of the spectrophotometer.

Figure 3.6: Comparison of 3 harvesting and storage conditions of *E. coli* DH5 α (fresh broth, frozen broth and clarified/frozen broth) and their effect on GST release when passed through an homogeniser for 5 passes at 500bar.

Figure 4.1: Decumulative particle size distribution measurements on a number basis for different sections of segregated STREAMLINE Phenyl matrix.

Figure 4.2: The effect of linear liquid velocity (100 and 300cm/hr) on the breakthrough of ADH loaded onto a segregated bed of STREAMLINE Phenyl consisting of the largest matrix particles in:

- a) Packed beds
- b) Expanded beds

Figure 4.3: The effect of particle size on the breakthrough of ADH loaded onto packed and expanded beds at constant linear liquid velocity:

- a) Smallest and largest particles in a packed bed compared at 300cm/hr.
- b) Smallest and largest particles in an expanded bed compared at 100cm/hr.
- c) Smallest and largest particles in an expanded bed compared at 300cm/hr.

Figure 4.4: Comparison of breakthrough rates of ADH in expanded beds of segregated matrix at various linear liquid velocities plotted against dimensionless experimental time (t/t_R):

- a) Largest particles compared at 100 and 300cm/hr.
- b) Smallest and largest particles compared at 100cm/hr.
- c) Smallest and largest particles compared at 300cm/hr.

Figure 5.1: The adsorption isotherm for the binding of GST to segregated beds of STREAMLINE DEAE. C_M is the concentration of GST (mg/mL) in the applied sample of C_S is the amount of GST (mg) bound to the matrix (mL).

Figure 5.2: The effect of linear liquid velocity (100 and 300 cm/hr) on the breakthrough of GST loaded onto a segregated bed of STREAMLINE DEAE consisting of the:

- a) Largest particles in an expanded bed.
- b) Smallest particles in an expanded bed.

Figure 5.3: The effect of particle size on the breakthrough of GST loaded onto expanded beds at constant linear liquid velocity:

- a) Smallest and largest particles in an expanded bed compared at 100cm/hr.
- b) Smallest and largest particles in an expanded bed compared at 300cm/hr.

Figure 5.4: Comparison of breakthrough rate of GST in expanded beds of segregated matrix at various linear liquid velocities plotted against dimensionless experimental time:

- a) Smallest and largest particles compared at 100cm/hr.
- b) Smallest and largest particles compared at 300cm/hr.

Figure 6.1: The chemical structures of the three prototype high salt tolerant anion exchange ligands.

Figure 6.2: The structure of a typical STREAMLINE Direct matrix bead (actual size is 130 μ m). The dark matter is the stainless steel core material utilised to densify the matrix allowing for high velocities.

Figure 6.3: The breakthrough of BSA in 10mL packed beds loaded onto three prototype high salt tolerant ligands.

Figure 6.4: The breakthrough of BSA in the presence of salt in 10mL packed beds loaded onto three prototype high salt tolerant ligands.

Figure 6.5: The breakthrough of GST in 10mL packed beds loaded onto three prototype high salt tolerant ligands.

Figure 6.6: The breakthrough of GST in the presence of salt in 10mL packed beds loaded onto three prototype high salt tolerant ligands.

Figure 7.1: The adsorption isotherm for binding of GST from *E. coli* homogenate to the prototype STREAMLINE Direct DAB. C_M is the concentration of GST (mg/mL) in the applied sample and C_S is the amount of GST (mg) bound to the matrix (mL).

Figure 7.2: The breakthrough of GST from whole *E. coli* homogenate loaded at 600cm/hr on 100mL STREAMLINE Direct DAB in a STREAMLINE 25 EBA column at a conductivity of 20mS/cm.

Figure 7.3: The breakthrough of GST found in the *E. coli* broth supernatant loaded at 600cm/hr on 100mL STREAMLINE Direct DAB in a STREAMLINE 25 EBA column at a conductivity of 20mS/cm.

Figure 7.4: The breakthrough of GST from the disrupted *E. coli* cell pellet loaded at 600cm/hr on 100mL STREAMLINE Direct DAB in a STREAMLINE 25 EBA column at a conductivity of 20mS/cm.

Figure 7.5: The breakthrough of GST from disrupted *E. coli* loaded onto 100mL of the three adsorbents (STREAMLINE Direct DAB, STREAMLINE DEAE and STREAMLINE Direct DEAE) at three conductivity levels (20, 10 and 2.5 mS/cm) and a velocity of 600cm/hr for the STREAMLINE Direct adsorbents and 160cm/hr for the STREAMLINE DEAE.

- a) GST breakthrough when loaded at a conductivity level of 20mS/cm.
- b) GST breakthrough when loaded at a conductivity level of 10mS/cm.
- c) GST breakthrough when loaded at a conductivity level of 2.5mS/cm.

Figure 8.1: The trade off between buffer consumption (mL) and processing time (min) when varying the operating flowrate and matrix particle size.

Figure 8.2: The trade off between buffer consumption and processing time in relation to the total ADH recovered in each process.

Figure 8.3: The effect of residence time, t_R , a measure of operating velocity and matrix particle size distribution on the total ADH recovered for each system set-up based on particle size and operating velocity.

ABBREVIATIONS

ADH:	Alcohol dehydrogenase
AIEX:	Anion exchange
BSA:	Bovine serum albumin
C:	Product concentration at the outlet
C ₀ :	Product concentration at the inlet
CDNB:	1-chloro-2,4-dinitrobenzene
CIP:	Clean-in-place
CST:	Cation salt tolerant
d ₁₀ :	The diameter at which 10% of the PSD is smaller; also a measure of the proportion of fines.
d ₅₀ :	The diameter at which 50% of the PSD is smaller; also the mean particle diameter.
d ₉₀ :	The diameter at which 90% of the PSD is smaller; also a measure of the proportion of large particles.
DAB:	1,4-diaminobutane
DAP:	1,3-diaminopropane
DCW:	Dry cell weight
DEAE:	Diethylaminoethyl
DOT:	Dissolved oxygen tension
DSP:	Downstream processing
EBA:	Expanded bed adsorption
<i>E. coli</i> :	<i>Escherichia coli</i>
EDTA:	Ethylenediaminetetraacetic acid
FDA:	Food and Drug Administration
GST:	Glutathione S-transferase
ΔH:	The difference in bed height due to extra expansion
HIC:	Hydrophobic interaction chromatography
ID _{column} :	Internal column diameter

ID _{tubing} :	Internal tubing diameter
IEX:	Ion exchange chromatography
IMAC:	Immobilised metal affinity chromatography
IQ:	Installation Qualification
IPTG:	Isopropyl β -D-thiogalactopyraoside
LALLS:	Low angle laser light scattering
LED:	Light emitting diode
L _{tubing} :	Tubing length
NAD ⁺ :	Nicotinamide adenine dinucleotide
N _p :	Number of particles
NTP:	Number of theoretical plates
OD:	Optical Density
OQ:	Operational Qualification
P&L:	Profit and Loss
PDR:	Project definition request
PPG:	Polypropylene glycol
PSD:	Particle size distribution
Q:	Volumetric flowrate (mL/ min)
RSF:	Regulatory support file
RTD:	Residence time distribution
SDS-PAGE:	Sodium dodecyl sulphate-polyacrylamide gel electrophoresis
SFA:	Stopped-flow analyser
SOP:	Standard operating procedure
SP:	Sepharose
TOC:	Total organic carbon
t _R :	Actual residence time within an expanded bed
t _{Rheight} :	Residence time due to extra expansion
t _{Rpacked} :	Residence time in a packed bed column
t _{Rsystem} :	Residence time as measured by an RTD test
t _{Rtubing} :	Residence time due to tubing

U:	Unit
V _L :	Total volume of liquid
V _M :	Total matrix volume
VMP:	Validation master plan
V _T :	Total volume in a matrix sample

1 INTRODUCTION

1.1 Introduction to the Engineering Doctorate

There were two main aims of the Engineering Doctorate (EngD) that was carried out in collaboration with Amersham Biosciences (now part of GE Healthcare):

1. To complete a research project of industrial relevance.
2. To develop skills appropriate to the working environment, in particular management and validation of bioprocesses, through a series of taught courses, examinations and work experience.

The research project that was agreed with Amersham Biosciences concentrated on the effects of matrix properties and operating parameters on the breakthrough behaviour and overall productivity of an expanded bed adsorption (EBA) step. In addition, Amersham Biosciences, at the time of this research, were in the process of developing second generation EBA matrices and columns that are now available commercially (STREAMLINE™ Direct columns and adsorbents). Work on some of these prototype matrices formed part of the research and were also the basis of the management project.

The bulk of this thesis is a description of the results and conclusions of the research carried out. In addition, as part of the EngD requirements, a description of the project management of a research and development (R&D) project is provided in Chapter 11 and the validation issues surrounding EBA are provided in Chapter 12.

This chapter will give an overview of EBA, including the traditional processing steps of a protein, general chromatography theory, and the development and operation of EBA.

1.2 Introduction to Expanded Bed Adsorption

The production of recombinant proteins for use in the treatment and prevention of diseases has increased dramatically in the last decade. Processing of these types of product, especially those proteins aimed for therapeutic use can require numerous steps, thus reducing product yields and increasing processing time. Processing strategies that can reduce the overall number of steps are an attractive and efficient solution to this type of challenge. EBA is such a solution as it combines clarification, concentration and purification into one processing step that can be employed early on in downstream processing. As such, processing times and hence the risk of product degradation are reduced and yields are increased by the use of EBA.

1.3 Traditional Processing Steps

Purification of recombinant proteins can essentially be divided into 3 stages (Protein Purification Handbook):

1. Capture
2. Intermediate Purification
3. Polishing

The capture step clarifies and concentrates the feedstock from the bioreactor. This is usually achieved by centrifugation and/or microfiltration to clarify, and either some adsorptive technique or ultrafiltration to concentrate. Clarification is crucial in order to apply the feedstock to a packed bed chromatography column and concentration can reduce processing time of the intermediate purification step. Expanded bed adsorption is used to replace all stages within the capture step.

Intermediate purification is used to remove the bulk of the contaminating proteins and impurities and is usually carried out in packed bed

chromatography. The most common type of chromatography at this stage is ion exchange (IEX), however hydrophobic interaction (HIC), immobilised metal affinity (IMAC) and affinity chromatography may be employed

The final polishing stages are to remove small amounts of impurities. This is usually achieved by IEX, gel filtration and/or reversed phase chromatography.

1.4 General Chromatographic Theory

Chromatography describes many different processes in both the chemical and biological fields. The broadest definition would be to say that chromatography is the separation of a substance (or substances) from a mobile phase by attachment onto a stationary phase. Separation of coloured dyes on filter paper by speed of travel is perhaps the simplest form of chromatography, and is known as one-dimensional chromatography. It is this principle that is still used for purification of proteins in biotechnology. The addition of a second “dimension” results in the mobile phase passing through a stationary column of adsorbent, where the cross-section of the column represents the second dimension. Most chemical and biological chromatographic purifications utilise a column of adsorbent or matrix of some kind and so are classed as two-dimensional chromatography. Two-dimensional chromatography has the major advantage of being able to handle large quantities of mobile phase.

Products and contaminants are separated as solutes in the mobile phase according to their interaction with the stationary phase (the matrix). If they have no affinity to the matrix, i.e. remain partitioned in the solvent of the sample, then they will pass straight through the column with no retardation. If they have a high affinity for the matrix they may totally adsorb onto it, and be impossible to remove without causing damage to the solute. These two scenarios are of little practicable use, except if the solute in question is an impurity in which case the first situation may be

desirable. There are two further possibilities; firstly the situation where the substance has an affinity for the matrix so mild that it is simply slowed down in its passage down the column, thus delaying its elution long enough for totally non-binding impurities to be washed off. In the cases of the fields being studied here however, the situation of interest is that where the solute binds to the matrix such that it is effectively stationary while the solvent used for loading is flowing through, but where conditions can be easily modified to elute the target solute when so desired.

Chromatography is widely used as a late or final stage in the purification of fine chemicals or biological products since as a process step it can achieve very high degrees of purity of final product. In addition chromatography does not place the substances involved under any high shear forces or create problems with heat generation or dissipation and as such can be considered a gentle process step.

The types of chromatography utilised in this thesis are IEX and HIC. A brief description of these is provided below.

1.4.1 Ion Exchange Chromatography

Ion exchange chromatography (IEX) is based on the interaction between charged solute molecules and oppositely charged moieties covalently linked to a chromatography matrix.

IEX is a very common form of chromatography for the separation and purification of proteins and other charged biomolecules as it is a very simple, powerful and controllable method (Ion Exchange Chromatography Principles and Methods). Separation is achieved by the difference in interaction between the various substances in the sample and the ion exchanger, which can be controlled by conditions such as ionic strength and pH. Differences in interaction arise from differences in charge, charge densities and charge distribution.

The ion exchanger is equilibrated to a state in terms of pH and ionic strength that promotes binding of the desired solute molecule. Upon sample application, the solute molecules displace the counter ions (usually simple ions such as chloride or sodium) from the equilibration buffer and bind reversibly to the matrix. The solute molecules can then be removed from the column usually by a change in ionic strength or pH.

In general, an increase in the conductivity of the sample leads to a reduction in binding of the solute molecule. As such, fermentation broths that typically have high conductivity levels that are loaded onto IEX EBA steps, require dilution in order to reduce the conductivity. However novel ion exchangers such as STREAMLINE Direct CST (see later for details) are able to operate effectively at high conductivity levels and offer similar performance as compared with the more typically utilised ion exchange matrices such as DEAE and SP.

1.4.2 Hydrophobic Interaction Chromatography

Hydrophobic interaction chromatography (HIC) utilises the fact that the surfaces of globular proteins have extensive hydrophobic patches in addition to the expected hydrophilic groups. These hydrophobic regions bind to the hydrophobic ligands, alkyl or aryl side chains on the gel matrix, under conditions favouring interaction e.g. aqueous solutions with high salt concentrations.

A large number of theories have been proposed to explain hydrophobic interaction chromatography. Most of the theories are essentially based upon the interaction of hydrophobic solutes and water (Tanfor, 1973; Creighton, 1984). None of the theories have enjoyed universal acceptance but common to them all is the central role of structure-forming salts and the influence they exert on the solute, solvent and adsorbent within the chromatography system.

The type and concentration of salt are two factors of great importance in hydrophobic interaction chromatography, as are additives that change the polarity of the solvent. The influence of salt on hydrophobic interaction follows the well known Hofmeister (lyotropic) series shown in Figure 1.1 (Pahlman *et al.*, 1977). Salts that promote hydrophobic interaction are to the left in the series. Hydrophobic interactions are increased in the presence of salts such as ammonium sulphate to a greater extent than salts lower down the Hofmeister series.

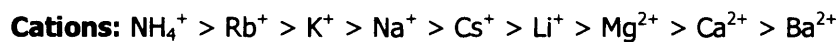
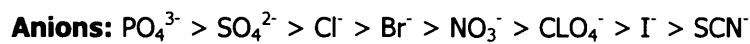


Figure 1.1: The Hofmeister Series on the effect of some anions and cations on promoting hydrophobic interactions.

Other factors to consider are the ligand and base matrix type and operating pH. The effect of pH is complicated. In general an increase in pH was found to decrease hydrophobic interaction (Porath *et al.*, 1973) probably as a result of the titration of charged groups leading to the increased hydrophilicity of the proteins. Other reports suggest that hydrophobic interaction increases as pH decreases (Halperin *et al.*, 1981).

Studies have shown that more than one ligand on the adsorbent must be involved in the binding of proteins to hydrophobic supports (Hjerten *et al.*, 1974). Hydrophobic interaction chromatography is, in general, a mild method due certainly to the stabilising influence of salts and the recoveries are often high (Scopes 1994).

1.5 Expanded Bed Adsorption

Expanded bed adsorption is a single pass operation in which products (usually proteins) are recovered from a crude feedstock. In this respect the operation seeks to combine the specificity of separation and overall volume reduction of chromatography with the clarification efficiency of a centrifugation and filtration system into one discrete step. This would be hoped to reduce the need for costly and time-consuming prior clarification steps such as centrifugation and filtration.

Expanded bed adsorption is suitable for the recovery of both extracellular and intracellular products; the former by direct capture from a fermenter or cell culture broth and the latter after homogenisation or cell lysis. As an effective operation it "came of age" in 1993 with the introduction of the STREAMLINE process range of expanded beds and matrices produced by Amersham Biosciences, Uppsala, Sweden and the FastLine range from UpFront Chromatography A/S, Copenhagen, Denmark.

The problem to which expanded bed operation became a solution was the requirement to combine three key aspects of the capture stage of a process - clarification, concentration and product stabilisation. Although filtration and centrifugation systems can achieve the first two objectives to varying degrees, some form of more specific separation is required to remove such things as proteases. If these are not removed then the product could be at risk and time constraints are enforced between the capture and later purification steps.

Initial attempts to combine both crude separation techniques and some form of chromatographic separation were hampered by the approaches adopted. Overly complex methods relied on keeping the adsorbent particles stationary at all times - in effect a packed bed but with greater voidage. In order to achieve this, a good deal of work (Chetty and Burns 1991; Terranova and Burns 1991) was carried out considering stabilising ferromagnetic adsorbent beads in an external magnetic field. This method

has had a good deal of success with virtually no mixing or movement of the particles and thus plug flow is achievable. However the drawbacks are great - the need for expensive and heavy-duty magnetic equipment coupled with the problem of heat generation, especially in systems which require the temperature to be kept low to prevent biodegradation.

Draeger and Chase (1991) looked at the possibility of using conventional packed bed matrices expanded in a column. Although they found that the matrix could be expanded to 2-3 times its settled height, this was achieved at very low flowrates thus limiting the possible applications to systems requiring very low throughput. In addition this can cause serious problems because the uniform density of the matrix beads causes inherent instability in the bed, resulting in turbulent flow and the accompanying eddies, backflow and dead spaces.

Since plug flow through a packed bed maximises the number of theoretical plates in the system (NTP), then an expanded bed exhibiting turbulent flow will have an inferior adsorption performance to an equivalent packed bed exhibiting plug flow. This greatly increases the amount of time needed to perform the separation and also the amount of debris retained by the column, often resulting in fouling of the matrix or the column. Although Chase (1994) has shown that when a bed is expanded where the solid-liquid density difference is minimal there is visually little mixing and the bed retains a uniform character during expansion, stability and complete plug flow would be unlikely. In addition a minimal density difference between the two phases precludes the use of high flowrates, or feedstocks of high viscosity, as the bed expands proportionally more under these situations.

Draeger and Chase (1991) also considered the adsorption characteristics of both Q-Sepharose (strong anion exchanger) for BSA solutions and Protein A Sepharose CL-4B (affinity) for human immunoglobulin G. They noted that when solutions of pure protein were used the breakthrough

characteristics were similar to that of the matrix in packed bed mode, however when cells or cell debris was introduced into the sample the adsorption performance greatly deteriorated. In addition the increase in viscosity of the sample caused over-expansion of the bed due to minimal density difference between the solid and liquid phases.

Consequently, in order for the true potential of expanded bed adsorption as a downstream processing operation to be realised, a method was needed to stabilise the bed under adsorption and ensure that the flow through the bed remained as close as possible to plug flow. Several methods have been suggested to aid this. The inclusion of baffles around the side of the column (Buijs and Wesselingh, 1980) is said to stabilise the bed when used in conjunction with standard packed bed matrices, but this does not solve the problem of small density differences between the solid and liquid phases, and so flowrates used were still minimal. The development of STREAMLINE adsorbents and columns designed specifically for EBA overcame these problems of stable fluidization and are described in 1.5.1.

1.5.1 STREAMLINE Expanded Bed Products

The work carried out by Draeger and Chase (1991) indicated the need for matrix particles with a higher sedimentation velocity (the full mathematical descriptions regarding fluidization are included in Appendix I). Their work also introduced the use of a purpose designed liquid distribution inlet providing plug flow in the column. In 1993 Amersham Biosciences introduced new columns and adsorbents called STREAMLINE specifically for use in EBA. Overall, the use of these products provided a single processing step to clarify, concentrate and purify the product, thereby increasing yields. An added advantage of EBA is the lack of cell damage that has been noted in the literature (Lutkemeyer *et al.*, 1999).

1.5.1.1 STREAMLINE Adsorbents

Almost all matrices used nowadays for fixed bed chromatography are porous structures. Increased porosity leads to high efficiency on account of reduced pore diffusion resistance and also allows for easier elution and washing of the matrix particles (Gondkar *et al.* 2001). The matrix is usually composed of hydrophilic polymer and in addition to this, certain other properties are desirable in the matrix. As well as hydrophilicity, an absence of groups to which proteins can spontaneously bind is desirable. A degree of physical and chemical stability is also required to cope with certain processes such as sanitisation (often 1M or stronger NaOH) and regeneration and repacking of columns after loss of activity. Other properties depend specifically on the process under consideration. Final important considerations include ensuring that the matrix material is porous enough to allow proteins to penetrate to an internal network of pores, thus ensuring maximum surface area for adsorption with minimum volume of matrix.

The most simple and effective system to stabilise an expanded bed is that use by Amersham Biosciences in their STREAMLINE adsorbents. By grading the adsorbent beads with a distribution of size or density, the system is most effective - the density and size gradient means that upon expansion the bed is stable as individual beads adopt a stable height in the bed based upon their density (Willoughby *et al.*, 2000(a)), and the heavy degree of matrix mixing observed in previous attempts is all but eradicated. To achieve the necessary particle gradients the beads are quartz-cored, thus giving a higher average density to the matrix than would normally be observed with fixed bed chromatography media (see Table 1.1 below). This has the additional benefit of allowing the system to support either higher flowrates or higher feedstock viscosities, as an increase in either of these tends to cause the bed to expand further but an increase in density of the matrix would result in a drop in expanded height.

Base Matrix	Ligand	Mean Density (kg/m ³)	Particle Size Distribution (μm)
Agarose-quartz	DEAE	1.15	100-300
Agarose-quartz	SP	1.15	100-300
Agarose-quartz	IDA	1.15	100-300
Agarose-quartz	Heparin	1.15	100-300
Agarose-metal	Protein A	1.3	80-165

Table 1.1: Illustration of densities and particle sizes for various types of STREAMLINE expanded bed adsorption matrices (Amersham Biosciences, 1997)

The physical properties under expansion of both of the ion exchange matrices (DEAE and SP) listed above have been reviewed by Chang *et al.* (1993) when compared to equivalent Sepharose Fast Flow matrices. They found that, under conditions of equal bed expansion, the flowrate in the STREAMLINE matrix was considerably higher.

Amersham Biosciences have widened greatly the varieties of STREAMLINE adsorbents available in the last few years. Initially only low specificity ligands such as ion exchangers and HIC groups were produced, because of concerns relating to the more harsh cleaning and regeneration steps required for processes which handle crude feedstocks. However, these ligands do not possess the high specificity for the separation product which is often required nowadays for maximum purity. Thus several new adsorbents have been developed based on the STREAMLINE system.

1.5.1.2 STREAMLINE Hardware

Experiments carried out for this thesis were conducted using STREAMLINE 25 and STREAMLINE 50 columns supplied by Amersham Biosciences. These are two of the smallest of the presently available expanded beds the company produce, and are intended for use in process development and method optimisation. The two columns have, respectively, 25 and 50 mm internal column diameters and are both 1 m in length.

The extra equipment required to run the STREAMLINE 25 and 50 columns is very similar to that required for standard packed bed chromatography. The system requires pumps, valves, fraction collection and on line spectroscopy/pH measurement/conductivity measurement as required. Details of system specifics can be found in Chapter 2 of this thesis.

Note that the upper adaptor in this system is hydraulic and can be raised or lowered by means of a pump feeding to a reservoir above the adapter. This allows for simple alteration of the adaptor height, which is important as bed height can vary considerably during a run and the bed is functioning most efficiently when the upper adaptor is positioned as close as possible to the top of the bed to minimise dead space. In addition to this, the hydraulic adapter opens up the possibility of eluting bound particles in the reverse direction (i.e. downwards) and therefore eluting the bed in packed mode rather than expanded mode.

In order to ensure efficient separation, it is important that the column is completely vertical. Misalignment of the column, even to degrees that are not detectable by visual inspection, can increase the liquid dispersion, leading to reductions in the separation efficiency (Bruce *et al.*, 1999(b)).

An expanded bed that exhibits stable behaviour under fluid flow conditions (such as a STREAMLINE system) can allow certain conclusions to be drawn concerning the hydrodynamic behaviour of the

bed under expansion. DeLuca *et al.* (1994) considered the effect of the design of the liquid distributor in terms of the effect on the bed expansion and on the hydrodynamic properties. They found that the value n in the Richardson-Zaki equation (Equation AI.11 in the appendix) depended on the design of the distributor, but also that the height of the bed upon expansion was reduced by having a lower settled bed height. This is not to be expected since the stable position (in terms of height) of any particle in an expanded bed depends on the density and size of the particle and the linear velocity of the fluid in the column but not on its starting height.

This led researchers to look more closely at the particle behaviour and draw the conclusion that the design of distributors was often causing channelling of liquid, especially in beds with low initial height, causing uneven expansion. They also stated that, to ensure channelling did not effect the stability of the bed, the distributor should be of a design such that fluid flow is even over the entire cross-section of the bed, and also that the height of the settled bed should be at minimum double the value of the diameter of the column. In general also it was noted that bed stability upon expansion increases with settled bed height, but in addition, as settled bed height is increased, constraints are placed on the maximum liquid linear velocity in the column and also the use of high viscosity solutions, both for reasons of excessive bed expansion.

In order to overcome these issues, STREAMLINE expanded beds are fitted with special flow adapters underneath the bottom mesh net of the column. These ensure the flow of liquid into the column is distributed evenly across the entire cross-section of the column. In addition the holes in the adapter and the mesh are large enough to allow the passage of particulate matter, even whole cells, but are small enough to confine the matrix within the column in settled or downward elution mode.

Custom built columns have been developed that allow the removal of liquid or particle samples from within the expanded bed. It has been

shown that in-bed sampling does not affect the separation efficiency and is a useful tool for investigating hydrodynamic and adsorption behaviour within the expanded bed (Bruce *et al.*, 1999(a), Bruce and Chase 1999, 2001 and 2002, Chase *et al.*, 1999, Willoughby *et al.*, 2000(a) and 2000(b)).

1.5.2 Operation

A typical chromatography process consists of six steps - matrix preparation, equilibration, loading (adsorption), washing, elution and column regeneration. These steps are similar in almost all forms of chromatography, but with variations depending on specific processes. A general description of these processes is given below, but more specific details depend on the exact process.

This section is not intended to replace the materials and methods sections in Chapter 2 but rather to provide the reader with an introduction to the general context of the operation.

1.5.2.1 Matrix Preparation

In the initial stages the bed must be prepared and fully expanded. The bed is intended to be run at a settled bed height of approximately 15cm (Amersham Biosciences recommendations). The bed must then be slowly expanded up to a linear flowrate of approximately 400 cm/hr. This allows all the particles to rearrange to their proper position in relation to their size/density and ensures that, once settled again the bed will be stable in future expansions. In addition it is often necessary, especially with prototype adsorbents, to elutriate the material during expansion to remove any excessive fine particles that may be present and that will prevent a sharp boundary on expansion between the bed and the liquid.

1.5.2.2 Bed Expansion and Equilibration

Initially the bed is expanded in an upwards direction using the equilibration buffer. According to Chang and Chase (1996) and Amersham Biosciences recommendations the bed should be expanded to

approximately 2-3 times the settled height. Hjorth (1997) suggests that for most adsorbents and buffers with viscosities in the order of that of water, this expansion can be achieved with a linear liquid flowrate of 300cm/hr.

1.5.2.3 Adsorption of Sample

When the bed is fully expanded and equilibrated at the required liquid flowrate and has stabilised, the liquid being passed through the column is switched to the load sample. The length of load period will depend on the specific conditions required. In some cases samples may be loaded until a specific percentage breakthrough of target substance is achieved, in other cases simply a fixed volume may be loaded.

For efficient adsorption the physiological conditions (pH, ionic strength) of the sample and the column must allow effective binding. Ideally the conditions should be optimal for the interaction between the substrate and the ligand. This can be achieved by various methods varying from simple pH alteration through desalting and chemical additions to complex modifications such as dialysis and buffer exchange. Although other primary recovery operations may well be necessary in order to clarify samples destined for fixed bed chromatography it is hoped that these will not be necessary when the sample is introduced to an expanded bed, with the possible exception of initial treatments to release intracellular products.

There is some degree of disagreement about methods of loading. Since the load samples are often of high viscosity relative to the buffers used then the bed expansion in the load step will be higher than in any other step. Consequently the liquid flowrate may need to be altered. Chang and Chase (1996) advocate keeping the bed height and therefore degree of expansion constant at all times by varying the liquid flowrates and show higher productivity can be achieved using these methods. On the other hand, Barnfield-Frej *et al.* (1994) suggest that the liquid flowrate should be kept constant allowing the bed expansion to vary according to the

viscosity of the liquid being loaded. This has the advantage that the bed height does not need to be monitored constantly, which is difficult when loading opaque liquids such as yeast homogenate or where other than borosilicate glass columns are used, although techniques to monitor bed height based upon ultrasonic waves (Thelen and Ramirez, 1999) or LED based sensors (Ghose *et al.*, 2000) have been suggested as possible solutions to this. In this thesis, all EBA experiments have been carried out at constant loading velocity in order to mimic scaled-up industrial processing conditions.

1.5.2.4 Washing

When the load step is complete the column is washed. This step is carried out to remove any traces of cell debris and non-binding substances such as contaminating proteins or weakly bound contaminants from the column.

In general washing is carried out using equilibration buffer for simplicity and ease of preparation. Draeger and Chase (1991) studied the effect of highly viscous wash buffers on volumes of liquid required and effects on elution and found that, while the addition of glycerol to wash buffers to increase viscosity reduced the wash volume required it also appeared to have a detrimental effect on elution. Equilibration buffer is run through the column until all waste material is removed from the system.

1.5.2.5 Elution

After washing, the required products and any remaining contaminants are removed from the column. This step is known as elution. In the event of other contaminants being still present on the column then the elution is carried out in such a way as to ensure the product is contaminant free (i.e. multiple step elutions). The method of elution varies depending on the method of chromatography but buffer changes, pH changes and salt gradients are common methods.

Elution from an expanded bed is frequently carried out with the bed in a packed configuration, i.e. the bed is allowed to settle after washing and the upper adapter lowered to the top of the settled bed. Elution is then most commonly carried out in a downward direction at a lower flowrate to minimise the elution peak width although either direction is possible (Hjorth, 1999, Lihme *et al.*, 1999). Elution can be carried out using a step or gradient protocol as with packed chromatography, although scale requirements mean that step elutions are favoured.

1.5.2.6 Regeneration

After elution the column must be cleaned. Clean-in-place (CIP) procedures for STREAMLINE matrices given in literature vary according to the type of matrix, usually due to the varying chemical stabilities of the different matrix functional groups. Most are based around a caustic wash, although strengths of NaOH solutions used tend to vary in the order of 0.1-1M NaOH. In addition some workers advocate an alternating acid/alkali wash (usually acetic acid) for enhanced cleaning, and storage is invariably in 20% ethanol. Specific matrices such as rProtein A are cleaned using agents such as 6M GuHCl since the immobilised protein A would be damaged by the action of NaOH.

If the column is to be immediately reused then it is usually regenerated by washing with equilibration buffer specific to the type of chromatography being carried out. Otherwise cleaning buffers are washed out of the system with water and the column stored in 20% ethanol or sodium azide solution to prevent bacterial growth.

1.6 Recent Developments - STREAMLINE Direct Expanded Bed Products

The next generation of STREAMLINE products, named STREAMLINE Direct are now available commercially and address the problems that were commonly encountered with the original STREAMLINE products.

1.6.1 STREAMLINE Direct Adsorbents

The work in this thesis provided the opportunity to work with prototype second generation STREAMLINE AIEX matrices (see Chapters 6 and 7). Whilst these are not available commercially, STREAMLINE Direct CST, a multi modal cation version is (Data File STREAMLINE Direct CST I), that is based on the same base matrix.

The density of the matrix beads has been increased from 1.15 to 1.8 g/mL as compared with the traditional STREAMLINE matrices. This allows higher operating velocities in the region of 600-900cm/hr thereby reducing processing time.

The adsorbent beads are smaller with a mean particle size of 135 μ m (compared to 200 μ m for STREAMLINE DEAE and SP). Smaller adsorbent particles are advantageous as they lead to an increased breakthrough capacity (Karau *et al.*, 1997).

In addition to this the ligand can withstand high ionic strength thus minimising the feed dilution required to reduce the conductivity, as is typically the case with IEX. Operation at these high conductivity levels has the additional benefit of preventing undesirable cell/adsorbent interactions that have been problematic and can lead to eventual bed collapse in IEX separations (Feuser *et al.*, 1999).

Combined, these developments reduce the processing time and buffer consumption, thereby increasing the overall processing economy.

This matrix is compatible with the existing STREAMLINE hardware and is also designed to operate in the new STREAMLINE Direct columns, described below.

1.6.2 STREAMLINE Direct Hardware

The new STREAMLINE Direct columns have been designed to overcome the problems of streaming, blocking and trapped air bubbles that are commonly encountered with the already available EBA columns. The

design is based on an oscillating distributor at the base of the column that removes the need for a bottom adaptor mesh (Data File STREAMLINE Direct 24 and 95 columns). Similar types of distribution systems have been positively reviewed in the literature (Zafirakos and Lihme, 1999). Due to this, all operations are carried out in an upwards flow, including the elution step. The new column is designed to work specifically with the new STREAMLINE Direct range of matrices.

1.7 Conclusions

This chapter has presented the theory and development of expanded beds and has also outlined the theory behind general chromatographic separations. This is all aimed at providing the reader with a basic understanding of this unit operation.

The next chapter outlines the materials and methods employed for all the experimental work carried out in this thesis.

2 MATERIALS AND METHODS

All chemical reagents used were laboratory grade obtained from Sigma Aldrich Fluka (Poole, Dorset, UK) and Amersham Biosciences (Uppsala, Sweden). Pre-made bacterial culture reagents were obtained from Oxoid (Hampshire, UK). All experiments were carried out in triplicate to ensure reproducibility.

2.1 Bacterial Cell Growth

Fermentation protocols were developed for *E. coli* DH5 α containing the ampicillin resistant plasmid pGEX-5X-1 (gift from Howard Chase, Cambridge University, Cambridge, UK), expressing GST under the control of the tac promoter, inducible with isopropyl β -D-thiogalactopyranoside (IPTG).

2.1.1 Cell Culture Media

2.1.1.1 Nutrient Broth No.2

Prepared according to manufacturers (Oxoid) guidelines by the addition of deionised H₂O. This was then sterilised by autoclave (121°C, 20min) and supplemented with 0.1g/L ampicillin via a 0.2 μ m sterile syringe filter (Whatman, Brentford, UK). This procedure was applied to both Nutrient Agar and Nutrient Broth.

2.1.1.2 Terrific Broth

Prepared according to manufacturers (Oxoid) guidelines by the addition of deionised H₂O and 10% w/v glycerol. This was then sterilised by autoclave (121°C, 20min) and supplemented with 0.1g/L ampicillin via a 0.2 μ m sterile syringe filter (Whatman).

2.1.1.3 High Cell Density Media

Prepared according to Korz (Korz *et al.*, 1995) supplemented with 10g/L of Yeast Extract (Oxoid). The base media, carbon source, trace elements, yeast extract and Fe Citrate media components were made up separately in solution to prevent precipitation and sterilised by autoclave (121°C, 20min). The thiamine and ampicillin were prepared as stocks and added via a 0.2µm sterile syringe filter (Whatman).

Base Media

KH ₂ PO ₄	13.3g/L
(NH ₄) ₂ HPO ₄	4.0g/L
Citric Acid	1.7g/L

Carbon Source

Glycerol	30.0g/L
MgSO ₄	1.2g/L

Trace Elements

EDTA	8.4 × 10 ⁻³ g/L
CoCl ₂	2.5 × 10 ⁻³ g/L
MnCl ₂	15.0 × 10 ⁻³ g/L
CuCl ₂	1.5 × 10 ⁻³ g/L
H ₃ BO ₃	3.0 × 10 ⁻³ g/L
Na ₂ MoO ₄	2.5 × 10 ⁻³ g/L
Zn(CH ₃ COO) ₂	13.0 × 10 ⁻³ g/L

Other Additions

Yeast Extract	10.0g/L
Thiamine	4.5g/L
Fe Citrate	10.0g/L
Ampicillin	0.1g/L

2.1.2 Glycerol stock preparation and maintenance

Nutrient agar plates were prepared as described in 2.1.1.1 with ampicillin added to select for cells harbouring the plasmid. Cells were applied to plates in a standard three way streak, and incubated at 37°C overnight.

Colonies were transferred aseptically to 50mL shake flasks containing 10mL nutrient broth prepared as per 2.1.1.1. The cultures were grown overnight until approximately 1 hour prior to stationary phase in an orbital shaker (New Brunswick Scientific, Hatfield, UK) at 37°C and an agitation rate of 200rpm. The culture was then suspended in sterile glycerol (50% w/v) and aliquoted into 2mL stocks. These master stocks were frozen at -70°C to be used for re-culturing fresh working stocks, by repeating the above procedure. The working stocks were frozen at -20°C to be used for cell culture and were given a two month life span after which time they were replaced.

2.1.3 Shake Flask Fermentation

2L shake flasks were prepared with 250mL of selected media, prepared as described in 2.1.1. These were inoculated aseptically using a working glycerol stock prepared as described in 2.1.2 that was thawed at room temperature. Cells were then grown in an orbital shaker at 30°C and 200rpm (New Brunswick Scientific). For growth and expression investigations, cells were grown until stationary phase and where appropriate, glutathione S-transferase (GST) expression was induced with the aseptic addition of 1mM IPTG; for inoculum preparation, cells were harvested approximately one hour prior to stationary phase.

2.1.4 5L Fermentation

Fermentations of *E. coli* DH5 α expressing GST were performed in 7L bioreactors with a 5L working volume supplied by LH Fermentation (Adaptive Biosystems, Luton, UK) with the offgas stream connected to a mass spectrometer (MM8-80S, VG Gas Analysis Ltd., Windsworth, UK).

Dissolved oxygen tension (DOT) and pH probes were calibrated and positioned within the fermenter along with the antifoam probe. The vessel was then filled with the desired volume of base media (allowing for any additions and inoculum) as the cells were grown in the High Cell Density media described in 2.1.1.3, which was then sterilised *in-situ* (121°C, 20min). To prevent precipitation, other media components were autoclaved separately where appropriate and added aseptically; media components that were not autoclaved were injected aseptically using a 0.2µm sterile syringe filter (Whatman).

Once all the media components had been added, the operating conditions were set and these were then controlled via feedback control. The pH was set to 6.7 and was then controlled by automated addition of acid (1M H₂SO₄) and base (4M NaOH). Foaming was monitored via the antifoam probe and was controlled by the automated addition of polypropylene glycol (PPG). Temperature was set and controlled at 30°C. Air flow was set and controlled at 5L/min and agitation rate was initially set and controlled at 500rpm. The DOT was maintained at a minimum of 40% using cascade control by increasing the agitation rate.

Two 2L shake flasks described in 2.1.3 were prepared using the High Cell Density media and were used to inoculate the fermenter. Throughout the fermentation, samples were taken at regular intervals to measure for optical density (OD_{600nm}) and GST activity. Cells were grown until an OD_{600nm} of approximately 20 was reached at which point GST expression was induced by the addition of 1mM IPTG via a 0.2µm sterile syringe filter. Cells were grown for a further three hours and then drained for downstream processing.

2.2 Downstream Processing

2.2.1 Cell Disruption

2.2.1.1 Sonication

Samples to a maximum of 5mL were chilled on ice and cells lysed by sonication for 1min with 10secs on/off pulse (Soniprep 150, Sanyo Scientific, Bensenville, IL).

For larger volumes to a maximum of 250mL, samples were chilled on ice and lysed by sonication for 10 mins with 9.9secs on/off pulse at 80% amplitude (Sonics Vibracell 750 Watt Model using 13mm probe, Newtown, CT).

2.2.1.2 Homogenisation

Volumes to a maximum of 5L were disrupted in a high pressure homogeniser (Lab 60, APV Ltd., Crawley, UK) fitted with a restricted orifice discharge valve for five discrete passes at 500bar with the temperature maintained at 5°C.

2.2.2 Clarification

Two types of centrifuge were used in this research; a bench microfuge for small scale clarification and a lab scale centrifuge for larger scale clarification.

2.2.2.1 Bench top centrifugation

A microfuge (Sanyo Scientific) was used to harvest cells or remove insoluble material. Cells were harvested for 5min and 13,000rpm.

2.2.2.2 Lab scale centrifugation

Clarification of larger volumes of material was carried out in a Beckman J2 centrifuge (Beckman Coulter, Fullerton, CA) fitted with a Ja-10 rotor at 10,000rpm for 30mins with cooling.

2.3 Biological Systems

This section describes the various biological systems used in this study and includes details of their preparation for use in both expanded and packed bed chromatography, along with details of the chromatography buffer/matrix/Clean-in-place (CIP) systems employed.

2.3.1 Alcohol Dehydrogenase/Yeast

2.3.1.1 Feedstock Preparation

Bakers' yeast in the form of pressed blocks (DCL Ltd., Clackmannanshire, UK) was used as a source of the intracellular protein Alcohol dehydrogenase (ADH). Yeast was made into a 250g/L (wet weight) suspension in 0.1M potassium phosphate buffer. This was then disrupted in a high pressure homogeniser as per section 2.2.1.2. The homogenised feed was then either clarified as per 2.2.2.2 for packed bed studies, or left unclarified for expanded bed runs. In each case, the feed was then assayed for ADH activity as described in 2.6.6 and diluted to 100 U/mL ADH activity ($\pm 20\%$). In the process, the feed was also made up to 0.78M ammonium sulphate for optimum binding to the matrix (Smith *et al*, 2002).

2.3.1.2 Chromatography Details

ADH was captured via hydrophobic interaction chromatography (HIC) using STREAMLINE Phenyl matrix. Separations were carried out in both packed beds with 20mL matrix equivalent to a 10cm bed height and expanded beds in the STREAMLINE 50 column described in 2.4.1 containing 200mL matrix, also equivalent to a 10cm settled bed height. Equilibration buffer used was 0.78M $(\text{NH}_4)_2\text{SO}_4$ + 0.1M KH_2PO_4 and elution buffer was 0.1M KH_2PO_4 . All chromatography runs were carried out with buffers and feed materials maintained at 4°C.

In order that each bed was challenged with the same quantity of ADH and to maintain the same product to matrix ratio, a feed of 1L volume was used for all expanded bed experiments and 100mL for packed bed experiments such that the matrices were challenged with 500Units ADH per mL matrix. In all cases, pooled samples of feed, load, wash and elution were collected in order to mass balance the process and determine the amount of product bound to the bed.

2.3.1.3 Clean-in-Place Procedure

The CIP procedure was carried out using 10 column volumes 1M NaOH followed by 120 minutes NaOH contact time, 3 column volumes 25% v/v acetic acid, 3 column volumes 30% v/v isopropyl alcohol and 5 column volumes 20% v/v ethanol. Each of these stages were interspaced with 3 column volume water washes.

2.3.1.4 Residence Time Determination

Residence Time Distribution (RTD) curves were obtained by recording the UV trace resulting from a step change from water + 0.5g/L blue Dextran 2000 to water and calculated as described below in 2.6.7 The choice of Blue Dextran 2000 as a marker is discussed in Chapter 4.

2.3.2 Glutathione S-Transferase/*E. coli*

2.3.2.1 Feedstock Preparation

E. coli expressing GST was grown in High Cell Density media either in shake flasks or 7L fermenter vessel (5L working volume) as per the methods of 2.1.3 and 2.1.4 respectively, dependent on the scale required. The broth was frozen in batches at -20°C until it was required at which point it was thawed at 4°C overnight. The feedstock preparation then followed one of the following routes dependant on its use:

Clarify, Disrupt and Clarify

The thawed broth was clarified as per 2.2.2 and the cell pellet was resuspended in 0.02M Tris/HCl pH 8.5 either with or without 0.2M NaCl added to adjust the conductivity. This was then disrupted as per 2.2.1 and the soluble protein was isolated via centrifugation as per 2.2.2.

Clarify and Disrupt

The thawed broth was clarified as per 2.2.2 and the cell pellet was resuspended in 0.02M Tris/HCl pH 8.5 containing 0.2M NaCl. This was then disrupted as per 2.2.1 and diluted as appropriate with 0.02M Tris/HCl pH 8.5.

Disrupt

The thawed broth was disrupted as per 2.2.1 and diluted to reduce the conductivity to 10mS/cm. In the process the feed was also made up to 0.02M Tris/HCl pH 8.5.

2.3.2.2 Chromatography Details

GST was captured via anion exchange chromatography (AIEX) using the following matrices (full details of the prototype ligands can be found in Chapter 6):

- STREAMLINE DEAE
- STREAMLINE base matrix coupled to DAB (prototype ligand)
- Prototype high density base matrix couple to DEAE
- Prototype high density base matrix coupled to 3 prototype high salt tolerant ligands.

Separations were carried out in both packed beds using 10mL matrix (equivalent to a 5cm bed height) and expanded beds in the STREAMLINE 25 column described in 2.4.2 containing between 75 - 100mL matrix equivalent to a 15 - 20cm settled bed height (total column height is 1m).

Equilibration buffer used was 0.02M Tris/HCl pH 8.5 and elution buffer was 50mM Potassium Phosphate containing 1M NaCl pH 6.0.

In all cases, pooled samples of feed, load, wash and elution were collected in order to mass balance the process and determine the amount of product bound to the bed.

2.3.2.3 Clean-in-Place Procedure

The CIP procedure was carried out as described in 2.3.1.3.

2.3.2.4 Residence Time Determination

Residence Time Distribution (RTD) curves were obtained by recording the UV trace resulting from a step change from water + 0.25% (v/v) acetone to water and calculated as described below in 2.6.7. The choice of acetone as a marker is discussed in Chapter 5.

2.3.3 Bovine Serum Albumin/Buffer

2.3.3.1 Feedstock Preparation

A 5mg/mL solution of Bovine Serum Albumin (BSA) was made up in 50mM Tris/HCl pH 7.5 buffer either with or without 0.25M NaCl added to adjust the conductivity.

2.3.3.2 Chromatography Details

BSA was captured via AIEX chromatography using the three prototype ligands coupled to the prototype high density base matrix detailed in Chapter 6. Equilibration buffer used was 50mM Tris/HCl pH 7.5 and elution buffer was 50mM Tris/HCl pH 7.5 containing 1M NaCl.

2.3.3.3 Clean-in-Place Procedure

The CIP procedure was carried out as described in 2.3.1.3.

2.4 Expanded Bed Chromatography

2.4.1 STREAMLINE 50

2.4.1.1 System Details

The STREAMLINE 50 column used for expanded bed separations was a modified, ported STREAMLINE 50 expanded bed described by Willoughby *et al*, 2000(b). The glass column (total length of 1m) was equipped with side ports every 5cm up the axis of the column. A total of 10 ports were made to cover the full expanded height of the bed (~50cm). These ports were plugged with rubber bungs when not needed. Selected sample ports, depending on the amount of matrix in the column were fitted with custom-made sampling tubes with mesh sinters to prevent matrix removal during liquid sampling. Peristaltic pumps (model 505DI, Watson-Marlow Ltd., Cornwall, UK) were used for buffer and feed application and to raise and lower the column hydraulic adaptor. All valves and equipment were from the Amersham Biosciences range. The automated CIP cycle was controlled via an LCC 500 Plus controller and a P-6000 pump (Amersham Biosciences). The output from the column was monitored for UV-absorbance at 280nm and conductivity using Amersham Biosciences monitors, and these values logged using a PE Nelson 900 interface and Turbochrom v4 (both Perkin Elmer Nelson Systems Inc., Boston, MA).

Samples were taken from the ported column, using a Gilson Minipuls multiroller peristaltic pump (Gilson, Villiers le Bel, France) at a flowrate of 2mL/min. This flowrate was selected to provide an adequate supply of fresh material for analysis without disturbing the bed stability (Willoughby *et al*, 2000(a)).

Samples were passed to the custom built stopped-flow analyser (SFA) described in more detail in 2.6.6 which operated on a split stream from

the 2mL/min sample line and enabled the removal of a small sample of liquid (approximately 1mL) for analysis every 55 seconds.

2.4.1.2 Mode of Operation

Expansion and equilibration were carried out at the running flowrate until the bed was fully equilibrated at which point feed was loaded onto the column in an upwards direction and at the same flowrate. On-line samples were taken at an axial height equivalent to the top of the matrix while the bed was expanded. Adaptor height was maintained approximately 5cm above the top of the bed. After loading, the bed was then switched back to equilibration buffer and the column washed upwards at the same flowrate until the UV 280nm trace had returned to baseline. As in the load step, on-line samples were taken at an axial height equivalent to the top of the matrix while the bed was expanded for the remainder of the wash. Flow was then halted and the bed allowed to settle. The hydraulic adaptor was then lowered to a height level with the top of the settled bed. The direction of flow was reversed and the product eluted in a downward direction at 75cm/hr until the product peak had been completely eluted. This took 20mins and was collected in two sample pools of equal volume. The CIP procedure was carried out at 90cm/hr immediately after elution in an upwards direction.

2.4.1.3 Matrix Elutriation and Segregation

In order to segregate STREAMLINE matrix into sections containing different particle size ranges, the STREAMLINE 50 column was filled with 300mL matrix and was elutriated in expanded mode to form three sections of equal settled matrix volume (100mL). By doing this, the individual sections corresponded to different particle size ranges since the top third of the expanded bed contains the smallest particles, and the bottom third the largest particles.

This procedure was repeated with a number of batches so as to prepare similar sections that were combined to generate “segregated” beds of the desired volume.

2.4.2 STREAMLINE 25

2.4.2.1 System Details

The STREAMLINE 25 expanded bed column (total column length is 1m) was connected to an AKTA Explorer 100 modified by the use of an AKTA STREAMLINE kit and controlled by Unicorn 4.1. The output from the column was monitored for UV-absorbance at 280nm and conductivity and these values logged via the Unicorn software. Fractions were collected where appropriate with a Frac-950 (all Amersham Biosciences).

2.4.2.2 Mode of Operation

Expansion and equilibration were carried out at the running flowrate until the bed was fully equilibrated at which point feed was loaded onto the column in an upwards direction and at the same flowrate. The adaptor was maintained approximately 5cm above the top of the bed. After loading, the bed was then switched back to equilibration buffer and the column washed upwards at the same flowrate until the UV 280nm trace had returned to baseline. Elution was then either carried out at the same running flowrate in an upwards direction, or flow was halted and the bed allowed to settle. In the latter case the hydraulic adaptor was then lowered to a height level with the top of the settled bed. The direction of flow was reversed and the product eluted in a downward direction at 75cm/hr until the product peak had been completely eluted. The CIP procedure was carried out at 90cm/hr immediately after elution in an upwards direction.

2.5 Packed Bed Chromatography

All packed bed separations were carried out in XK16 columns containing the desired quantity of expanded bed matrix that had been packed by employing a fluid downflow in excess of the running flowrate, and according to guidelines from Amersham Biosciences. Separations and CIP procedures were controlled by an AKTA Explorer 100 running Unicorn version 4.1 in a downwards direction with fractions being collected throughout the load, wash and elution where appropriate with a Frac-950 (all Amersham Biosciences).

2.6 Monitoring and Analysis

2.6.1 Optical Density

Optical density was determined using sample absorbance at 600nm, as measured against a blank of the media being used for cell culture. A Uvikon 922 UV/VIS spectrophotometer (Kontron Instruments S.p.A, Milan, Italy) was used. Samples were diluted as necessary with ultra pure water in order to adjust the absorbance below one unit at a wavelength of 600nm (the limit of linearity of the spectrophotometer).

2.6.2 Dry Cell Weight

To determine the dry cell weight within the cell cultures, 1mL samples from the fermentation were placed into Eppendorf tubes that had been dried at 105°C for 24 hours and pre-weighed. Cells were then recovered by centrifugation as per 2.2.2.1, supernatant was discarded, and the sample was dried at 105°C for 24 hours and weighed. Dry cell weight was then determined by subtraction of the original Eppendorf weight.

2.6.3 GST Assay

The detection of GST was based on the change in absorbance at 340nm as GST catalyses the reaction between 1-chloro-2,4-dinitrobenzene (CDNB) and glutathione resulting in a CDNB-glutathione product with a strong molar absorption at 340nm. GST activity was determined following the method described in the GST detection module (Amersham Biosciences). In this assay a sample of GST is incubated in a reaction buffer containing 100mM CDNB and 30.8mg/mL glutathione for 5 minutes and the initial rate is used to determine GST concentration.

Assays were performed at room temperature in 1cm path length cuvettes with 1mL assay mix in a UVIKON 922 UV/VIS spectrometer. The reaction was started by the addition of the enzyme. Sample volumes were adjusted and where necessary were diluted with potassium dihydrogen phosphate buffer (100mM, pH 6.5) to produce a linear change in absorbance between 0.1-0.8 AU. Assays were reproducible to $\pm 5\%$.

Results were expressed in terms of units of enzyme activity where one unit (U) is defined as the amount of GST required to react 1 μ mol/min of glutathione with CDNB. Activity was converted to units using the molar extinction coefficient of the CDNB-glutathione product at 340nm, $\epsilon=9.6/\text{mM}/\text{cm}$. An activity of 9.96U/mg GST was assumed (Kaplan *et al.* 1997).

2.6.4 Total Protein (Bradford) Assay

The Bradford assay was used to determine total protein levels (Bradford, 1976). The assay is based on the shift in absorbance from 465nm to 595nm which occurs when Coomassie blue G-250 dye binds to proteins in acidic solution. A commercially available dye was used (Bio-Rad, Hemel Hempstead, UK). Bovine Serum Albumin was used to construct a calibration curve with a range of 0.1-1.0mg/mL. Protein concentration was then obtained from the calibration curve.

2.6.5 SDS-PAGE Gels

Samples from cell cultures were investigated by SDS-PAGE. Electrophoresis was carried out using the discontinuous buffer system and method of Laemmli (Laemmli, 1970).

2.6.5.1 Protein Preparation

Cells were harvested by centrifugation as per 2.2.2.1. Pellets were resuspended and boiled in appropriate amounts of sample buffer (40mM Tris/HCl pH 6.8, 20% (v/v) glycerol, 2% (w/v) Sodium dodecyl sulphate (SDS), 5% (v/v) β -mercaptoethanol and trace bromophenol blue). 50 μ L of protein was loaded.

2.6.5.2 Gel Preparation, Running and Staining

12% monomer resolving gels were prepared using ProtoGel (National Diagnostics, Hull, UK). The gel solution contained 40% ProtoGel, 26% ProtoGel Buffer, and 34% ultra pure H₂O. Following pouring, gels were cast with the addition of 1mL 10% (w/v) ammonium persulphate (freshly prepared), and 100 μ L TEMED to result in 100mL of resolving gel solution. Gels were run at 200V for 35min in MES electrode buffer (Invitrogen).

Gels were stained using 0.1% (w/v) Coomassie brilliant blue R-250 in 50% (v/v) methanol, and 10% (v/v) acetic acid for 2 hours on a rocker. Gels were destained using fast destain (40% (v/v) methanol, 10% (v/v) acetic acid) for 2 hours, followed by slow destain (10% (v/v) methanol, 10% (v/v) acetic acid) for 4 hours.

2.6.6 ADH Assay

ADH monitoring was based on the initial rate of absorbance change at 340nm as ADH catalyses the reduction of NAD⁺. Alcohol dehydrogenase (ADH) activity was determined following the method of Bergmeyer (Bergmeyer, 1979). All assays were performed in 1cm path length

cuvettes and the reaction was started by the addition of the enzyme sample. Potassium dihydrogen phosphate buffer (100mM, pH 6.5) was used to dilute samples to produce a linear change in absorbance less than 0.5 AU/min.

The assay was carried out using a custom built stopped-flow analyser (SFA) connected to a computer-controlled spectrophotometer (Amersham Biosciences) equipped with controllable twin cuvettes (with 1mm and 10mm pathlengths respectively). ADH concentration was determined using an initial rate assay carried out for 15 seconds after which the flowcells were automatically washed and the next sample analysis began. The total system time was 55 seconds and assays were carried out to a duplicate accuracy of $\pm 5\%$.

Dilution of the samples was achieved in the SFA delivery system prior to analysis. The more concentrated samples were diluted one in 236 and the more dilute one in 17. Further dilution for the product (ADH) rate assays could be achieved by using different cuvette path lengths.

The results were logged by PC and plotted on screen to allow on-line operator monitoring of the system. All instruments were linked to a computer through serial RS232 and A/D connections to facilitate data logging and instrument control. The software used for these purposes was based on LabVIEW (National Instruments, Austin, TX). Full details of the SFA method can be found in other publications (Habib *et al*, 1997; Richardson *et al*, 1996).

2.6.7 Residence Time Determination

System residence times ($t_{Rsystem}$) were determined for both packed and expanded beds. In both systems, residence time distribution (RTD) curves were obtained by recording the UV trace resulting from a step change from tracer molecule to water at the desired flowrate using the packed and expanded bed systems described above. RTD tests were carried out

in triplicate to yield the number of theoretical plates (NTP), reproducible to within $\pm 20\%$.

2.6.7.1 Packed Bed Operation

Once the residence time for the system ($t_{Rsystem}$) had been measured, it was necessary to correct for the time delay due to tubing prior to and after the column ($t_{Rtubing}$) by measuring tubing length, cm (L_{tubing}) and internal diameter, cm (ID_{tubing}), such that:

$$t_{Rtubing} = \frac{L_{tubing} \times \pi \times \left(\frac{ID_{tubing}}{2}\right)^2}{Q} \times 60 \quad (2.1)$$

where Q is the volumetric flowrate, mL/min through the tubing.

The true residence time for the bed was then:

$$t_{Rpacked} = t_{Rsystem} - t_{Rtubing} \quad (2.2)$$

2.6.7.2 Expanded Bed Operation

The true residence time in expanded beds was determined in a similar fashion to that of the packed beds. During the RTD tests the adapter was maintained at a height equivalent to the top of the expanded matrix, and a UV monitor was placed in the outlet stream of the bed. Once the residence time for the system ($t_{Rsystem}$) had been measured, it was necessary to correct for the time delay due to tubing prior to and after the column and also for the difference in residence time attributed to the change in the degree of expansion achieved with the biological system applied to the column, as compared with water ($t_{Rheight}$).

The difference in bed height, ΔH (cm) due to expansion in the more viscous biological fluid was accounted for by measuring the difference in expanded height when the system was run with water as compared with the biological system. Given that the matrix mass and volume are constant, the change in system volume is solely due to an increase in bed voidage. Such a change will increase the system residence time. The

internal diameter, cm (ID_{column}) of the column was known and hence using the flowrate at which the experiment was run (Q , mL/min), it was possible to calculate the residence time for the extra height, $t_{Rheight}$ (sec) by:

$$t_{Rheight} = \frac{\Delta H \times \pi \times \left(\frac{ID_{column}}{2}\right)^2}{Q} \times 60 \quad (2.3)$$

The true residence time for the segregated bed (t_R) was then calculated by subtracting from the measured residence time ($t_{Rsystem}$) the residence time due to the tubing ($t_{Rtubing}$) and subsequently adding on the residence time due to the extra height ($t_{Rheight}$), therefore:

$$t_R = t_{Rsystem} - t_{Rtubing} + t_{Rheight} \quad (2.4)$$

2.6.8 Matrix Particle sizing

Particle size ranges for each of the various matrix samples were determined using a Malvern Mastersize 2000 laser sizer (Malvern Instruments, Worcestershire, UK). This device employs a Low Angle Laser Light Scattering (LALLS) method to measure particles in the range 0.1 to 2000 microns. Samples were added to a recirculating cell within the sizer.

The values noted were the number diameter statistics d_{10} , d_{50} and d_{90} . These are defined as the point on the particle distribution where, respectively, 10%, 50% and 90% of the particles are smaller than the stated diameter. The d_{10} statistic is an indicator of the proportion of fines in a particle size distribution, whilst d_{50} gives the mean particle diameter and d_{90} a measure of the proportion of large particles present. These statistics were selected in order to characterise the sample particle distributions.

2.6.9 Number of Matrix Particles

RTD curves were recorded as described above in 2.6.7 in XK16 columns containing a known settled matrix volume (V_T) using 0.5g/L Blue Dextran as a marker. V_T can be defined as the total volume of matrix, consisting of matrix particles (V_M) and liquid (V_L) such that:

$$V_T = V_M + V_L \quad (2.5)$$

Once the true residence time, $t_{Rpacked}$ described in 2.6.7.1 had been determined, and given the volumetric flowrate, Q mL/min, through the column it was possible to calculate the volume of liquid in the sample of matrix from:

$$V_L = Q \times t_{Rpacked} \quad (2.6)$$

Rearranging equation 2.5 allows the volume of matrix in a sample to be calculated as:

$$V_M = V_T - V_L \quad (2.7)$$

The number of particles (N_p) in a 1mL sample can then be defined as:

$$N_p = \frac{V_M}{\frac{4}{3}\pi(d_{50}/2)^3} \quad (2.8)$$

Where d_{50} is the mean diameter of a particle described in 2.6.8.

2.6.10 Total Binding Capacity Measurements

Total binding capacities were determined for various matrices using a finite bath method, whereby sample containing product prepared according to the guidelines outlined above was assayed for product and diluted to the required concentration ($[Product]_0$) and applied in excess to 0.5mL samples of matrix in sealable tubes. These were then sealed and placed on a shaking rack and left for 5 hours. The supernatant was then assayed for product until a constant value was achieved ($[Product]_{eqm}$). The difference in $[Product]_0 - [Product]_{eqm}$ was taken as the total binding capacity of the matrix for product at the given product concentration.

Various product concentrations of the same sample were used to prepare adsorption isotherms for segregated beds of STREAMLINE DEAE and the prototype high density base matrix coupled to the prototype high salt tolerant ligand DAB.

3 THE PRODUCTION AND ANALYSIS OF GST FROM *E. COLI*

3.1 Introduction

The overall aims of this study are to investigate the effects of operating parameters on the productivity of an EBA unit. Chapter 4 will look at these using a Yeast/Alcohol Dehydrogenase (ADH) system. In order to establish the generic nature of the findings it is necessary to see if these results are transferable across different systems. A second system based on the purification of glutathione S-transferase (GST), an untagged intracellular protein, from an unclarified *E. coli* homogenate will be used to provide this test. GST (26kDa) is part of a family of proteins that catalyse the conjugation of reduced glutathione with a variety of hydrophobic chemicals containing electrophilic centres (Habig *et al.*, 1974).

The use of EBA to purify ADH from yeast homogenate has been well characterised (Smith *et al.* 2002, Willoughby *et al.* 2000(b)) as has the purification of GST from *E. coli* homogenate (Clemmitt *et al.* 2002), however, little work has been published on the production of GST from *E. coli*. In this chapter *E. coli* DH5 α containing the plasmid pGEX-5X-1 (Amersham Biosciences) expressing GST inducible with isopropyl β -D-thiogalactopyranoside (IPTG), has been grown in a variety of fermentation media in order to determine *E. coli* growth and GST expression and assess the conditions necessary to maximise material from the minimum number of fermentations. Based on these results, a choice of media was made for scale-up and it was then possible to explore the disruption and storage conditions needed for GST release. Finally the GST assay, as described in chapter 2, was examined with respect to the effects of reaction time and sample dilution level in order to identify

appropriate conditions necessary for the monitoring of this system and to enable rapid throughput and analysis of GST.

3.2 Fermentation Development

3.2.1 Effect of culture media on *E. coli* growth

In the first instance it was necessary to investigate the effect of the culture media on the growth of *E. coli* DH5 α . Shake flask cultures were grown according to the methods in section 2.1.3 using three different media:

- a) Nutrient Broth (Oxoid)
- b) Terrific Broth (Oxoid)
- c) High Density Media (Korz *et al.*, 1995) supplemented with 10g/L of Yeast Extract (Oxoid)

In each case, *E. coli* was grown aerobically at 30°C and 200rpm in 2L shake flasks (250mL working volume) until cell death, supplemented with 0.1g/L ampicillin. During growth, two 1mL samples were removed every hour for measurement of optical density according to the methods in section 2.6.1 and dry cell weight (DCW) according to section 2.6.2 until growth had ceased, at which point the fermentation was stopped. All fermentations were carried out in triplicate. The growth curves for each of the media are shown in Figure 3.1 and the relationship between optical density and dry cell weight are shown in Figure 3.2.

These growth curves in Figure 3.1 demonstrate that *E. coli* DH5 α can be grown reproducibly in each of the 3 media. Terrific Broth produced a greater dry cell weight of 10mg/mL, approximately 2 fold higher than the high cell density media and 10 fold higher compared to nutrient broth.

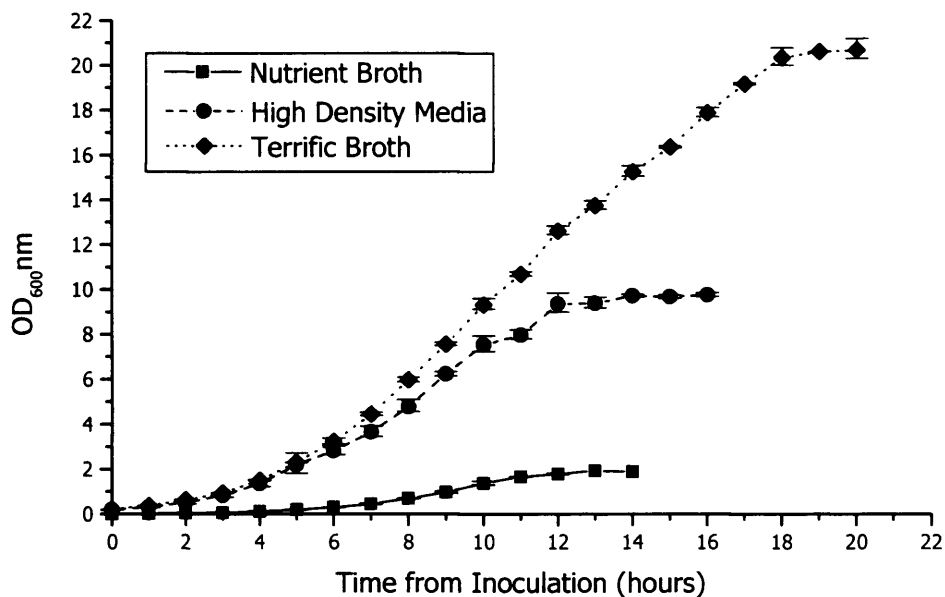


Figure 3.1: Growth of *E. coli* DH5α within 3 different media. Cultures were grown in 2L shake flasks with a 250mL working volume at 200rpm and 30°C.

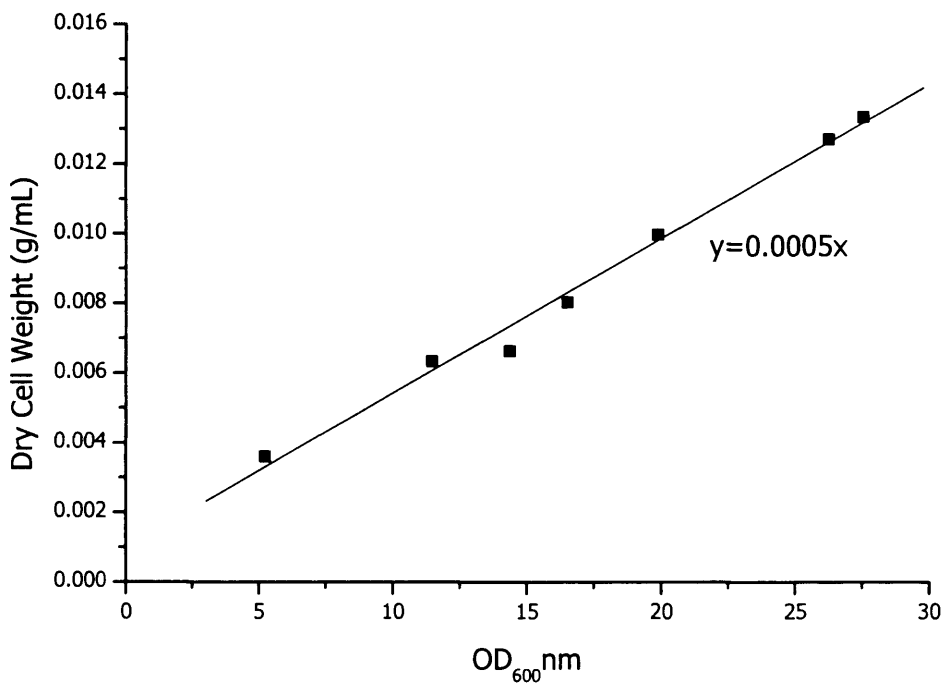


Figure 3.2: Relationship between optical density measurements (OD_{600nm}) and dry cell weight of *E. coli* DH5α grown in High Density Media.

3.2.2 Effect of culture media on GST expression

Based on the growth curve results, the obvious choice would be to use Terrific Broth as this produced the highest dry cell weight of *E. coli*, however the aim here is to reproducibly produce high levels of GST and therefore it is important to investigate the GST expression in each of the three media. The shake flask fermentations were repeated and GST production was induced in each of the above media by the addition of IPTG to 1mM. In each case, based on the growth curves obtained in Figure 3.1, IPTG was added 1 hour prior to the end of growth i.e. for Nutrient Broth, at an OD_{600nm} of 0.9-1.0AU, for Terrific Broth, at an OD_{600nm} of 15-16AU and for High Density Media, at an OD_{600nm} of 6-7AU.

The cultures were incubated for a further 3 hours. Samples were removed every hour post induction for analysis. Each sample was disrupted using an ultrasound sonicator for 1min as per section 2.2.1.1 and levels of GST were determined using the GST detection module (Amersham Biosciences) described in 2.6.3. Results are shown in Table 3.1.

The final sample taken 3 hours post induction was also assayed for total protein using the Bradford assay (Bradford, 1976) as per 2.6.4 and was subsequently centrifuged as per 2.2.2.1. The supernatant was assayed for total protein and GST, and the remaining debris containing any trapped soluble product was resuspended in 100mM Tris/HCl pH 7.5 buffer and also assayed for total protein and GST. These results are shown in Table 3.2.

SDS-PAGE gels were also run as per the methods in 2.6.5 for each media to carry out an analysis of the protein fractions (Figure 3.3 a, b and c for each media) in order to confirm assay results.

Time from Induction (hours)	Nutrient Broth	Terrific Broth	High Density Media
0	0	0.375	0.042
1	0.029	0.398	0.055
2	0.075	0.656	0.157
3	0.121	1.444	0.266

Table 3.1: Levels of GST (mg/mL) detected in sonicated *E. coli* samples taken each hour post induction with 1mM IPTG in three media grown in 2L shake flasks with a 250mL working volume at 200rpm and 30°C.

Sample		Nutrient Broth	Terrific Broth	High Density Media
GST	Whole Broth sonicate	0.121	1.444	0.266
	Supernatant	0.112	1.053	0.217
	Resuspended Pellet	0.017	0.125	0.01
Protein	Whole Broth Sonicate	0.295	1.749	0.871
	Supernatant	0.2175	1.402	0.85
	Resuspended Pellet	0.16	0.5715	0.241

Table 3.2: Total protein and GST levels (mg/mL) detected in sonicated *E. coli* cell culture, resuspended pellet and supernatant taken 3 hours post induction with 1mM IPTG.

Figure 3.3: SDS-PAGE gels of proteins detected in *E. coli* samples taken each hour post induction in three media grown in 2L shake flasks with a 250mL working volume at 200rpm and 30°C.

Figure 3.3a: Nutrient Broth

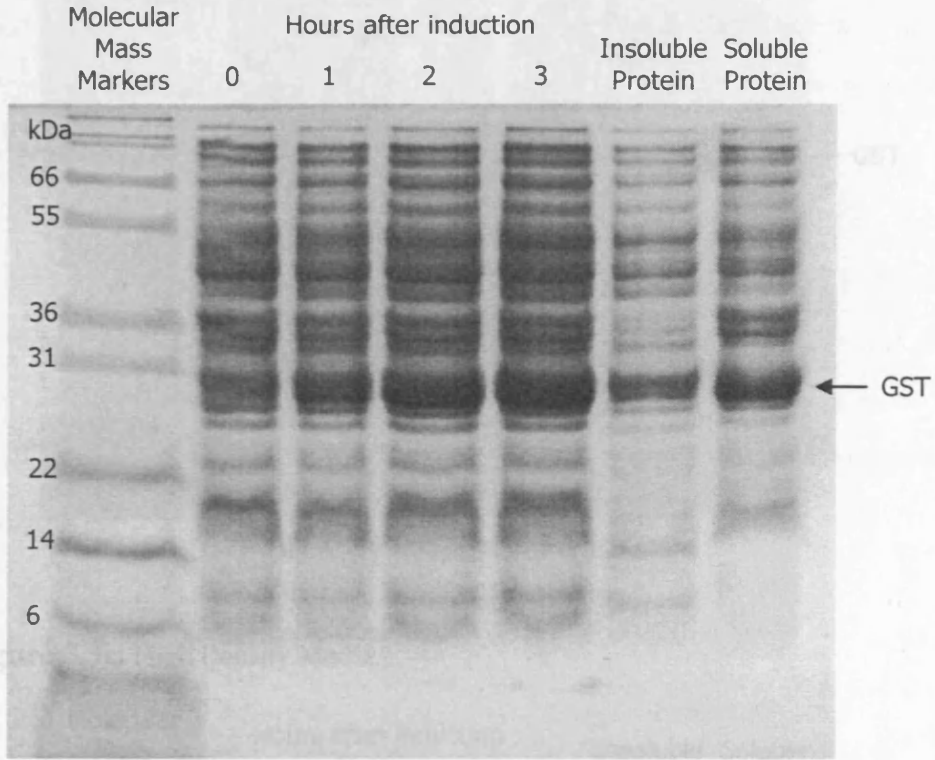


Figure 3.3b: Terrific Broth

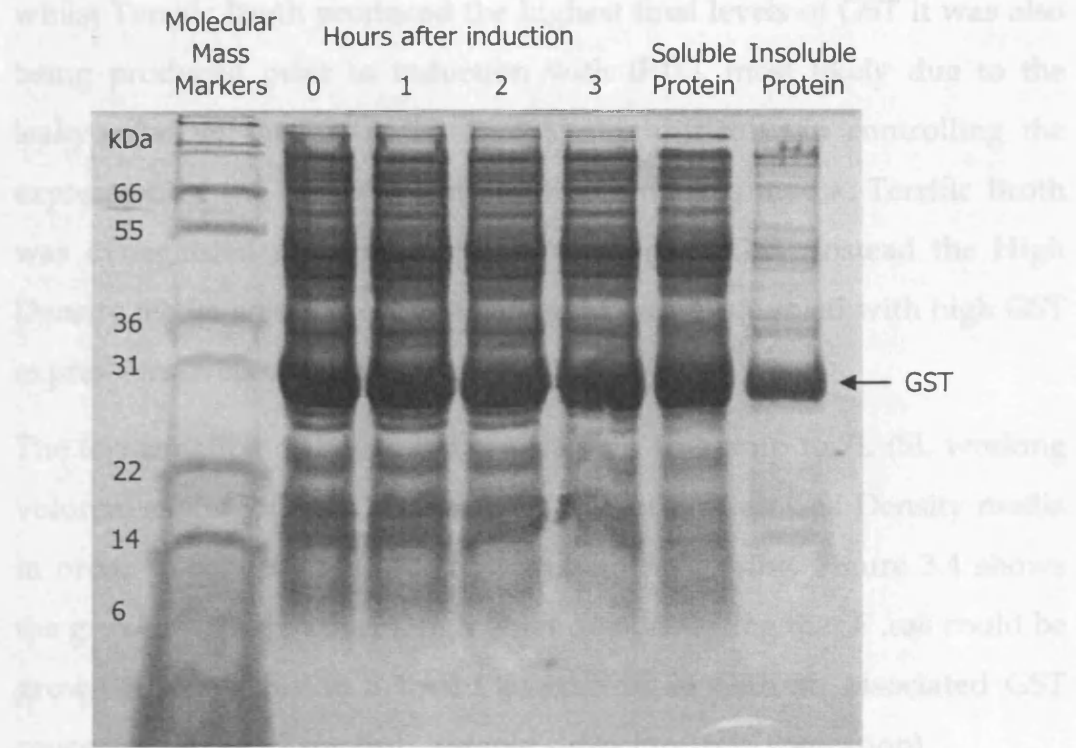
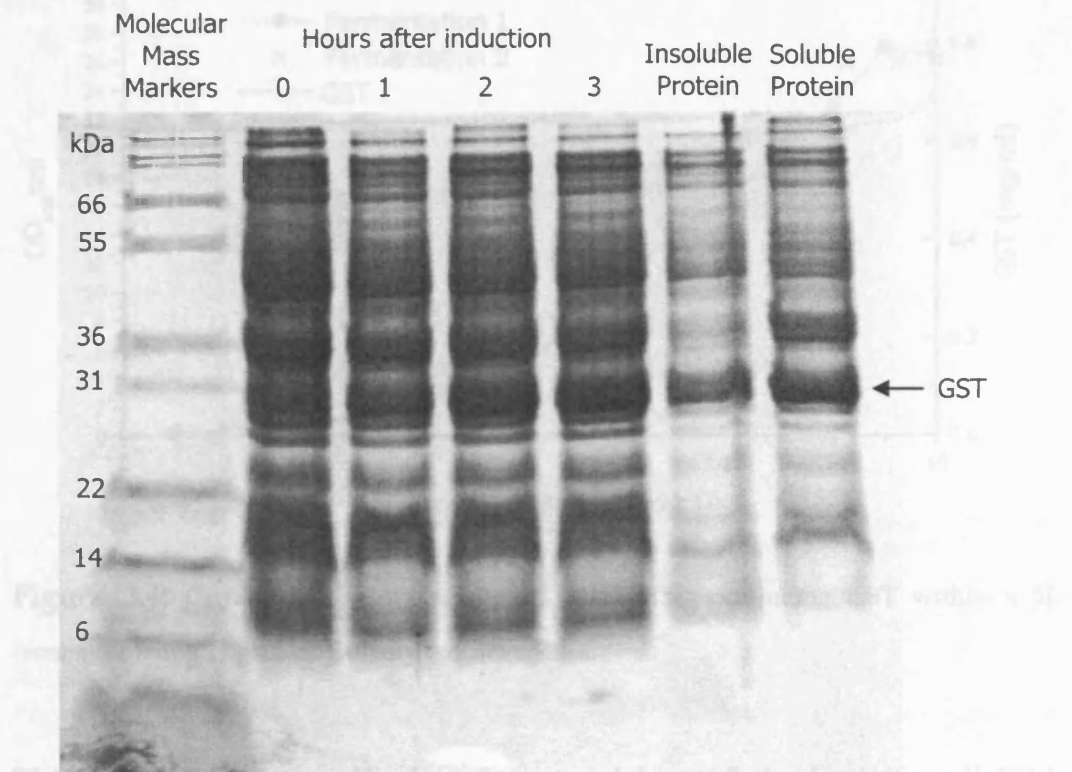


Figure 3.3c: High Density Media



Assay analysis of GST levels in the three fermentation media showed that whilst Terrific Broth produced the highest final levels of GST it was also being produced prior to induction with IPTG, most likely due to the leaky effect of the promoter. Due to this difficulty in controlling the expression of the plasmid while growing on this media, Terrific Broth was disregarded as a choice for production of GST. Instead the High Density media was chosen as it had good growth coupled with high GST expression levels in soluble form.

The fermentation of *E. coli* DH5 α was then scaled up to 7L (5L working volume) as described in section 2.1.4 using the High Cell Density media in order to produce GST for downstream processing. Figure 3.4 shows the growth curves in the 5L fermenter demonstrating that *E. coli* could be grown reproducibly to a final OD_{600nm} of 26 with an associated GST concentration of 0.7 mg/mL (sample subject to 1min sonication).

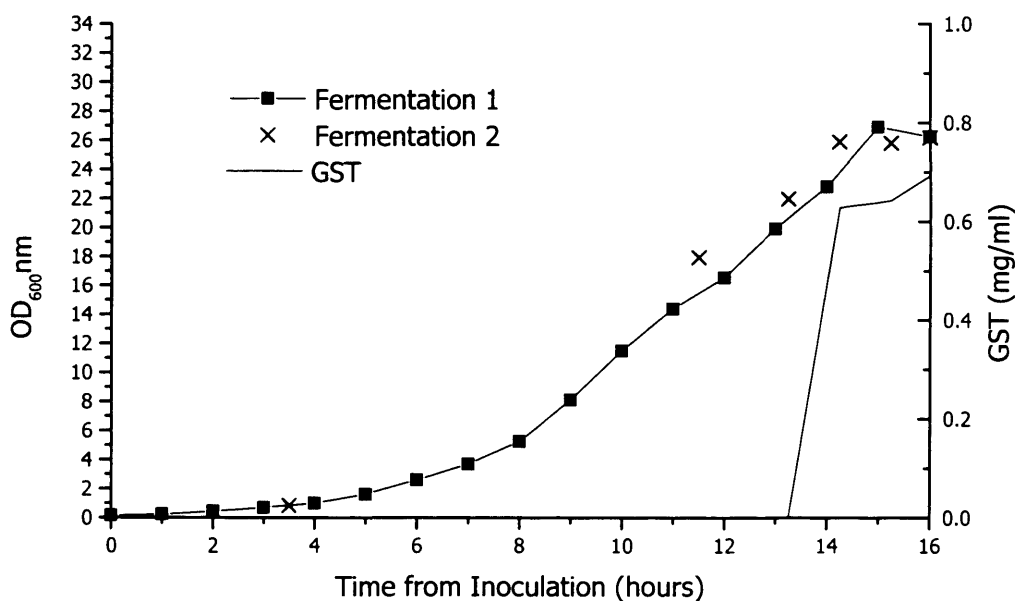


Figure 3.4: Growth and expression of *E. coli* DH5 α producing GST within a 5L fermenter using High Cell Density culture media.

This material and the developed protocol formed the basis for all EBA studies of GST that are reported in the remainder of this thesis.

3.3 GST Assay Development

Once GST had been successfully produced it was possible to investigate the assay conditions necessary to achieve reproducible analysis of the EBA process step. According to the assay guidelines detailed in 2.6.3, the detection of GST is based on a rate assay at A_{340} where absorbance measurements are made every minute for 5 mins and should fall between 0.1 and 0.8AU. In order to test these guidelines the effect of sample dilution and time of reaction on the assay results were investigated.

A sample of fermentation broth, three hours post induction was sonicated for 10 mins. The critical assay parameters were then tested by diluting the sample to different levels and assaying for GST, and also by measuring the absorbance over a 5 min period, with readings being taken every 10 sec in the first minute to check that the rate was linear. The GST concentration was then determined for each sample based on 1 and 5 mins reaction time. These results are shown in Figure 3.5.

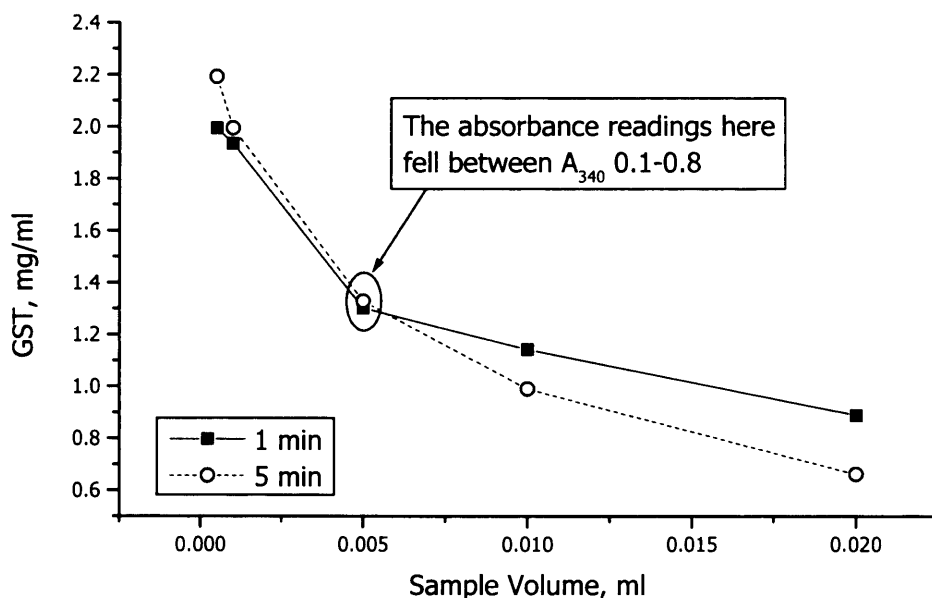


Figure 3.5: Effect of assay sample volume and reaction time on the measured concentration of GST produced in *E. coli* DH5 α . The highlighted points are those where the absorbance readings fell within the linear range of the spectrophotometer.

It can be seen in Figure 3.5 that a decrease in sample dilution i.e. an increase in overall sample volume in the assay leads to an apparently decreasing GST concentration when running the assay on the same sample source. At both high and low dilution levels, the assay was difficult to reproduce to within $\pm 5\%$. The most reproducible assay results were when the absorbance readings fell between 0.1-0.8AU as per the guidelines. This is identified in Figure 3.5 as occurring at a sample volume of 0.005mL for this particular sample under investigation. In this region of dilution, the differences in measured GST concentration upon reducing the reaction time from 5mins to 1min was only 2%. These results provided the basis for a consistent GST assay used throughout the study to gain rapid data on the EBA process. The sensitivity of the assay to the sample preparation methods indicates the importance of establishing robust methods for each system under examination.

3.4 GST Release

During the course of the GST assay development it was noted that the GST concentration measured after sonicating for 10mins was more than double that compared with 1 min (1.5 mg/mL *cf* 0.7 mg/mL) implying that maximum GST release was not achieved when sonicating for 1min. This led to an investigation of GST release kinetics and of the effect of harvest/storage conditions on GST levels.

A sample of fresh fermentation broth 3 hours post induction was passed through a Lab 60 homogeniser for 5 passes at 500bar as described in 2.2.1.2 ("*fresh*"). Samples were removed at each pass and assayed for GST concentration.

In order to investigate the impact of harvesting and storage conditions of the fermentation broth on subsequent GST release, a sample of fresh fermentation broth 3 hours post induction was frozen at -20°C and then thawed at room temperature and passed through the homogeniser. This material was termed "*frozen*". Another sample of fresh fermentation

broth 3 hours post induction was clarified as per section 2.2.2 and the cell pellet and supernatant were frozen separately at -20°C , then thawed at room temperature and recombined and passed through the homogeniser. This material was termed “*spun*”. GST concentration (mg/mL) at each pass for the above samples is shown in Figure 3.6.

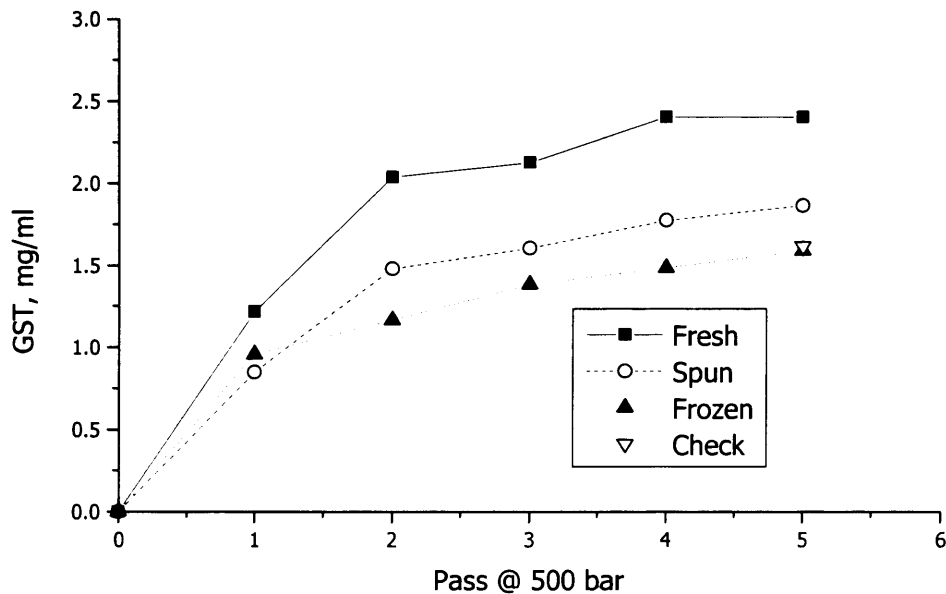


Figure 3.6: Comparison of 3 harvesting and storage conditions of *E. coli* DH5 α (fresh broth, frozen broth and clarified/frozen broth) and their effect on GST release when passed through an homogeniser for 5 passes at 500bar.

As can be seen from Figure 3.6 each of the samples achieve the highest measured level of GST release after 5 passes through the homogeniser. It would appear that the fresh broth contains the most GST as compared with the frozen and spun broth. However it was noted that the fresh broth was the first sample to be assayed. The sample was re-assayed after completing all the other samples. The new GST concentration was lower (see check point) and appears to have dropped relative to the initial measurement.

The explanations for the results reported in sections 3.2 - 3.4 are discussed in the following section.

3.5 Discussion

Three culture media were evaluated for growth of *E. coli* and expression of GST. It was possible to reproducibly grow *E. coli* in each of the media. Nutrient broth produced the least *E. coli* and Terrific broth produced the most. However upon investigation of GST expression, it was found that in the case of Terrific broth GST was present at the point of induction with IPTG indicating that control of plasmid expression was difficult in Terrific broth. Due to this, Terrific broth was disregarded as a culture media and the High Cell Density media was chosen for further work as growth levels were high, coupled with good plasmid control and expression.

This media was then successfully and reproducibly scaled up to 5L working volume. The levels of *E. coli* increased 3 fold as compared to the shake flask (from a dry cell weight of 5mg/mL to 13mg/mL) as did the levels of GST (from 0.27mg/mL to 0.7mg/mL) when comparing using similar disruption strategies. This is to be expected as the oxygen transfer is vastly improved in a fermenter coupled with the ability to control pH.

Work was then carried out on the GST assay using the same sample source to investigate the effect of sample dilution and reaction time. It was found that over or under dilution of the sample led to inaccurately high or low GST concentrations respectively. To produce consistent results, it was necessary to dilute the sample such that the $A_{340\text{nm}}$ absorbance readings fell between 0.1-0.8AU, as per the assay guidelines. Once this criteria was met it was possible to consider the effect of reaction time on the assay output.

The assay guidelines suggest a reaction time of 5mins, however decreasing this reaction time to 1min leads to a difference in GST

concentration of only -2%. Considering that the assay is accurate to within $\pm 5\%$, it was decided that the reaction time could be safely reduced to 1 min for all future work provided the $A_{340\text{nm}}$ absorbance readings fell between 0.1-0.8AU.

Despite assays having been carried out as per the assay guidelines it was observed that samples from the 5L working volume fermenter that had been sonicated for 1min had GST levels of 0.7mg/mL compared with samples that had been sonicated for 10mins that had GST levels of 1.5mg/mL. This would indicate that maximum GST release was not achieved in 1min of sonication. To verify this, samples were disrupted in a high pressure homogeniser to investigate the GST release kinetics. Various harvest and storage conditions were also investigated at this point to determine their impact on cell strength and consequently their effect on GST release.

Results demonstrated that the highest measured GST release is achieved after 5 passes at 500bar for all harvest and storage conditions investigated. It would appear on initial inspection that the broth which was homogenised immediately after fermentation released the most GST, however this sample was re-assayed once all other assays were complete. It was found at this point that the level of GST in this sample had dropped from 2.2mg/mL to 1.5mg/mL, putting it in line with the other samples. Fresh assay mix was used in the first sample and hour old assay mix was used for the check result. This implies that the assay mix degrades over time, most likely due to the reaction of glutathione with CDNB in the absence of GST that forms a chemical moiety that absorbs at 340nm. All subsequent measurements in this thesis were based upon fresh assay mix.

3.6 Conclusions

Conclusions that may be drawn from this work are that *E. coli* can be reproducibly grown to a dry cell weight of 13mg/mL and GST produced to a concentration of 1.5mg/mL in a 5L working volume fermentation employing High Cell Density media.

The highest measured GST release is achieved by 10mins sonication or 5 passes at 500bar in a homogeniser. Harvest and storage conditions do not have an impact on the apparent cell strength and hence GST release indicating that frozen cell paste can be used as the basis for downstream processing studies. This is a key result as it enables a break point to be established between culture and subsequent processing studies.

GST can be reproducibly detected to within $\pm 5\%$ using the GST assay and a reaction time of 1 min providing the assay mix is fresh and absorbance readings at 340nm fall within 0.1-0.8AU.

The work carried out in this chapter provides the basis for an analysis of the effect of expanded bed adsorption operating parameters and matrix properties on the purification of GST from *E. coli* (detailed in Chapter 5) as compared to those when investigating the purification of alcohol dehydrogenase from Yeast homogenate, in Chapter 4. This GST/*E. coli* system will also be employed when studying prototype expanded bed matrices, in Chapters 6 and 7.

4 THE EFFECT OF MATRIX PARTICLE SIZE DISTRIBUTION AND OPERATING VELOCITY ON THE PURIFICATION OF ALCOHOL DEHYDROGENASE FROM YEAST

4.1 Introduction

In the study of expanded beds, little consideration has been given to the impact of having matrix particles of different sizes present within an expanded bed adsorption (EBA) column during product breakthrough. Previously Willoughby *et al.*, 2000(a), 2000(b), Bruce and Chase, 2002, 2001, 1999 and Chase *et al.*, 1999 studied various aspects of expanded bed behaviour and in particular used in-bed sampling and on-line monitoring to consider the breakthrough of products and contaminants along the axis of the bed. Of particular interest was the observation (Willoughby *et al.*, 2000(b)) that the largest particles (those that remained in the bottom third of the bed during expansion) were seen to provide over 60% of the binding capacity of the column in a typical 10% product breakthrough loading strategy.

Karau *et al.*, 1997 demonstrated with a single component system that small matrix particles had an enlarged breakthrough capacity as compared with large particles and it was speculated that smaller particles may lead to mass transfer limitations upon expansion due to the increased bed voidage, especially when applying viscous feedstocks such as yeast homogenates.

Breakthrough curves at the column outlet of expanded beds are typically much shallower than those observed in traditional packed bed chromatography (Smith *et al.*, 2002) and a possible explanation for this is that the utilisation of the matrix is a function of particle size distribution

(PSD). By contrast in a packed bed there is no significant particle size gradient along the axis and hence the bed capacity is constant in the axial direction.

The variation in binding potential along the expanded bed axis implies that a better bed productivity might be gained via an improved understanding of these effects. This and the next chapter set out to gain such knowledge of the effects of matrix PSD utilising the smallest and largest particles available from within a typical EBA matrix and operating flowrate on the breakthrough behaviour observed in an EBA column. This chapter will consider the purification of alcohol dehydrogenase (ADH) from Yeast homogenate via hydrophobic interaction chromatography (HIC) and the productivity implications of the results will be discussed in Chapter 8.

4.2 Matrix Segregation and Characterisation

STREAMLINE Phenyl matrix was elutriated as described in 2.4.1.3 and the particle size ranges of these samples were measured as described in 2.6.8 to confirm that the elutriation successfully separated the original bed into three segregated beds (termed "*smallest*", "*medium*" and "*largest*") each internally consistent in terms of size but with dissimilar particle size distributions (PSD's). A graph of decumulative PSD is shown in Figure 4.1. Table 4.1 contains the number diameter statistics d_{10} , d_{50} and d_{90} defined in 2.6.8 demonstrating the variation in particle size distributions for the different segregated beds.

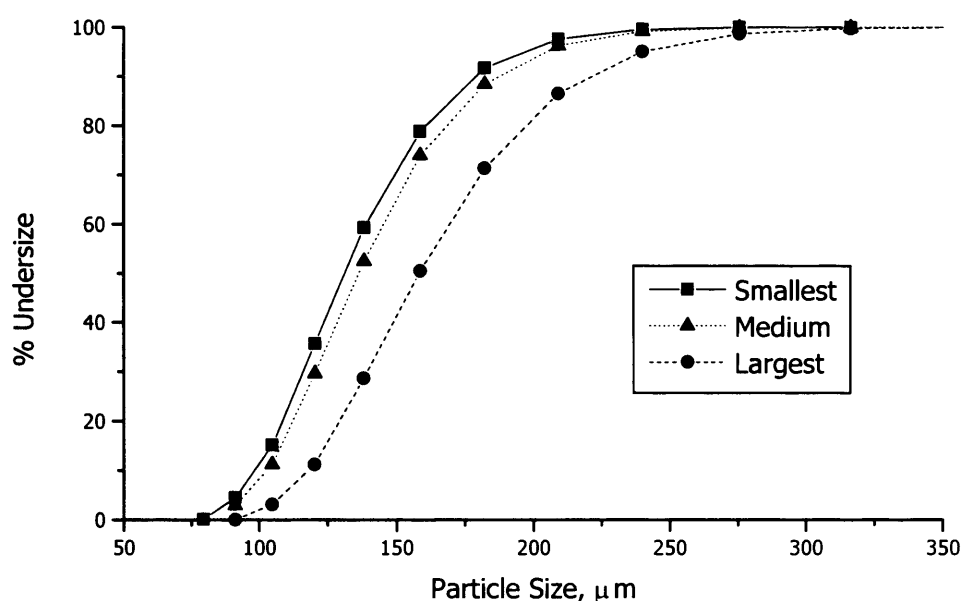


Figure 4.1: Decumulative particle size distribution measurements on a number basis for different sections of segregated STREAMLINE Phenyl matrix.

	d_{10} , μm	d_{50} , μm	d_{90} , μm
Smallest	114	150	204
Medium	119	156	214
Largest	136	181	251

Table 4.1: Particle size range variations as shown by d_{10} , d_{50} and d_{90} measurements on a number basis for different sections of segregated STREAMLINE Phenyl matrix.

The segregated beds were further characterised by calculation of the number of particles in 1mL of matrix for each of the beds, based on the methods in 2.6.9. The total binding capacity (based on the methods in 2.6.10) of ADH in g/L when applying yeast homogenate prepared as described in 2.3.1.1 was also determined. These results are summarised in

Table 4.2 for the largest and smallest particles only, as these provided the widest extremes of particle size.

	Total Binding Capacity (grams of ADH per L matrix)	Number of particles (N_p) per mL of settled matrix
Largest	1.94	209,837
Smallest	3.89	336,005

Table 4.2: Characterisation of segregated STREAMLINE Phenyl detailing the total binding capacity for ADH when applied at a concentration of 100U/mL and the number of matrix particles per mL of settled matrix.

4.3 Velocity and Particle Size Effects on Breakthrough

Purification of ADH from Yeast homogenate prepared as described in 2.3.1.1 was carried out according to the methods in 2.4.1.2 for expanded bed chromatography and 2.5 for packed bed chromatography, using the buffer system described in 2.3.1.2. The STREAMLINE Phenyl segregated beds consisting of the smallest and largest particles were used in order to enable the effect of particle size to be determined. These sections were chosen as they contained the widest extremes of particle size. 200mL of matrix was used in the STREAMLINE 50 column described in 2.4.1.1 as this corresponded to a settled bed height of 10cm, the minimum height recommended for this column to achieve stable expansion (Hjorth *et al.*, 1995); 20mL of matrix was used in the XK16 columns, equivalent to 10cm bed height.

In order to investigate the effect of load velocity on the recovery and breakthrough characteristics of ADH, experiments were carried out on these segregated beds at flowrates of 100 and 300 cm/hr in both packed and expanded modes of operation.

The breakthrough curves for the expanded and packed bed runs are shown plotted in Figures 4.2 and 4.3, with Figure 4.2 demonstrating the effect of flowrate on a segregated bed of the largest particles in both a packed (4.2a) and an expanded bed (4.2b) and Figure 4.3 demonstrating the effect of particle size at various velocities in both packed (4.3a) and expanded beds (4.3b and c). As the velocity was varied, Figure 4.2 is plotted on a volume loaded basis for ease of comparison. Figure 4.3 is plotted against time.

Figure 4.2: The effect of linear liquid velocity (100 and 300 cm/hr) on the breakthrough of ADH loaded onto a segregated bed of STREAMLINE Phenyl consisting of the largest matrix particles in a) packed and b) expanded beds.

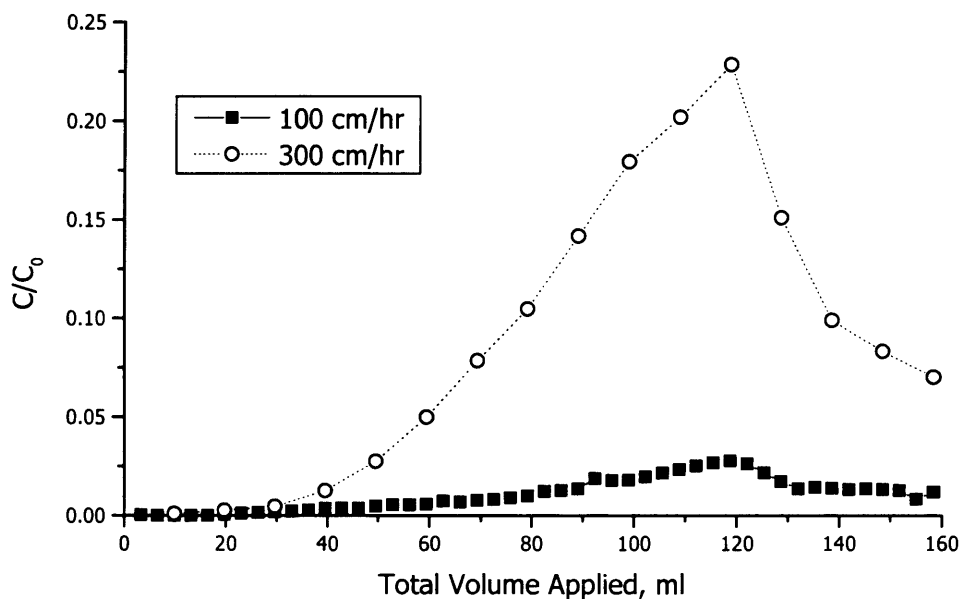


Figure 4.2a: Largest particles in a packed bed compared at 100 and 300 cm/hr.

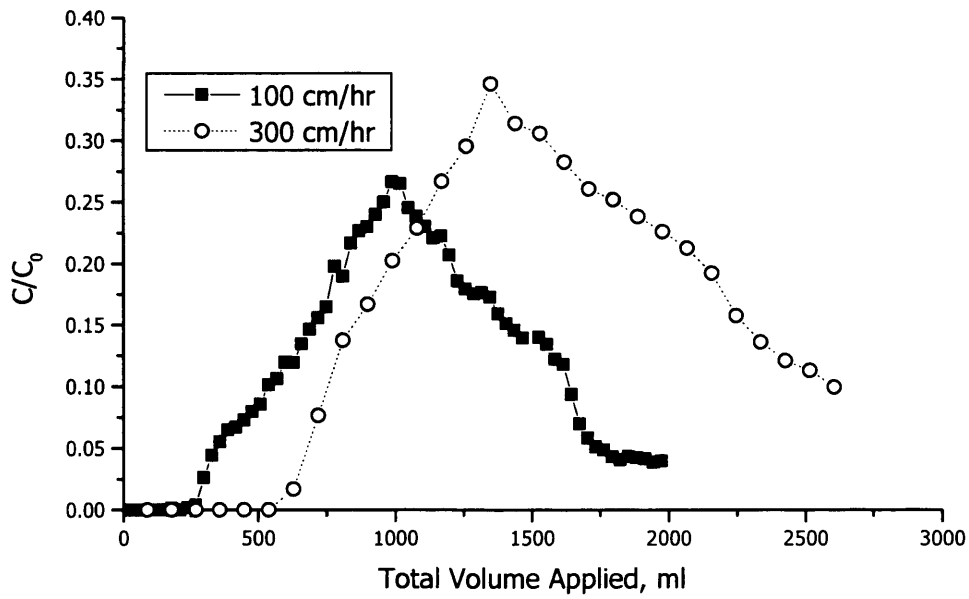


Figure 4.2b: Largest particles in an expanded bed compared at 100 and 300 cm/hr.

Figure 4.3: The effect of particle size on the breakthrough of ADH loaded onto packed and expanded beds at constant linear liquid velocity.

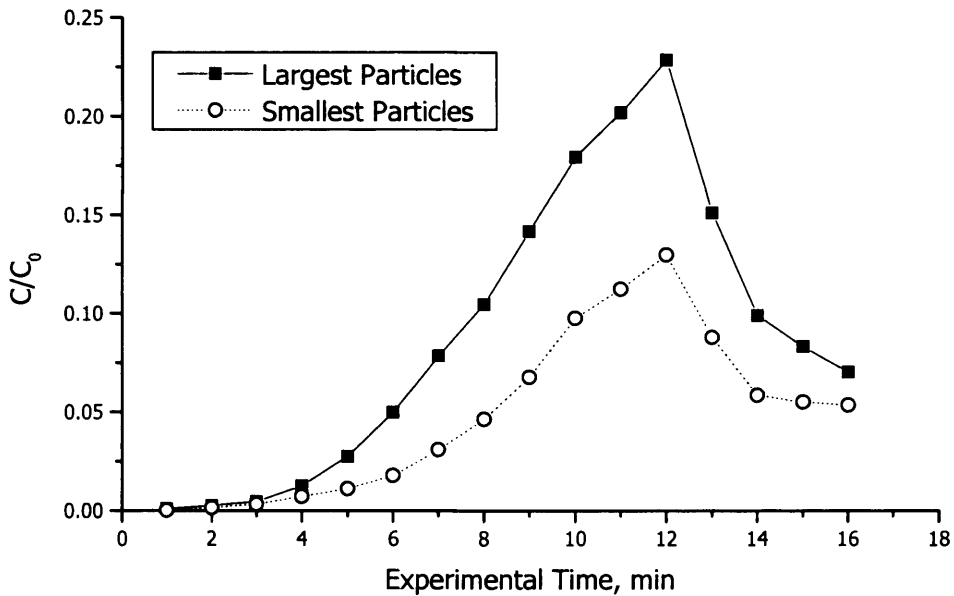


Figure 4.3a: Smallest and Largest particles in a packed bed compared at 300cm/hr.

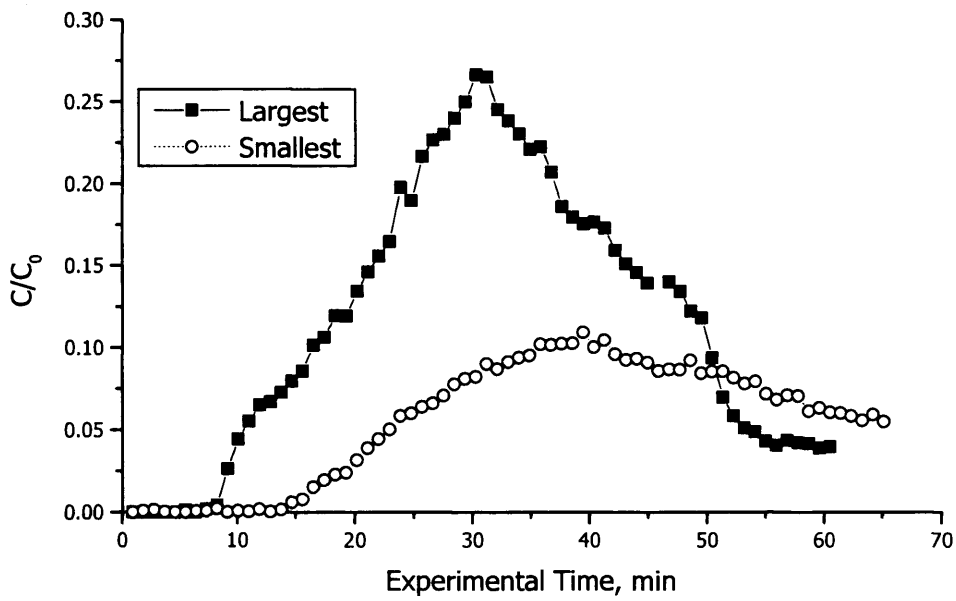


Figure 4.3b: Smallest and Largest particles in an expanded bed at 100cm/hr.

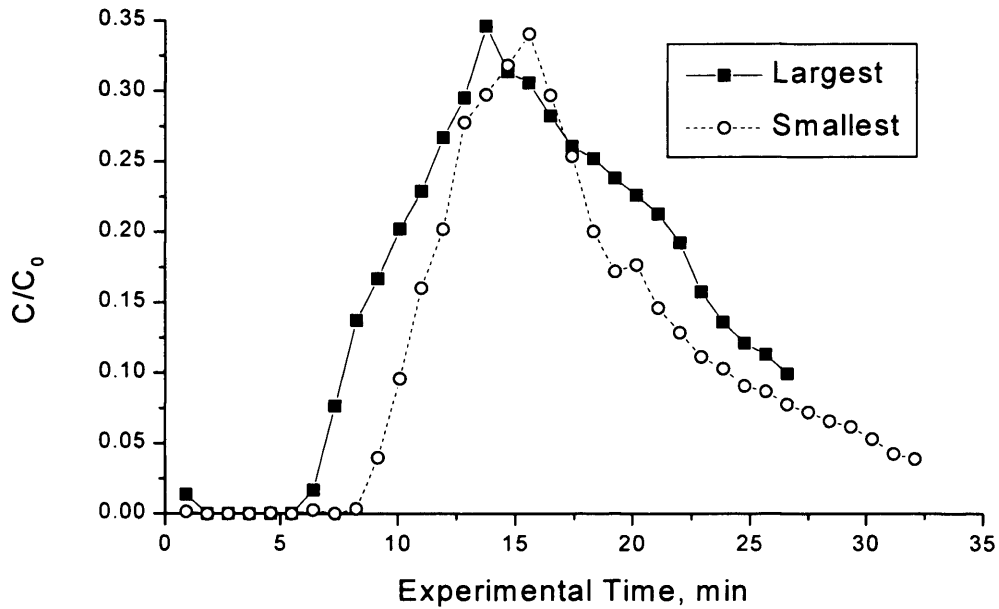


Figure 4.3c: Smallest and Largest particles in an expanded bed at 300cm/hr.

4.4 Impact of Residence Time on Breakthrough Profiles

For each expanded bed set-up (i.e. small and large particles; 100cm/hr and 300cm/hr) RTD tests were carried out as described in 2.6.7.2 using 0.5g/L Blue Dextran as tracer molecule. The results are summarised in Table 4.3, giving details of the residence times due to tubing and that due to the extra degree of expansion while processing the homogenate. The number of theoretical plates (NTP) values are also presented. The results were also used to calculate t/t_R where t is the experimental time (secs) and t_R is calculated as described in 2.6.7.2. This was used in the breakthrough curves analysis at varying fluid velocities and PSD, shown in Figure 4.4.

Residence Time (sec)	Large Particles		Small Particles	
	100cm/hr	300cm/hr	100cm/hr	300cm/hr
$t_{Rsystem}$	579	282	663	338
$t_{Rtubing}$	202	68	202	68
$t_{Rheight}$	108	120	198	144
t_R	485	334	659	414
NTP	19.8	13.7	26.1	15.8

Table 4.3: Variation in residence time (sec) with bed arrangement.

4.5 Discussion

The objective of this work was to consider the effects on expanded bed performance of changes in the size distribution of matrix particles and the loading velocity. Elutriation of the original bed yielded 2 beds for study each containing quite different PSD's. The size difference between the elutriated particle samples is illustrated in Figure 4.1 and quantified in

Table 4.1. On a number basis the mean size of the smallest particles was 150 μm compared to 181 μm for the largest particles.

Table 4.2 summarises the main characteristics of the segregated beds. The total binding capacity was found to be almost double for the smaller particles compared with the larger particles, suggesting that the binding with ADH is predominantly external bead surface area binding (or the spherical surface area of the bead), as the smaller particles have a higher specific surface area than the large particles. The number of particles per mL of settled bed matrix was found to be higher for the smaller particles than the larger particles as would be expected, as a small particle, based on their average diameter of 150 μm , would individually take up less space than a large particle of 181 μm .

The number of theoretical plates was measured in each expanded bed at the three different linear velocities used for breakthrough and as expected, the number of plates decreased with both increasing particle size and increasing linear liquid velocity. This can be seen in Table 4.3. These results show that at the higher velocities the reduction in number of theoretical plates relates to a corresponding increase in axial dispersion in the bed. This might be expected to produce an earlier point of initial breakthrough coupled with a shallower profile for the higher velocities but, as can be seen in Figure 4.2, this effect does not seem to be significant. Differences in theoretical plate numbers between the largest and smallest particles at the same linear velocity are not large enough (<25% in all cases) to be significant when compared with the reproducibility of the measurement ($\pm 20\%$).

Figure 4.2 illustrates the effect of velocity on binding behaviour of a segregated matrix in both packed beds and expanded beds. As the velocity was varied for each experiment, the breakthrough curves are plotted against total volume loaded for ease of comparison. This is the conventional form of data presentation for both expanded and packed

bed chromatography. From the breakthrough curves in the packed bed (Fig 4.2a), it is clear that increasing liquid velocity increases the rate of product breakthrough for particles of comparable size. This is to be expected and is a reflection of the mass transfer limitations experienced at higher velocities coupled with the reduction in contact time. Comparing this with Figure 4.2b in an expanded bed, whilst higher overall levels of breakthrough are achieved at a higher velocity, consistent with the packed bed data, the curves show that the breakthrough occurs earlier at the lower velocity. This is not the case in the packed bed. The difference in expanded bed behaviour is due to the extra degree of expansion that occurs at higher velocities in expanded beds.

Figure 4.3 illustrates the effect of particle size on breakthrough behaviour. Product breakthrough in the packed bed at 300 cm/hr is more rapid and reaches higher levels with the larger particles compared to smaller particles at the same velocity (shown in Fig 4.3a). This is to be expected as the higher specific surface area of the smaller particles leads to a higher capacity for product per unit volume of matrix. This is particularly true of ADH, a relatively large protein (~140 kDa) such that penetration of the matrix bead interior will be slowed by its size. Relatively limited penetration of matrix beads during loading has been illustrated using confocal microscopy of matrix beads (Linden *et al.*, 1999) meaning that substantially only the matrix surface area is utilised for binding. This is confirmed by the total binding capacity experiments where it was found that the smaller particles had a total binding capacity double that of the large particles and would thus be expected to exhibit a later and shallower product breakthrough.

As the binding of ADH is mainly on the matrix surface the tracer molecule for the RTD tests was chosen to reflect this. Blue Dextran 2000 has a very high molecular weight and thus does not penetrate the interior of the matrix particles, hence only passing through the voids between the

particles (Willoughby *et al.*, 2000(a)). This marker was therefore also used when determining the number of particles since it can be used to provide a measure of the excluded column volume i.e. the interstitial voidage.

If we compare Figure 4.3b to Figure 4.3a, effects noticed in the packed beds in 4.3a due to the particle size are also noticed in the expanded bed at low velocities (100 cm/hr), shown in Figure 4.3b. However, despite there being an obvious difference in the shape of the breakthrough curves between the small and large particles at low velocities, when running at higher velocities (300 cm/hr) breakthrough profiles are almost identical, with the small particles breakthrough shifted only slightly later in time than the larger particles (Figure 4.3c). This shift in time is due to the smaller particles expanding to a greater extent than the larger particles and thus, on a straight time or volumetric basis, the product breakthrough will be further retarded by the longer residence time of the bed.

The change in bed residence time as a function of matrix size and operating velocity makes direct comparison of product breakthrough characteristics in expanded beds of different diameter particles difficult. The standard approach of using time or volume to plot product breakthrough does not allow for the increase in residence time caused, for example, by the greater expansion of smaller particles relative to the larger size material. In order to compensate for this, a dimensionless residence time group was defined, t/t_R , where t is the experimental time and t_R is the residence time for the bed as defined by equation 2.4 in Chapter 2. This group takes into account differences in velocity and PSD as t_R is a measurement of the time taken for liquid to pass through the column, itself dependent on velocity, but also on the degree of expansion and hence voidage, which are functions of the PSD.

Re-plotting the data in Figures 4.2b, 4.3b and 4.3c now using the dimensionless ratio t/t_R as described earlier yields Figures 4.4 a - c

respectively (the packed bed data was not replotted since the residence time was constant due to the small volume of matrix used; 120 secs at 100 cm/hr and 39 secs at 300 cm/hr for the beds formed from both small and large particles). This figure demonstrates the difference in breakthrough curves obtained when running at different velocities and using different PSD's of matrix.

Analysing these new curves reveals that breakthrough curves remain similar in profile, but as expected the delay in breakthrough seen on a straight time or volume basis has been offset. The result is that breakthrough curves for the differently sized particles and at different liquid velocities can now be compared directly.

The effect of increasing velocity in limiting the mass transfer is still obvious when comparing similar segregated beds and in fact is easier to distinguish in an unambiguous fashion as the earlier breakthrough at the lower velocity seen in Figure 4.2b which is a product of the degree of expansion, has now been compensated for (Figure 4.4a).

The data also show that the effect of particle size is negated with increasing velocity in the expanded bed. At 100 cm/hr (Figure 4.4b) there is a noticeable delay in, and a lower overall rate of, breakthrough for the smaller particles when compared to the larger particles. This is consistent with the higher surface area of the smaller particles leading to a higher dynamic binding capacity.

Figure 4.4: Comparison of breakthrough rates of ADH in expanded beds of segregated matrix at various linear liquid velocities plotted against dimensionless experimental time (t/t_R).

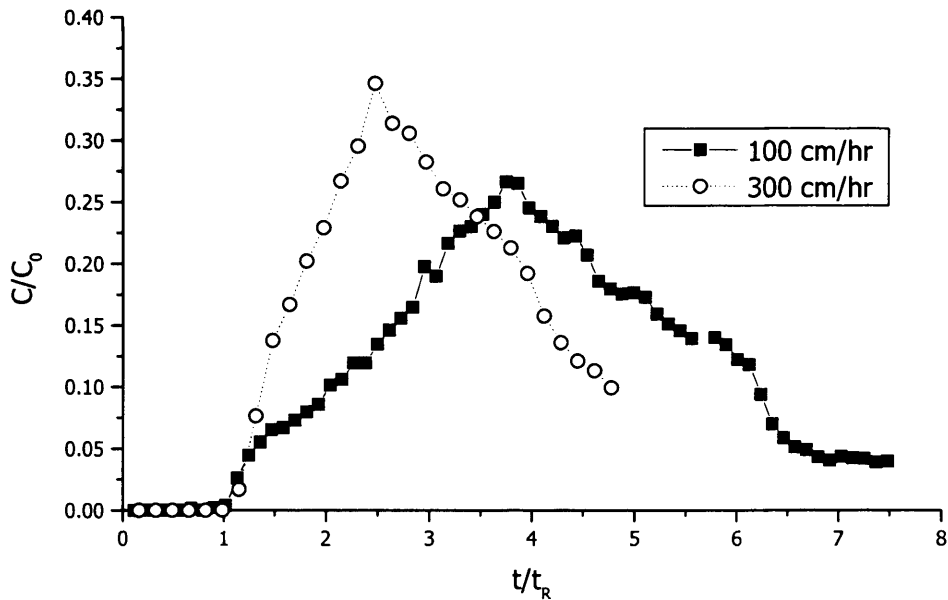


Figure 4.4a: Largest particles compared at 100 and 300 cm/hr.

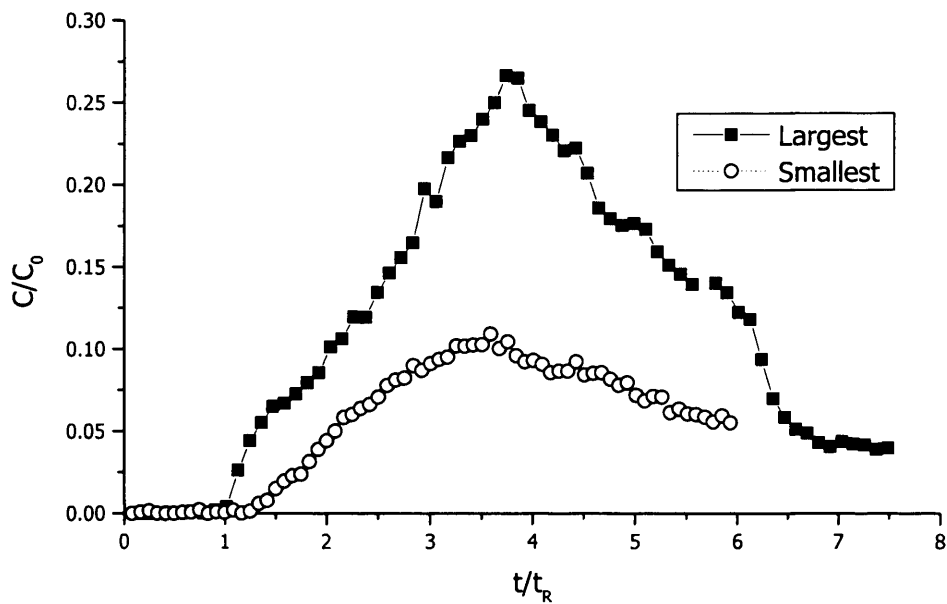


Figure 4.4b: Smallest and largest particles compared at 100 cm/hr.

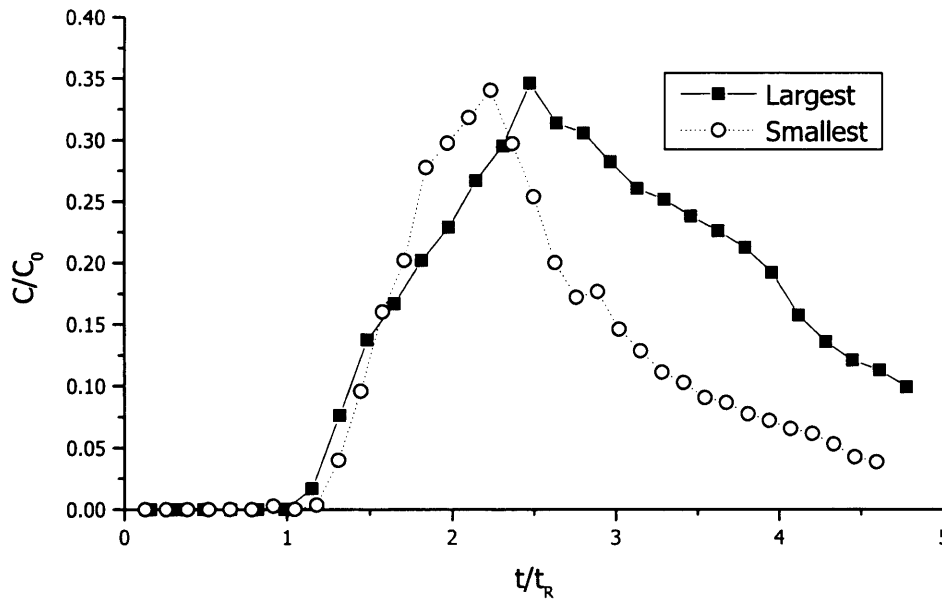


Figure 4.4c: Smallest and largest particles compared at 300 cm/hr.

We would expect this behaviour for the smaller particles to be maintained as the velocity is increased, as suggested by the packed bed results at 300 cm/hr (Figure 4.3a). However, this is not seen to be the case. At 300 cm/hr in the expanded bed (Figure 4.4c) there is no delay or difference in breakthrough for the smaller particles relative to the larger particles.

Taken together the results from these experiments would suggest that the binding at high velocities is limited by a factor other than surface area alone. Since the change in binding behaviour is more pronounced at higher velocities it seems likely that the effect of surface area is negated by the increased void volume achieved between small and large particles at high velocities (Willoughby *et al.*, 2000(a)) leading to a reduced frequency of particle/product collision and hence an observed fall off in the observed binding efficiency.

4.6 Conclusions

The work described here illustrates the variation in the adsorptive behaviour of expanded beds formed from differently sized particles. The use of a dimensionless residence (t/t_R) time allows for a direct comparison of breakthrough behaviour between such beds since it accounts for the changes in bed height due to variations in particle size and velocity. This approach has allowed us to demonstrate that, for the particular protein under study, the expected improved dynamic capacity of smaller beads is negated at velocities in excess of 100 cm/hr most probably by mass transfer limitations of the product binding to the matrix coupled with the effects of an increased void volume at higher velocities. With conventional time or volume based analysis such a conclusion would have been more difficult to infer.

Expanded beds are typically run at liquid velocities of up to 300 cm/hr. In the work presented here, use of t/t_R analysis has enabled us to show that for the particular protein examined where the kinetics of binding are relatively slow, the EBA performance is not optimal under conditions of high liquid velocities that are used for EBA operation. This necessity to run at significantly lower velocities would tend to negate some of the advantages of EBA in terms of reducing early downstream processing times and minimising the risk of product degrading over time.

Continuation of this work in Chapter 5 examines the effect of matrix PSD and operating velocity on the purification of a product not limited by its size to adsorbance by surface area binding. The use of a dimensionless experimental time in this situation will be also be discussed. The productivity implications for both of these biological systems will be considered in Chapter 8.

5 THE EFFECT OF MATRIX PARTICLE SIZE DISTRIBUTION AND OPERATING VELOCITY ON THE PURIFICATION OF GLUTATHIONE S-TRANSFERASE PRODUCED IN *E. COLI*

5.1 Introduction

In Chapter 4 it was stipulated that the productivity of an expanded bed column may be improved by careful selection of matrix particle size distribution. It was found for the system under investigation (ADH produced in Yeast and purified via HIC) where product binding was mainly limited to surface area binding, that at low velocities, the small matrix particles bound more product than the large matrix particles. However, when running at velocities in excess of 300cm/hr, this effect was negated due to mass transfer limitations. Due to the difficulty in comparing breakthrough behaviour in expanded beds at different velocities containing different matrices, the concept of a dimensionless experimental time was also introduced. This chapter seeks to extend this analysis to a different experimental system that is not limited by surface area binding.

The system under investigation will be the *E. coli*/GST system developed in Chapter 3 whereby the GST is purified via anion exchange chromatography (AIEX). Studies will investigate whether differences are observed in breakthrough between the small and large particles at both low and high velocities and will consider the applicability and utility of the dimensionless residence time in the analysis of such a system.

5.2 Matrix Segregation and Characterisation

STREAMLINE DEAE matrix was elutriated as described in 2.4.1.3 and the particle size ranges of the samples were measured as described in 2.6.8 to confirm that the elutriation successfully separated the original beds into three segregated beds each internally consistent but with dissimilar PSD's. The decumulative PSD graphs were extremely similar to those found with STREAMLINE Phenyl in Chapter 4 Figure 4.1 and so are not shown here. Instead, the number diameter statistics are summarised in Tabular form in Table 5.1 demonstrating the variation in particle size distributions for the different segregated beds of STREAMLINE DEAE.

	$d_{10}, \mu\text{m}$	$d_{50}, \mu\text{m}$	$d_{90}, \mu\text{m}$
Smallest	120	145	208
Medium	116	158	213
Largest	137	178	249

Table 5.1: Particle size range variations as shown by d_{10} , d_{50} and d_{90} measurements on a number basis for different sections of segregated STREAMLINE DEAE matrix.

As the PSD's were similar to that of the segregated STREAMLINE Phenyl, the number of particles was not recalculated. However in order to understand the kinetics of GST binding to STREAMLINE DEAE of varying PSD's, adsorption isotherms were produced for the smallest and largest particle size ranges. These were produced as described in 2.6.10 by challenging samples of matrix with *E. coli* homogenate prepared as described in 2.3.2.1 containing varying concentrations of GST. The adsorption isotherms are shown in Figure 5.1.

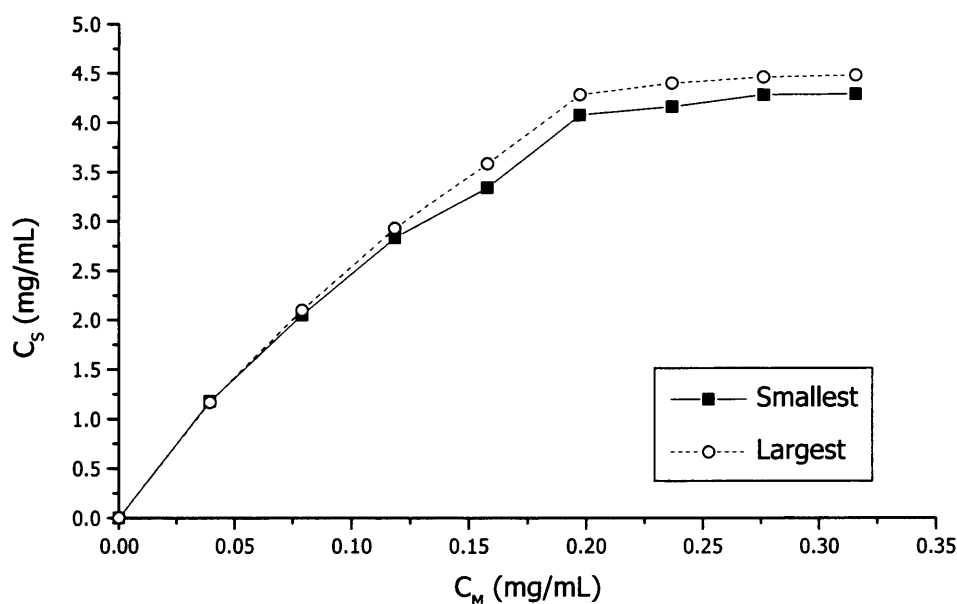


Figure 5.1: The adsorption isotherm for the binding of GST to segregated beds of STREAMLINE DEAE. C_M is the concentration of GST (mg/mL) in the applied sample and C_s is the amount of GST (mg) bound to the matrix (mL).

As can be seen in Figure 5.1, there is very little difference in binding between the segregated beds consisting of the largest and smallest particles.

5.3 Velocity and Particle Size Effects on Breakthrough

Expanded bed purification of GST from *E. coli* homogenate prepared as described in 2.3.2.1 was carried out according to the methods in 2.4.2.2 and the buffer system described in 2.3.2.2. This buffer system was based on the work carried out by Clemmitt and Chase (2002), however a step change in pH, used in conjunction with an increase in salt concentration and hence conductivity, was utilised in place of the salt gradients utilised by Clemmitt and Chase. This was in order to elute the maximum amount of GST and to mimic large industrial processes.

In each case, the STREAMLINE DEAE was challenged with 1000mL disrupted *E. coli* containing 0.3mg/mL GST. The segregated beds

consisting of the smallest and largest particles were used in order to consider the effect of particle size. These sections were chosen as they contained the widest extremes of particle size. 50mL of matrix was used in the STREAMLINE 25 column described in 2.4.2.1 as this corresponded to a settled bed height of 10cm, the settled bed height utilised in the Yeast/ADH system in Chapter 4.

In order to investigate the effect of load velocity on the recovery and breakthrough characteristics of GST, experiments were carried out on these segregated beds at velocities of 100 and 300 cm/hr.

The breakthrough curves for the expanded bed runs are shown plotted in Figures 5.2 and 5.3, with Figure 5.2 demonstrating the effect of velocity on a segregated bed of the largest particles (5.2a) and smallest particles (5.2b) and Figure 5.3 demonstrating the effect of particle size at 100 and 300 cm/hr (5.3 a and b respectively).

Figure 5.2: The effect of linear liquid velocity (100 and 300 cm/hr) on the breakthrough of GST loaded onto a segregated bed of STREAMLINE DEAE consisting of the a) largest matrix particles and b) smallest matrix particles.

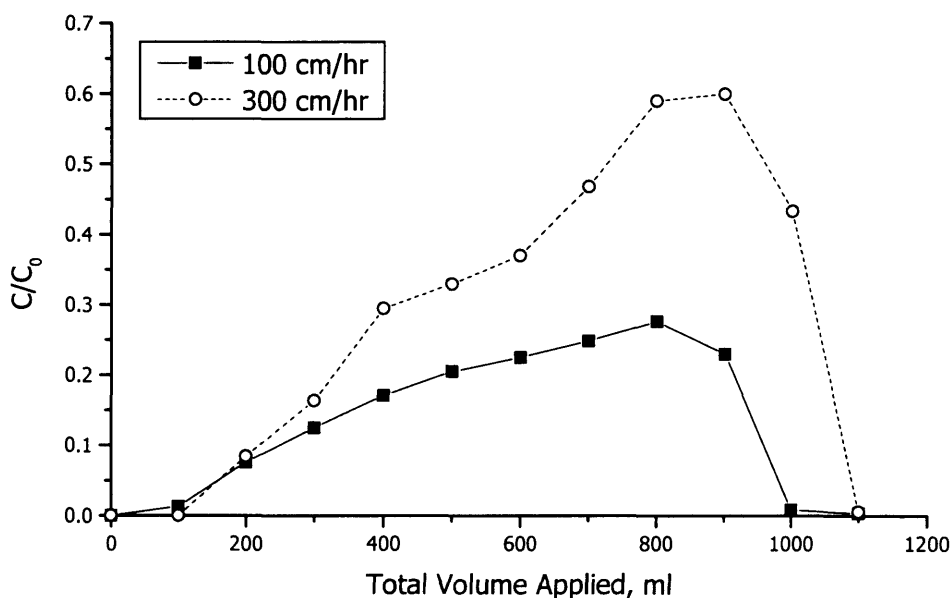


Figure 5.2a: Largest particles in an expanded bed compared at 100 and 300 cm/hr.

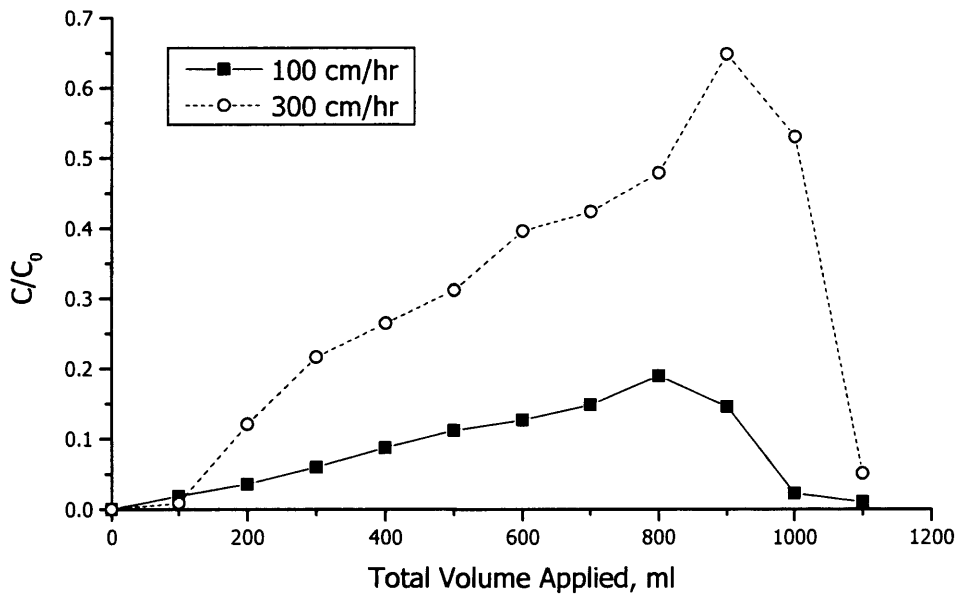


Figure 5.2b: Smallest particles in an expanded bed compared at 100 and 300 cm/hr.

Figure 5.3: The effect of particle size on the breakthrough of GST loaded onto expanded beds at constant linear liquid velocity.

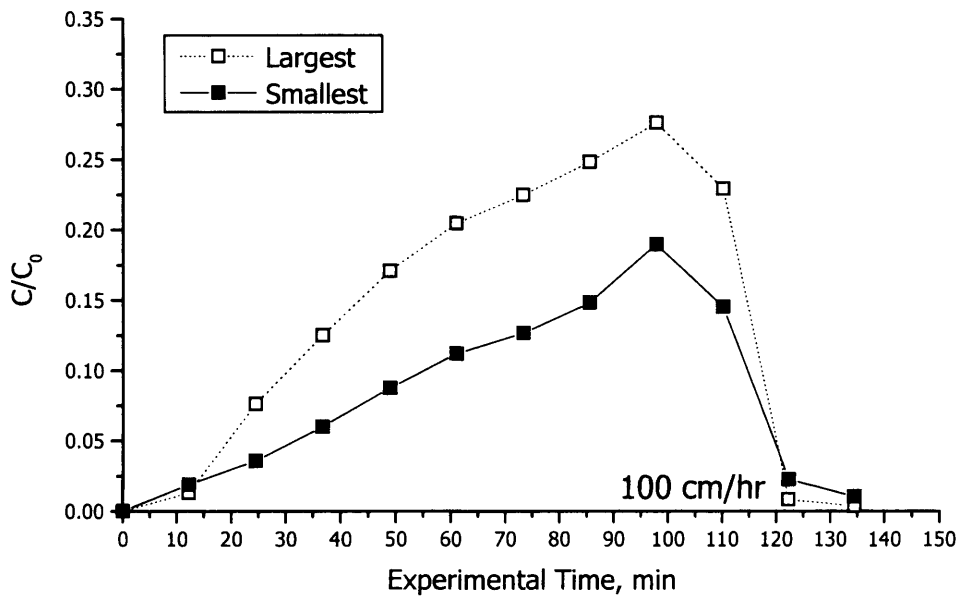


Figure 5.3a: Smallest and Largest particles in an expanded bed compared at 100cm/hr.

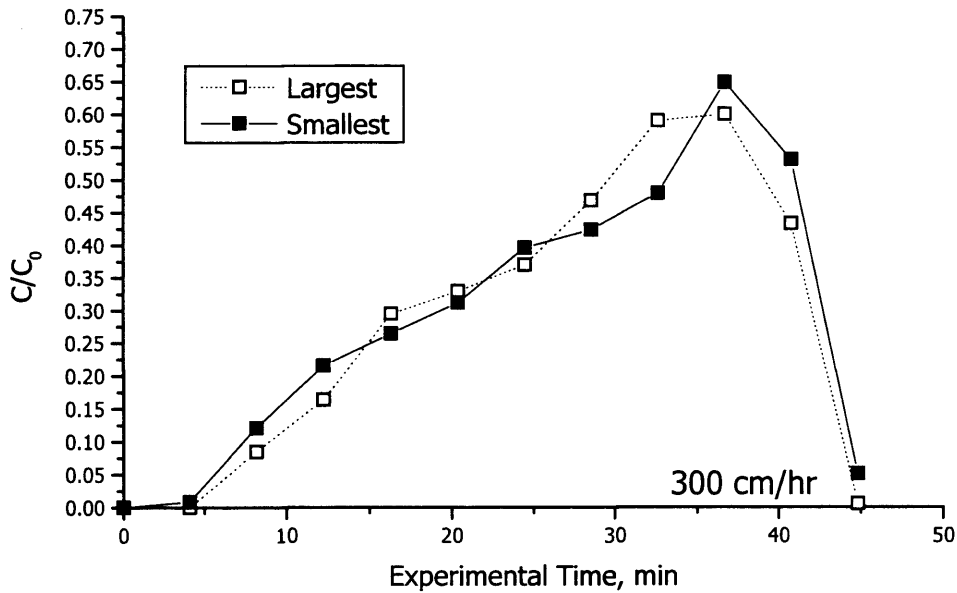


Figure 5.3b: Smallest and Largest particles in an expanded bed compared at 300cm/hr.

5.4 Impact of Residence Time

For each expanded bed set-up (i.e. small and large particles; 100 cm/hr and 300cm/hr) the RTD tests were carried out as described in 2.6.7.2 using 0.25% v/v acetone as tracer molecule. The results are summarised in Table 5.2, giving details of the residence time due to tubing and that due to the extra degree of expansion while processing the homogenate.

Residence Time (sec)	Largest Particles		Smallest Particles	
	100cm/hr	300cm/hr	100cm/hr	300cm/hr
$t_{Rsystem}$	640	345	618	326
$t_{Rtubing}$	219	73	219	73
$t_{Rheight}$	162	72	216	132
t_R	583	344	615	385

Table 5.2: Variation in residence time (sec) with bed arrangement.

The values obtained for t_R were then used to calculate t/t_R where t is the experimental time (secs) for the analysis of breakthrough curves at varying fluid velocities and PSD, shown in Figure 5.4.

5.5 Discussion

The objective of this chapter was to consider the effects on expanded bed performance of changes in the size distribution of matrix particles and the loading velocity using a system where adsorbance of the target molecule was not limited by its size to surface area binding as in Chapter 4. The matrix under study was elutriated into 2 beds for further study each containing different PSD's. The size difference between the elutriated particles is quantified in Table 5.1. As can be seen in this table, the number diameter statistics for the beds are very similar to those obtained in Chapter 4. This is to be expected as both of the adsorbents under study consisted of the same base matrix; the only difference between them were the ligands to which they were coupled i.e. Phenyl and DEAE.

The adsorption isotherms for the segregated beds consisting of the smallest and largest particles can be seen in Figure 5.1. As this Figure clearly illustrates, there is very little difference in the binding potential between the smallest and the largest particles. In fact, the large particles have a slightly higher binding capacity than the small particles when challenged with higher concentrations of GST. This is most likely due to a larger volume of matrix available for binding within the large particles compared with the small particles. This confirms that GST is not limited by surface area binding, as was the case with ADH where the smallest particles bound almost double the quantity of ADH compared with the large particles. Due to the ability of GST to bind to the full volume of the matrix rather than just the surface, a penetrative tracer molecule was chosen to perform the residence time distribution tests. In this case, acetone was selected.

Figure 5.2 illustrates the effect of velocity on binding behaviour of the segregated matrices. As the velocity was varied for each experiment, the breakthrough curves are plotted against total applied volume for ease of comparison. As can be seen, the behaviour follows similar patterns for both the small and large particles in that a higher overall breakthrough is achieved at the higher velocities due to mass transfer limitations and it occurs earlier at the lower velocities in both cases. This is consistent with the results obtained in Chapter 4, however the delay in breakthrough at the higher velocity is not as obvious as is the case for the results in Chapter 4. This is in part due to the larger intervals between data points obtained with the GST system.

Figure 5.3 illustrates the effect of particle size on breakthrough behaviour. Product breakthrough at the lower velocity is more rapid and reaches higher levels with the larger particles compared to the smaller particles at the same velocity (Figure 5.3a). However, despite there being a difference in behaviour at the low velocity, running at higher velocities (300cm/hr) leads to identical breakthrough profiles. There is no delay in breakthrough with small particles as observed with the yeast/ADH system in Chapter 4. This is discussed below.

If we now consider the impact of residence time on the observed breakthrough behaviours, and re-plot the data in Figures 5.3 (a & b) to yield Figures 5.4 (a & b) by application of the dimensionless time concept introduced in Chapter 4 (t/t_R), it is clear that the breakthrough curves in Figures 5.4 (a & b) shown below do not differ greatly from those in Figures 5.3 (a & b).

Figure 5.4: Comparison of breakthrough rate of GST in expanded beds of segregated matrix at various linear liquid velocity plotted against dimensionless experimental time.

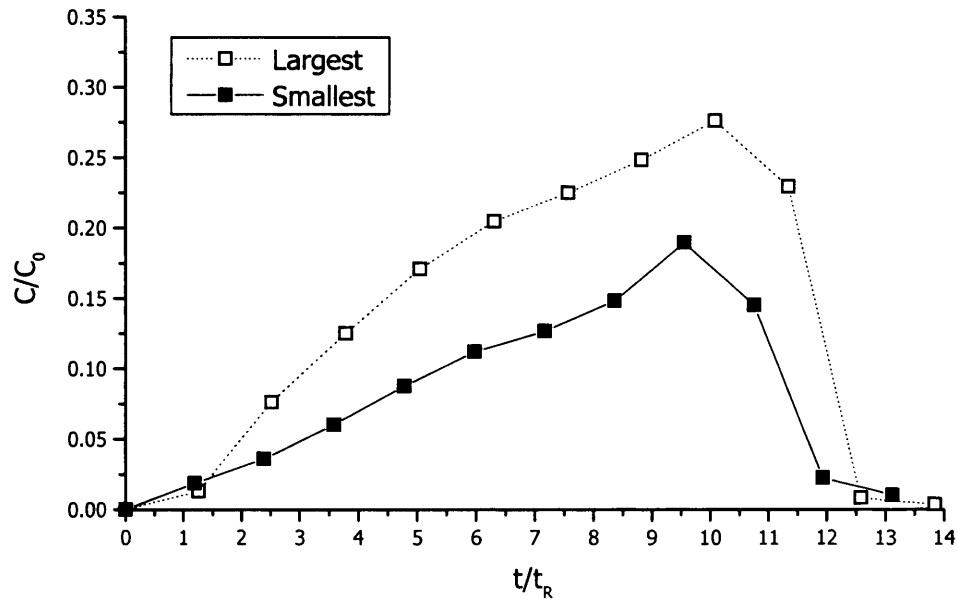


Figure 5.4a: Smallest and largest particles compared at 100cm/hr.

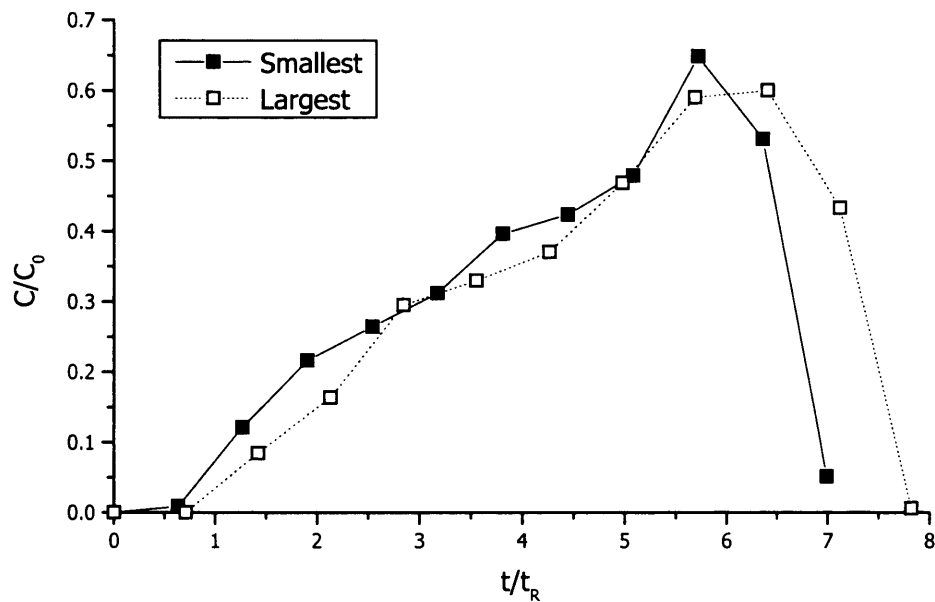


Figure 5.4b: Smallest and largest particles compared at 300cm/hr.

This is due to the similarity in residence time at the same linear liquid velocity between the PSD's, quantified in Table 5.2 (583 and 615 secs at 100cm/hr for the largest and smallest particles respectively and 344 and 385 secs at 300cm/hr for the largest and smallest particles respectively). In addition the binding behaviour of GST is not limited to surface area binding, as was the case with ADH, but can utilise the full volume of the matrix. Hence the larger particles have a higher capacity available for binding. This is confirmed by the GST isotherms as the larger particles bound more GST than the small particles.

The higher capacity observed in the large particles is then effectively negated in an expanded bed by the extra degree of expansion obtained with the small particles. This leads to similar residence times for the small and large particles when comparing at the same linear liquid velocity. This similarity in residence time can then account for the lack of delay in breakthrough mentioned above.

If we now analyse the curves in Figure 5.4 similar conclusions can then still be drawn. At low velocities, the small particles perform slightly better than the large particles due to the slight increase in residence time that this system offers (30 secs more). However, at high velocities, whilst this difference in residence time still exists between the small and large particles, it offers no obvious advantage in terms of product binding. This is due to the binding at high velocities being affected by factors other than the residence time. As in Chapter 4, this is most likely due to the increased void volume observed between the small and large particles coupled with mass transfer limitations at this higher velocity.

Normalisation of breakthrough curves by t/t_R for this system is not as obviously beneficial as when applied to the yeast/ADH system as the overall conclusions reached are the same without its application. However the use of residence time is still useful as it provides a deeper understanding of the differences observed in binding - for example the

difference in performance between the small and large particle at low velocities can be attributed to the increased residence time observed with the small particles upon expansion.

5.6 Conclusions

The work presented in this chapter illustrates that at low operating velocities small matrix particles offer an advantage in terms of product binding due to the increased residence time observed in these beds as compared to those consisting of only the large matrix particles. This is despite the large particles having a higher capacity for the product due to their larger volume available for binding.

When operating at higher liquid velocities, no advantage is offered when using the small matrix particles. This is due to the relatively large increase in the void volume in the small particle system coupled with mass transfer limitations. Given that expanded beds are generally run between 200-300cm/hr, no significant benefit would be offered through careful selection of the matrix particle size distribution in the case of GST which is a relatively small and hence mobile molecule.

The overall conclusions reached in this chapter are in agreement with those results in Chapter 4 even for products subject to different binding kinetics. Whilst it was possible to reach these conclusions without the use of a dimensionless time as introduced in Chapter 4, this is still a worthwhile measurement as it allows a deeper understanding of the results obtained.

The following chapters utilise the GST system from this chapter to investigate the effect of feed conductivity on expanded bed adsorption. Chapter 6 examines various prototype ligands for use in the conductivity studies, and Chapter 7 compares the performance of the selected prototype ligand with that of the more standard AIEX ligand, DEAE.

Chapter 8 then considers the productivity implications of the work carried out in these chapters.

6 PROTOTYPE HIGH SALT TOLERANT ANION EXCHANGE LIGAND EVALUATION

6.1 Introduction

Expanded beds have been successfully utilised to recover proteins directly from crude feedstocks. In many situations, affinity ligands are employed due to their specificity for the target molecule, however they can be a complex and expensive solution. Alternatives such as ion exchange provide less selectivity but offer cost advantages. Problems arise with these adsorbents due to their inability to perform well under conditions of high conductivity typical of many fermentation broths.

As expanded beds are used early on in downstream processing, feed volumes are already at their maximum. The need to dilute further these feeds to reduce ionic strength leads to high buffer consumption and long processing times.

In order to minimise the need to dilute, Amersham Biosciences have developed prototype ion exchange ligands that can operate at high ionic strengths. Three of these prototype anion exchange ligands will be considered in this chapter for their use in protein purification.

The ligands will be compared for their binding of BSA from a buffer solution and GST from the *E. coli* system developed in Chapters 3 and 5 at high and low salt conditions and one will be chosen for further comparison studies with DEAE in Chapter 7.

6.2 Adsorbent Characteristics

Three high salt tolerant anion exchange ligands were evaluated for their binding capacity for both Bovine Serum Albumin (BSA) and Glutathione S-Transferase (GST). The structure of the multi-modal ligands is detailed in Figure 6.1 below.

6.3 Purification of Bovine Serum Albumin

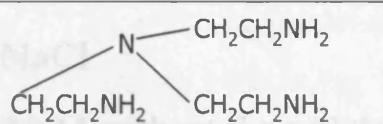
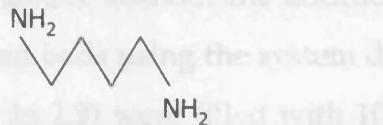
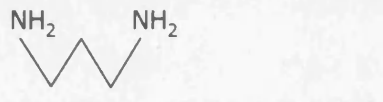
Tris (2-aminoethyl) amine (Tris)	
1,4-diaminobutane (DAB)	
1,3-diaminopropane (DAP)	

Figure 6.1: The chemical structures of the three prototype high salt tolerant anion exchange ligands.

The ligands were each attached to the newly developed high density STREAMLINE Direct adsorbent beads. These are cross-linked agarose beads modified by the inclusion of an inert stainless steel core material to provide a high density allowing for high flow velocities up to 900cm/hr. They are spherical with a particle size range of 80 to 165 μ m and a mean particle size and density of 135 μ m and 1.8g/mL respectively. A typical bead is shown in Figure 6.2.

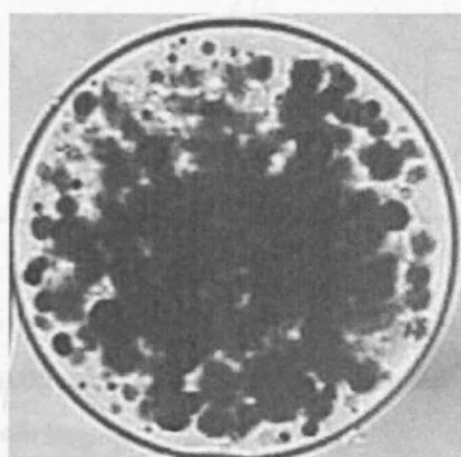


Figure 6.2: The structure of a typical STREAMLINE Direct matrix bead (actual size is 130 μ m). The dark matter is the stainless steel core material utilised to densify the matrix allowing for high velocities.

6.3 Purification of Bovine Serum Albumin

6.3.1 Without the addition of NaCl

BSA was prepared as described in 2.3.3.1 without the addition of NaCl. Purification was carried out in packed beds using the system described in 2.3.3.2. The packed beds (described in 2.5) were filled with 10mL matrix corresponding to a 5cm bed height.

Feed was applied at a velocity of 100cm/hr until 90% breakthrough was reached at which the point the bed was washed and then the BSA was eluted. Breakthrough curves for the three ligands are shown in Figure 6.3. The total BSA in the elution fraction for the three ligands is quantified in Table 6.1.

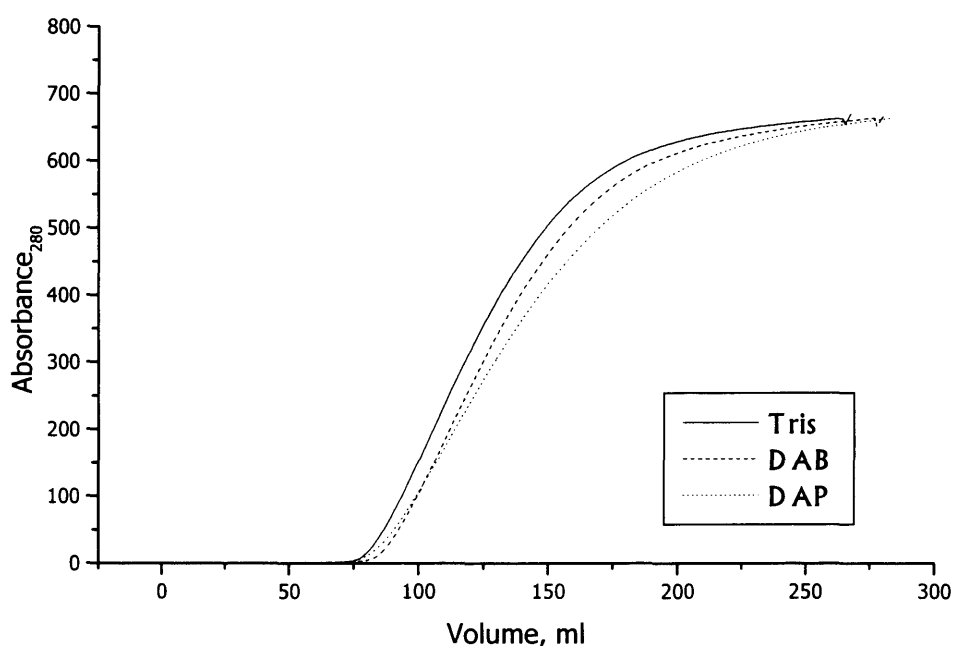


Figure 6.3: The breakthrough of BSA in 10mL packed beds loaded onto three prototype high salt tolerant ligands.

6.3.2 With the addition of NaCl

BSA was prepared as described in 2.3.3.1 with the addition of 0.25M NaCl. Purification was carried out in packed beds using the system described in 2.3.3.2. The packed beds (described in 2.5) were filled with 10mL matrix corresponding to a 5cm bed height.

Feed was applied at a velocity of 100cm/hr until 90% breakthrough was reached at which the point the bed was washed and then the BSA was eluted. Breakthrough curves for the three ligands are shown in Figure 6.4. The total BSA in the elution fraction for the three ligands is quantified in Table 6.1.

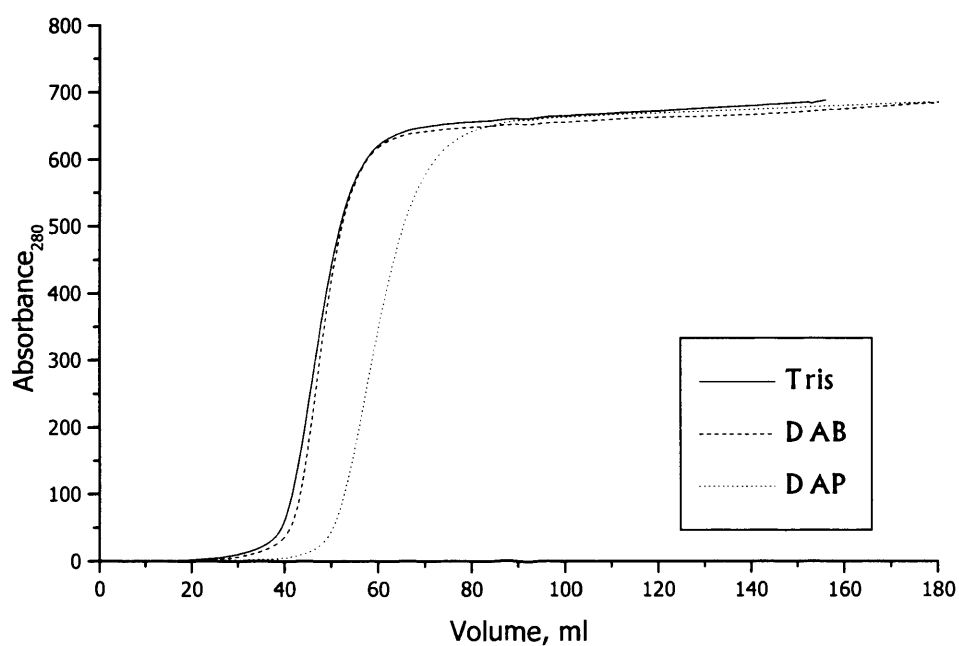


Figure 6.4: The breakthrough of BSA in the presence of salt in 10mL packed beds loaded onto three prototype high salt tolerant ligands.

6.4 Purification of Glutathione S-Transferase

6.4.1 Without the addition of NaCl

GST from *E. coli* homogenate was prepared as described in 2.3.2.1 without the addition of NaCl. Purification was carried out in packed beds using the system described in 2.3.2.2. The packed beds (described in 2.5) were filled with 10mL matrix corresponding to a 5cm bed height.

Each ligand was challenged with 100mL of clarified *E. coli* homogenate containing approximately 3.5mg/mL GST. The feed was applied at a velocity of 100cm/hr. After loading the bed was washed and then the GST was eluted. Breakthrough curves for the three ligands are shown in Figure 6.5. The total GST in the elution fraction for the three ligands is quantified in Table 6.1.

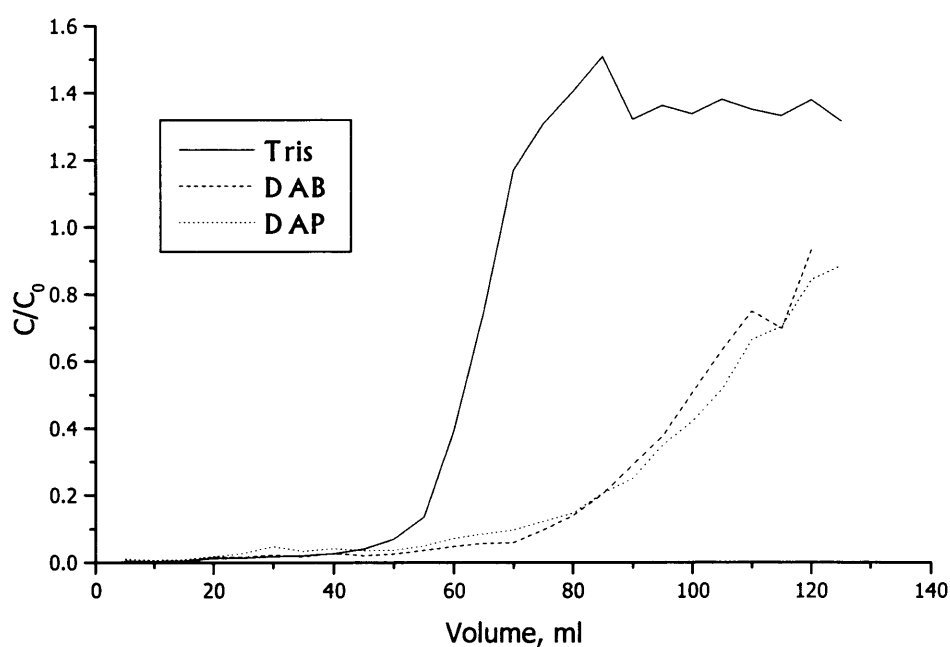


Figure 6.5: The breakthrough of GST in 10mL packed beds loaded onto three prototype high salt tolerant ligands.

6.4.2 With the addition of NaCl

GST from *E. coli* homogenate was prepared as described in 2.3.2.1 with the addition of 0.2M NaCl. Purification was carried out in packed beds using the system described in 2.3.2.2. The packed beds (described in 2.5) were filled with 10mL matrix corresponding to a 5cm bed height.

Each ligand was challenged with 100mL of clarified *E. coli* homogenate containing approximately 3.5mg/mL GST. The feed was applied at a velocity of 100cm/hr. After loading the bed was washed and then the GST was eluted. Breakthrough curves for the three ligands are shown in Figure 6.6. The total GST in the elution fraction for the three ligands is quantified in Table 6.1.

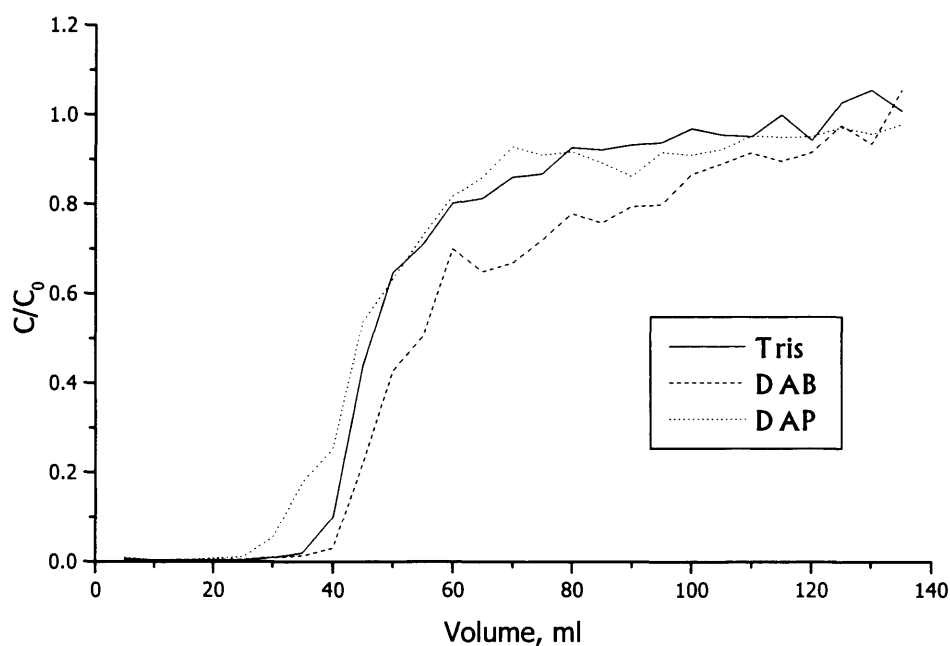


Figure 6.6: The breakthrough of GST in the presence of salt in 10mL packed beds loaded onto three prototype high salt tolerant ligands.

	BSA (mg/ml)		GST (mg/ml)	
	No Salt	With Salt	No Salt	With Salt
Tris	52	16	16	9
DAB	57	18	18	16
DAP	50	22	20	12

Table 6.1: Total BSA and GST (mg/mL) captured on each prototype high salt ligand both with and without the presence of salt to adjust the conductivity. Numbers in bold highlight the highest capacity achieved for each product and conductivity level.

6.5 Discussion

The three prototype high salt tolerant ligands under investigation were developed to cope with high conductivity levels typical of fermentation broths (~20mS/cm) such that the need for feed dilution would be reduced. In addition to this, their performance at low conductivity levels should be similar or better than the performance of the currently available STREAMLINE DEAE. The structure of the ligands shown in Figure 6.1 would suggest that DAB and DAP may produce comparable results due to their structural similarity.

The breakthrough of BSA without the addition of salt is shown in Figure 6.3 and it can be seen that the breakthrough curves are very similar for each ligand. It is also seen in Table 6.1 that the total BSA eluted from the matrix (mg BSA/mL matrix) is very similar for each ligand and is in excess of 50mg/mL in each case. This compares well with STREAMLINE DEAE for which it is noted in the literature that the binding capacity for BSA should be in excess of 40mg BSA/mL adsorbent (Data File STREAMLINE SP/STREAMLINE DEAE).

With the addition of NaCl to the BSA feed to increase the conductivity level to ~25mS/cm it can be seen in Figure 6.4 that the breakthrough curves are again very similar for each ligand. If we compare these curves to those in Figure 6.3 it can be seen that breakthrough occurs earlier and is much steeper in the presence of salt, indicating that the binding performance will be reduced. This is confirmed with the total BSA bound shown in Table 6.1 where it can be seen that it has been reduced in the presence of higher salt levels for each ligand to 16 - 22 mg BSA/mL matrix.

If we now consider the breakthrough of GST without the addition of salt, shown in figure 6.5, we can see that the breakthrough curves for DAB and DAP are very similar, however the breakthrough on the Tris ligand occurs earlier and is much steeper. In addition to this, breakthrough levels achieved are in excess of 1.0 indicating that the GST is not the only, nor is it the most strongly, bound component of the feed and it is being displaced by some other component. Competitive displacement of adsorbed proteins has been described in model studies on competition between lysozyme and BSA when binding to similar adsorbents (Skidmore and Chase, 1990). If we then consider the total GST eluted from the matrices, quantified in Table 6.1, it can be seen that the Tris ligand binds the least GST as compared to DAB and DAP. The difference in GST bound (mg/mL) is not as extreme as may be expected by analysis of the breakthrough curves. This suggests that it may be more difficult to elute the GST from the DAB and DAP ligands than from the Tris ligand. In order to confirm this, the processes were mass balanced, data is shown in Table 6.2.

	Tris		DAB		DAP	
	No Salt	With NaCl	No Salt	With NaCl	No Salt	With NaCl
Load	385	376	330	354	385	366
Flowthrough	217	279	94	151	106	163
Elution	158	88	183	156	200	120
In minus Out	10	9	53	47	79	83

Table 6.2: Total GST (mg) in each collected fraction for all three of the prototype ligands both with and without the presence of salt to adjust the conductivity. Numbers in bold highlight the quantity of GST that was lost in the process.

For the DAB ligand approximately 50mg GST was “lost” in the mass balance i.e. it was not possible to elute the full amount that had bound. The accuracy of the GST assay would only account for around 5mg of this thereby suggesting that the majority of the GST that was lost was due to the difficulty in eluting this protein from this ligand. Consequently this GST was then lost in the CIP. The DAP ligand retained 80mg GST after elution that was lost in the CIP.

With the addition of NaCl to the GST feed the breakthrough curves for the three ligands are now very similar, shown in Figure 6.6. If these curves are compared to those in Figure 6.5 it can be seen for the DAB and DAP ligands that the breakthrough occurs earlier and is much steeper, indicating that the binding performance will be reduced. This is confirmed with the total GST bound (mg/mL) shown in Table 6.1 where the total GST bound has been reduced for each ligand. Once again the processes were mass balanced (shown in Table 6.2) and it was found that all the GST bound to the Tris ligand was eluted. However DAB and DAP retained 50 and 80mg GST respectively that was lost in the CIP.

Taking all of these results into account, the Tris ligand was disregarded for further experimental investigations as it did not bind the most BSA nor GST in any situation. In addition, the GST also appeared to be displaced by some other protein.

The performance of DAB and DAP was comparable, which was expected due to the similarities in their chemical structure. Careful analysis of their performance led to the choice of DAB for further studies. This was based on the fact that the highest level of GST was eluted from this ligand in the presence of salt, coupled with that fact that there was very little difference in the performance of this ligand at high or low salt concentrations. In addition it was easier to elute GST from DAB than from DAP.

6.6 Conclusions

The results from the packed bed experiments indicate that these prototype salt tolerant ion exchange ligands compare well with the currently available expanded bed matrix STREAMLINE DEAE. In particular DAB, which is to be used for further conductivity experiments, has a BSA capacity of 57mg/mL and a GST capacity of 18mg/mL.

This ligand will be used to investigate the effect of feed conductivity on the purification of GST from *E. coli* homogenate in Chapter 7 and the productivity implications will be considered in Chapter 8.

7 INVESTIGATION INTO THE EFFECT OF CONDUCTIVITY ON THE BINDING OF GLUTATHIONE S-TRANSFERASE

7.1 Introduction

The effect of high conductivity levels in a fermentation broth on ion exchange chromatography frequently leads to the need to dilute the feed in order to reduce the ionic strength to such a level that allows binding of the target protein. Typically, this is in the 2-5 mS/cm range and can require a 4-fold dilution. This is particularly problematic for expanded bed adsorption which is used early on in downstream processing as the feed volume is already at a process maximum straight out of the fermenter. A solution to this problem can be to use affinity ligands, however these are a very costly alternative. More recently, attention has focused on the use of multi-modal ligands that operate as ion exchangers at high salt concentrations. These have been developed for large-scale use and a high salt tolerant cation exchanger is now available commercially.

In Chapter 6 three high salt tolerant anion exchange ligands were evaluated for their performance when challenged with BSA and GST from *E. coli* homogenate both at high and low salt concentrations. The ligand DAB was chosen for further investigation into the effect of conductivity on the binding of GST. This chapter seeks to challenge this ligand in an expanded bed adsorption column with *E. coli* homogenate containing GST at a variety of conductivity levels. The DAB is coupled to new high density base matrix, STREAMLINE Direct to facilitate EBA operation at linear velocities in the range 300-900cm/hr.

The performance of the DAB matrix will be compared with that of the currently available STREAMLINE DEAE matrix. Furthermore, as the

DAB ligand under investigation is coupled to a second generation expanded bed base matrix that is densified, allowing operation at velocities in the region of 300-900 cm/hr, the effect of this base matrix and of operating at high velocities will be investigated by comparison to a third adsorbent - DEAE coupled to the high density base matrix STREAMLINE Direct.

These three adsorbents will be challenged with the same feed at varying conductivity levels and their performance in terms of total GST bound compared. The relative productivity of each system will be considered in Chapter 8 with a view to determining the best possible process alternative for EBA application to high ionic strength feeds.

7.2 Adsorbent Verification and Characterisation

7.2.1 Purification of Bovine Serum Albumin

A new batch of STREAMLINE Direct DAB was produced specifically for this work and prior to commencing any GST purification runs, the adsorbent performance was verified by testing its capacity for BSA in a STREAMLINE 25 expanded bed column. BSA was prepared in buffer as described in 2.3.3.1 both without and with the addition of NaCl to increase the conductivity. The BSA was purified according to the methods in 2.4.2 using 100mL matrix corresponding to a 20cm bed height. The operating velocity was chosen in order to achieve double expansion, this was found to be 600cm/hr. Feed was applied until 90% breakthrough was reached at which point the bed was washed and the BSA was eluted in an upwards direction. The elution fraction was collected and analysed for BSA concentration.

The BSA dynamic capacity at 90% breakthrough without salt was found to be 46 compared with 57 mg BSA/mL matrix in the packed bed. In the presence of salt (0.25M NaCl with a corresponding conductivity level of

25mS/cm), this was reduced to 20 (at 97% breakthrough) compared with 18 mg BSA/mL matrix (at 90% breakthrough) in the packed bed.

7.2.2 Adsorption Isotherm for GST

In order to further characterise this matrix, the adsorption isotherm for GST was produced as described in 2.6.10 by challenging samples of matrix with *E. coli* that was clarified and disrupted as described in 2.3.2.1 containing varying concentrations of GST. The GST concentrations varied between 0 - 4mg/mL such that the highest concentration far exceeded the GST levels produced in the fermentation (typically 1.5mg GST/mL). The isotherm is shown in Figure 7.1.

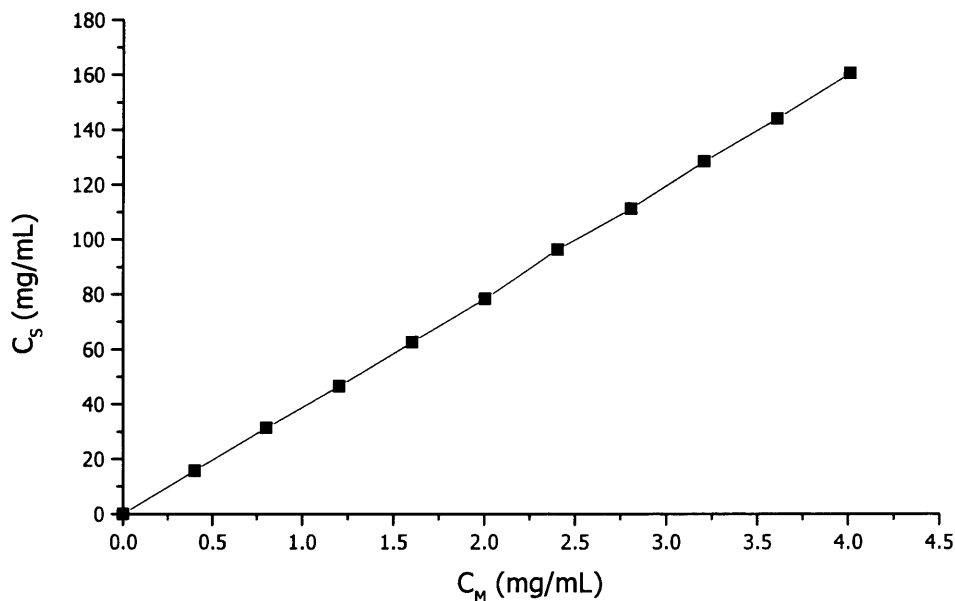


Figure 7.1: The adsorption isotherm for binding of GST from *E. coli* homogenate to the prototype STREAMLINE Direct DAB. C_M is the concentration of GST (mg/mL) in the applied sample and C_S is the amount of GST (mg) bound to the matrix (mL).

7.2.3 Determination of Feed Volume for Conductivity Investigations

In order to establish the volume of feed to be used in each experiment, the STREAMLINE Direct DAB was loaded with *E. coli* homogenate to determine the quantity of feed containing GST required to achieve 10%

GST breakthrough. The feed was prepared as described in 2.3.2.1 and the GST was purified according to the methods in 2.4.2.2 and the buffer system described in 2.3.2.2. A typical breakthrough curve is shown in Figure 7.2.

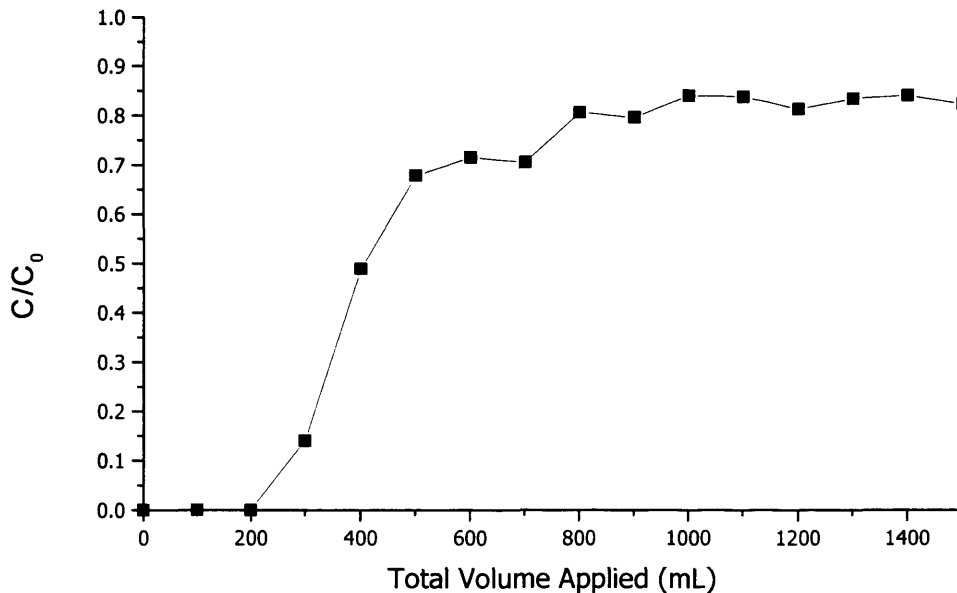


Figure 7.2: The breakthrough of GST from whole *E. coli* homogenate loaded at 600cm/hr on 100mL STREAMLINE Direct DAB in a STREAMLINE 25 EBA column at a conductivity of 20mS/cm.

The breakthrough occurred much earlier than expected and rose very dramatically. The total GST eluted was found to be 1mg GST/mL matrix and only 1% of the applied GST was recovered. This was in contrast to the 16mg GST/mL matrix found in the packed bed experiments. Upon consideration, it was hypothesised that there may be some entity in the fermentation broth that was binding more strongly to the matrix than the GST. This hypothesis was reinforced when considering the conditions of feed preparation between the packed bed and expanded bed systems. For the packed bed experiments, the *E. coli* broth was clarified and the pellet then resuspended in buffer for disruption. This disrupted sample was

then clarified to prevent loading of debris onto the packed bed. In the case of the expanded bed, the *E. coli* broth was disrupted and loaded directly onto the bed after pH adjustment. For the packed bed preparation this effectively removed the fermentation broth and its components from the feed loaded onto the column, whereas these remained in the feed loaded onto the expanded bed.

In order to test the hypothesis that some component(s) in the fermentation broth that remained in the EBA feed led to the reduction in capacity for GST, the *E. coli* broth was clarified as per 2.2.2. The cell broth supernatant was adjusted to pH 8.5 and loaded onto the expanded bed. The cell broth supernatant was found to contain 1mg/mL GST. The cell pellet was resuspended in buffer for disruption. After disruption the pH was adjusted to 8.5 and this homogenate was loaded onto the expanded bed. Breakthrough curves are shown in Figures 7.3 and 7.4 for cell broth supernatant and homogenised pellet respectively.

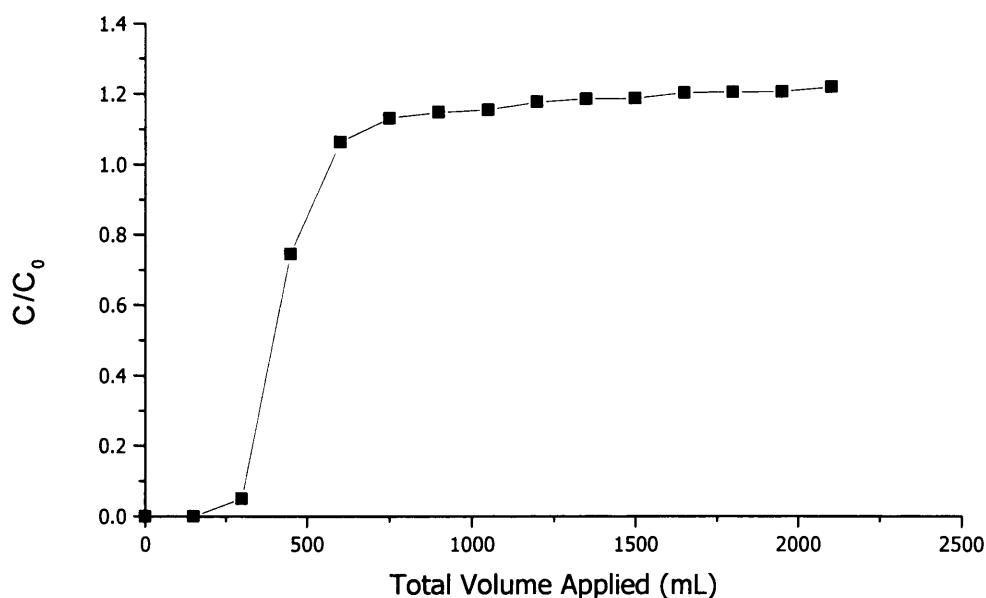


Figure 7.3: The breakthrough of GST found in the *E. coli* broth supernatant loaded at 600cm/hr on 100mL STREAMLINE Direct DAB in a STREAMLINE 25 EBA column at a conductivity of 20mS/cm.

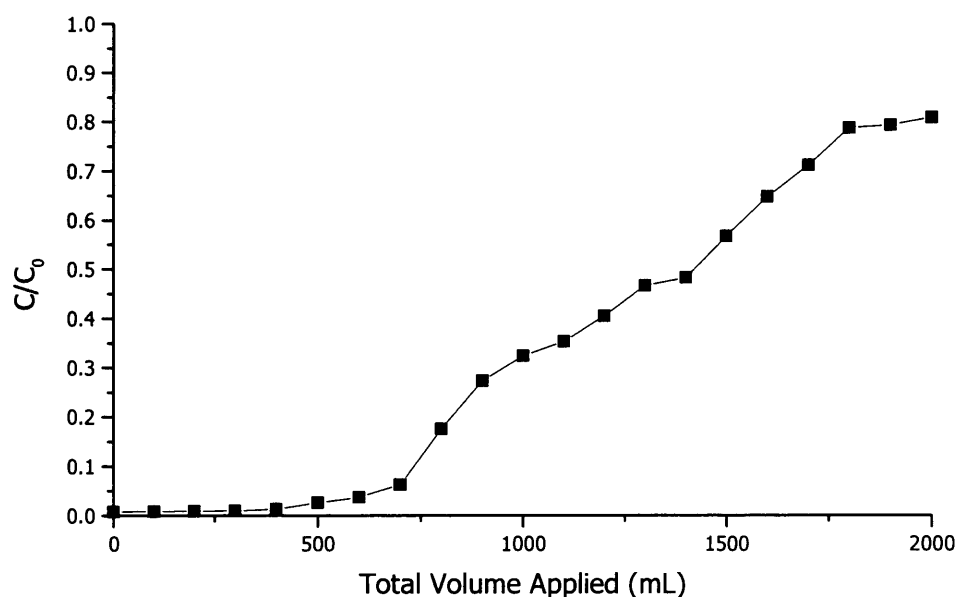


Figure 7.4: The breakthrough of GST from the disrupted *E. coli* cell pellet loaded at 600cm/hr on 100mL STREAMLINE Direct DAB in a STREAMLINE 25 EBA column at a conductivity of 20mS/cm.

When the cell broth supernatant was applied it was found that the total GST eluted was 0.6mg GST/mL matrix with 2% of the applied GST being recovered in the elution. When the disrupted pellet was loaded it was found that the total GST eluted was 8mg GST/mL matrix with 55% of the applied GST recovered in the elution. These results support the hypothesis that there was some entity in the fermentation broth preventing GST binding. As such, for further purifications, the *E. coli* broth was clarified as per 2.2.2 and the pellet resuspended in buffer for disruption.

From Figure 7.4 it was established that 700mL of clarified and disrupted *E. coli* with a GST concentration of 0.8mg/mL ($\pm 10\%$) and a conductivity level of 20mS/cm would be needed to achieve 10% GST breakthrough on the STREAMLINE Direct DAB. This provided the base-line for the next phase of studies.

7.3 Conductivity Studies

In the previous section, it was established that 700mL of undiluted, clarified and disrupted *E. coli* containing 0.8mg/mL GST at a conductivity level of 20mS/cm was needed to achieve 10% GST breakthrough on the STREAMLINE Direct DAB adsorbent. This feed was prepared and loaded onto the three adsorbents under investigation:

1. STREAMLINE Direct DAB
2. STREAMLINE DEAE
3. STREAMLINE Direct DEAE

For each adsorbent, the flowrate was chosen such that the matrix height upon expansion in equilibration buffer was double that of the settled bed height (20cm for each adsorbent). This was found to be 600cm/hr for the STREAMLINE Direct adsorbents and 160cm/hr for the STREAMLINE DEAE.

To investigate the effect of conductivity the feed prepared as described above was diluted with equilibration buffer as appropriate to reduce the conductivity to 10 and 2.5mS/cm i.e. 1 in 2 and 1 in 8 dilutions respectively. The breakthrough curves at each conductivity level are shown in Figure 7.5 and the total GST collected in the elution is summarised in Table 7.1.

	20mS/cm	10mS/cm	2.5mS/cm
STREAMLINE Direct DAB	482	516	495
STREAMLINE Direct DEAE	140	461	431
STREAMLINE DEAE	328	541	562

Table 7.1: The total GST (mg) eluted at each conductivity level (20, 10 and 2.5 mS/cm) and from 100mL of each adsorbent (STREAMLINE Direct DAB, STREAMLINE DEAE and STREAMLINE Direct DEAE).

Figure 7.5: The breakthrough of GST from disrupted *E. coli* loaded onto 100mL of the three adsorbents (STREAMLINE Direct DAB, STREAMLINE DEAE and STREAMLINE Direct DEAE) at three conductivity levels (20, 10 and 2.5 mS/cm) and a velocity of 600cm/hr for the STREAMLINE Direct adsorbents and 160cm/hr for the STREAMLINE DEAE.

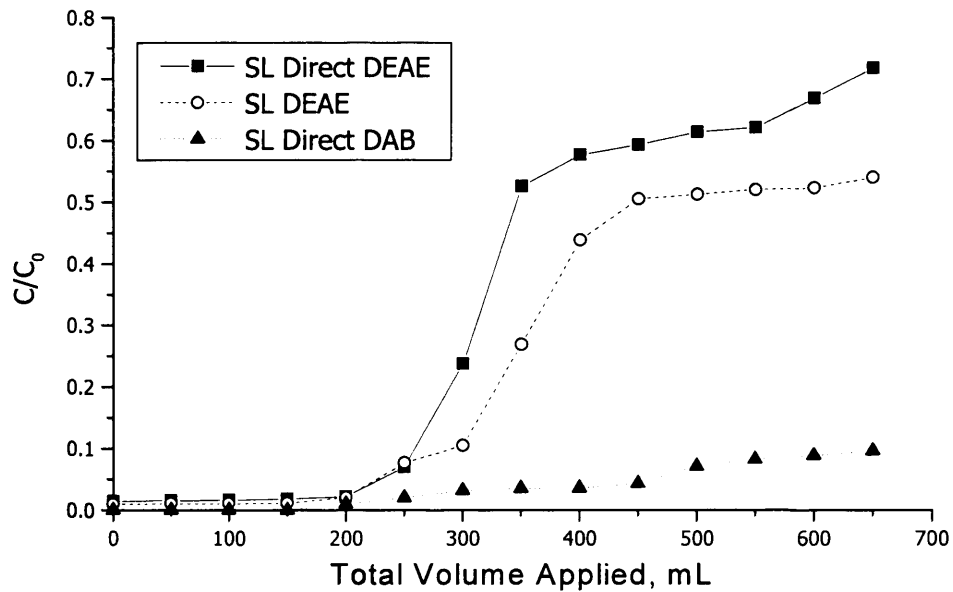


Figure 7.5a: GST breakthrough when loaded at a conductivity level of 20mS/cm.

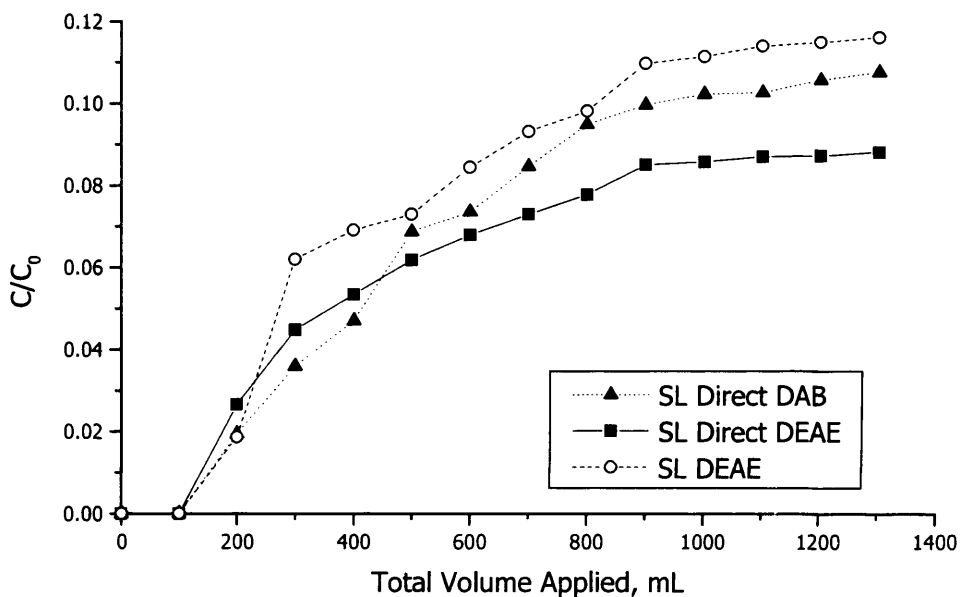


Figure 7.5b: GST breakthrough when loaded at a conductivity level of 10mS/cm.

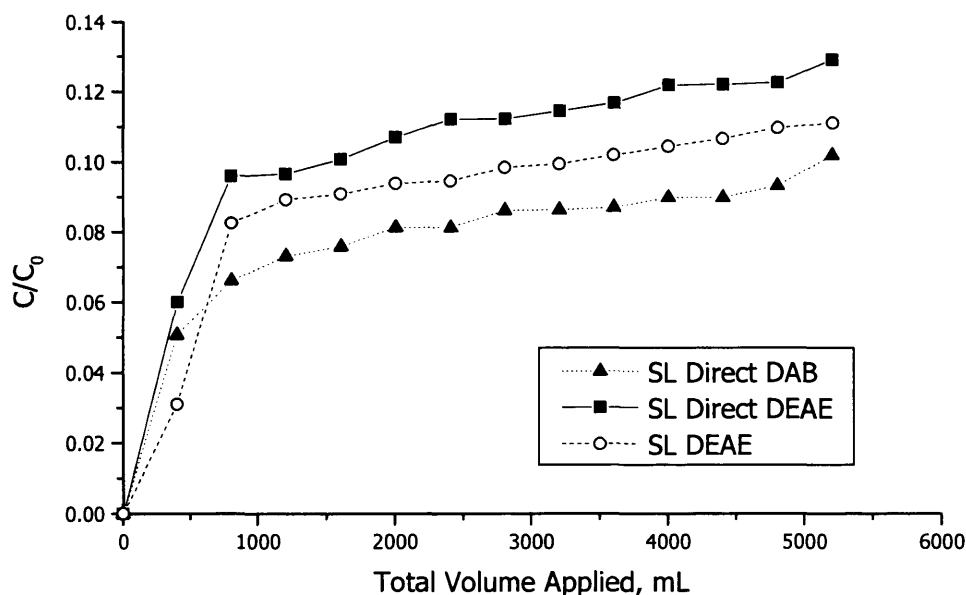


Figure 7.5c: GST breakthrough when loaded at a conductivity level of 2.5mS/cm.

7.4 Discussion

The new batch of STREAMLINE Direct DAB was tested in an expanded bed for its binding capacity to BSA prepared in buffer. As this was a prototype adsorbent, no standard operating procedures were in place for large scale production of the base matrix or ligand coupling and therefore testing was required to ensure its performance was comparable with that of the small volume samples evaluated in Chapter 6. The results compared well with those observed in the packed bed. Without the addition of NaCl, the dynamic capacity at 90% breakthrough was slightly reduced in the expanded bed compared with the packed bed from 57 to 46mg BSA/mL matrix. This reduction in the capacity is to be expected with expanded beds and is due to the reduction in NTP observed in expanded beds. This leads to shallower breakthrough curves in expanded beds as compared to the packed beds. This then coupled with the increase in operating velocity which limits the mass transfer as observed in Chapters 4 and 5 leads to lower binding capacities. With the addition of salt to increase the conductivity, the dynamic capacity was found to be

20mg BSA/mL matrix at 97% breakthrough in the expanded bed, compared with 18mg BSA/ml matrix in the packed bed. The slightly higher dynamic binding capacity observed in the expanded bed can be attributed to the fact the breakthrough in the packed bed only reached 90%. The dynamic binding capacity at 90% in the expanded bed was calculated based on the breakthrough curves. This was found to be 15mg/mL and therefore is consistent with the packed beds results coupled with the reduced capacity in the expanded bed, discussed above.

In order to test further this new batch of DAB adsorbent and to understand the binding of GST to DAB, the adsorption isotherm was prepared. It can be seen in Figure 7.1 that the isotherm in the concentration range tested is linear. The GST concentrations applied to the matrix for preparation of the isotherm (0 - 4mg/mL GST) were such that they far exceeded the concentrations produced in the fermentation (1.5mg/mL GST) and as such the concentration that would be applied to the expanded bed. The implications of this linear adsorption isotherm are that maximum capacity of the adsorbent has not yet been reached.

After this initial testing, it was concluded that the new batch of STREAMLINE Direct DAB was behaving as expected both with BSA and GST. The next stage was to determine the quantity of GST and hence volume of feed to be applied to each of the three adsorbents under investigation. It was decided that the quantity of GST applied should be such that the GST had reached 10% breakthrough on the STREAMLINE Direct DAB.

In order to establish this, whole *E. coli* fermentation broth was disrupted and the pH adjusted to 8.5 and this was loaded onto the STREAMLINE Direct DAB matrix in the expanded bed. The resulting breakthrough curve is shown in Figure 7.2. Based on experiences in the packed bed, the breakthrough occurred much faster than anticipated, going from 0% at 200mL applied feed volume to 70% GST breakthrough at 500mL applied

volume. The process was mass balanced and it was found that only 1% of the applied GST was recovered in the elution, equivalent to a dynamic binding capacity of 1mg GST/mL matrix. This was in contrast to the 16mg GST/mL matrix obtained in the packed bed.

Given that this batch of matrix had successfully bound GST in the isotherm experiments, the feed preparation method was examined. For both the packed bed and isotherm experiments, the *E. coli* fermentation broth was clarified and the supernatant discarded. The pellet was then resuspended in buffer prior to disruption. For the expanded bed experiment, the whole fermentation broth was disrupted. This indicated the possibility that there may be some entity in the supernatant that was binding more strongly to the matrix than the GST.

To test this theory, supernatant was loaded onto the expanded bed. Despite GST being an intracellular protein, the supernatant was found to contain 1mg/mL GST. This was most likely due to partial cell lysis during the freezing process. In this test, only 2% of the applied GST was recovered in the elution, equivalent to a dynamic binding capacity of 0.6mg GST/mL matrix.

E. coli was then clarified and the supernatant discarded. The cell pellet was resuspended in buffer, disrupted, and the pH adjusted to 8.5 prior to loading onto the expanded bed. In this case, 55% of the applied GST was recovered with a dynamic binding capacity of 8mg GST/mL matrix. This compared more favourably with the packed bed results.

These tests indicated that GST binding was suppressed in the presence of cell broth supernatant. The colour and odour of the elution fraction when the bed was loaded with supernatant suggested that the competitive entity may be some component of the yeast extract, a highly complex organic nitrogen source containing a variety of vitamins, minerals and other growth factors. This has been observed in other studies (Calado *et al.* 2002).

When the cell pellet minus the cell broth supernatant was used for feed preparation, the capacity for GST in the expanded bed was half that observed in the packed bed. This decrease was to be expected for the reasons outlined above when comparing the capacity for BSA.

From these tests it was established that 700mL of feed containing 0.8mg/mL GST prepared from disrupted *E. coli* cell pellet with a conductivity of 20mS/cm would be needed to reach 10% GST breakthrough on the STREAMLINE Direct DAB. In an industrial process the fermentation broth would typically not be clarified prior to disruption if an EBA step was to be utilised. However since the purpose of this study was to compare binding performance of these adsorbents with the given feed no further fermentation development was considered to evaluate the interaction with DSP.

Instead, the common feed was loaded onto equal volumes of 100mL of each of the three adsorbents under study such that they were each challenged with the same total quantity of GST. The breakthrough curves are shown in Figure 7.5a. From these curves it can be seen that the STREAMLINE Direct DAB reaches the lowest overall breakthrough. The two DEAE adsorbents reach high levels of breakthrough rapidly, with the STREAMLINE Direct DEAE reaching the highest overall breakthrough. The results are further quantified in Table 7.1 where it can be seen that the STREAMLINE Direct DAB binds the most GST (482mg), followed by the STREAMLINE DEAE (328mg) with the STREAMLINE Direct DEAE binding the least GST (140mg). As the DEAE ligand is not designed to operate at high conductivity levels, these results are in-line with expectations.

The difference in the total GST bound by the two DEAE adsorbents can be attributed to the effect of operating velocity. The total GST bound by the STREAMLINE DEAE adsorbent loaded at a velocity of 160cm/hr is double that bound by the STREAMLINE Direct DEAE, loaded at a

velocity of 600cm/hr. This increase in velocity leads to a reduction in contact time which in a mass transfer limited situation will lead to a reduction in dynamic binding capacity.

In the subsequent experiments, conductivity of the feed was then reduced to 10mS/cm by dilution of the original 700mL feed with 700mL of equilibration buffer. Breakthrough curves at this conductivity level can be seen in Figure 7.5b. At this conductivity level, the behaviour of the three adsorbents is comparable, not only in terms of breakthrough curves, but also in the total GST bound, summarised in Table 7.1.

Comparing the behaviour of the three adsorbents at this conductivity level with that at the higher conductivity level of 20mS/cm, it can be seen that there is no difference in performance for the STREAMLINE Direct DAB adsorbent. The performance of the two DEAE adsorbents has improved with a reduction in the conductivity and their behaviour is now comparable with that of the STREAMLINE Direct DAB. Again, as observed at the higher conductivity level, the STREAMLINE DEAE adsorbent outperforms the STREAMLINE Direct DEAE. This is most likely due to the difference in operating velocities, discussed above.

A further reduction in the conductivity level to 2.5mS/cm by dilution of the original feed with 4900mL equilibration buffer does not offer any obvious advantage in terms of the performance and behaviour of the three adsorbents. If the results at this conductivity level are compared with those at 10mS/cm, it can be seen that both the breakthrough curves in Figure 7.5c and the total GST bound detailed in Table 7.1 are very similar in shape and that the differences in amount of GST bound are now small relative to saturation levels.

Taken together, these results demonstrate that the STREAMLINE Direct DAB performs consistently in the range of conductivities tested. In order for the DEAE ligand to bind similar quantities of GST, the conductivity must be halved.

7.5 Conclusions

The multi-modal ligand DAB was designed to operate at high conductivity levels typical of fermentation broths (approximately 20mS/cm). As these experiments indicate, this ligand performed consistently in the range of conductivity levels tested (2.5 – 20mS/cm). Its performance was comparable with that of the commercially available DEAE ligand at low conductivity levels where the latter ligand is designed to be optimal.

As expected the performance of the DEAE ligand was reduced at high conductivity levels. The dilution required for acceptable performance was 1 in 2, reducing the conductivity to 10mS/cm. At this conductivity level, performance was comparable with that of DAB ligand at 20mS/cm.

The STREAMLINE Direct DEAE was consistently outperformed by the STREAMLINE DEAE adsorbent at all conductivity levels. This was due to the operating velocity in each of these systems. The STREAMLINE Direct DEAE was operated at a velocity of 600cm/hr, 3.75 fold higher than that of the STREAMLINE DEAE (160cm/hr). This increase in velocity led to an accentuation of mass transfer limitations and a reduction in the contact time.

The full implications of these observed differences in ligand behaviour and the effect of the base matrix and ligand design on the productivity of each adsorbent will be considered in the next chapter.

8 THE PRODUCTIVITY IMPLICATIONS OF VARYING OPERATING PARAMETERS AND MATRIX PROPERTIES

8.1 Introduction

In Chapters 4 and 5, the effect of matrix particle size distribution and operating velocity on protein binding in an expanded bed was examined. It was found for both systems under study that when operating at velocities typically utilised in EBA, no benefit in terms of performance was offered through careful selection of the particle size distribution in the range of sizes commercially available.

In Chapter 7, the effect of conductivity was considered on protein binding to three adsorbents, different in both their ligand chemistry and their base matrix. The multi-modal ligand was found to operate most effectively at high conductivity levels, thereby reducing the need to dilute the feed. The performance of the commercially available ligand DEAE was improved by operating at low velocities.

In all of these studies, performance was examined only in terms of the product breakthrough. The overall productivity of each scenario was not considered. Productivity can be defined and expressed in a variety of forms, ranging from the simple, where for example processing time is considered, to the complex, where time, buffer, matrix and costs are considered. In industry, productivity is a key parameter as ultimately, no matter what its definition, an improvement in the productivity of the overall process leads to cost benefits.

This chapter seeks to examine a number of productivity definitions using the Yeast/ADH system investigated in Chapter 4 to illustrate their meaning. This will provide the basis for a productivity definition that will

be used to evaluate all of the processes examined in this thesis. In order to provide a realistic productivity expression, this definition will be based on the total ADH recovered in the elution fraction. However as no elution development was carried out in this thesis, 100% product recovery in the elution is unlikely. Instead it will be assumed for comparison only that the breakthrough curves can be integrated for the Yeast/ADH processes in order to calculate the total quantity of product bound. Furthermore, the 5% dynamic binding capacity will be calculated for each of the Yeast/ADH processes as a reflection of the likely levels to be encountered in processing. Productivity levels can be evaluated based on these figures.

8.2 Productivity Definition Evaluation

The Yeast/ADH system examined in Chapter 4 considered the impact of operating velocity and matrix particle size on the HIC purification of ADH from unclarified Yeast homogenate. Results in terms of breakthrough curves indicated that no benefit was offered by careful selection of matrix particle size distribution at flowrates typical of an EBA process (300cm/hr).

The impact of increasing operating velocity offers savings in terms of processing time, but the trade off is that buffer consumption is higher. The smaller matrix particles expand more than the larger particles at a given velocity and so require longer processing times and higher buffer consumption. Taking this into consideration, the Yeast/ADH processes were re-examined in terms of their buffer consumption and processing time, as shown in Figure 8.1.

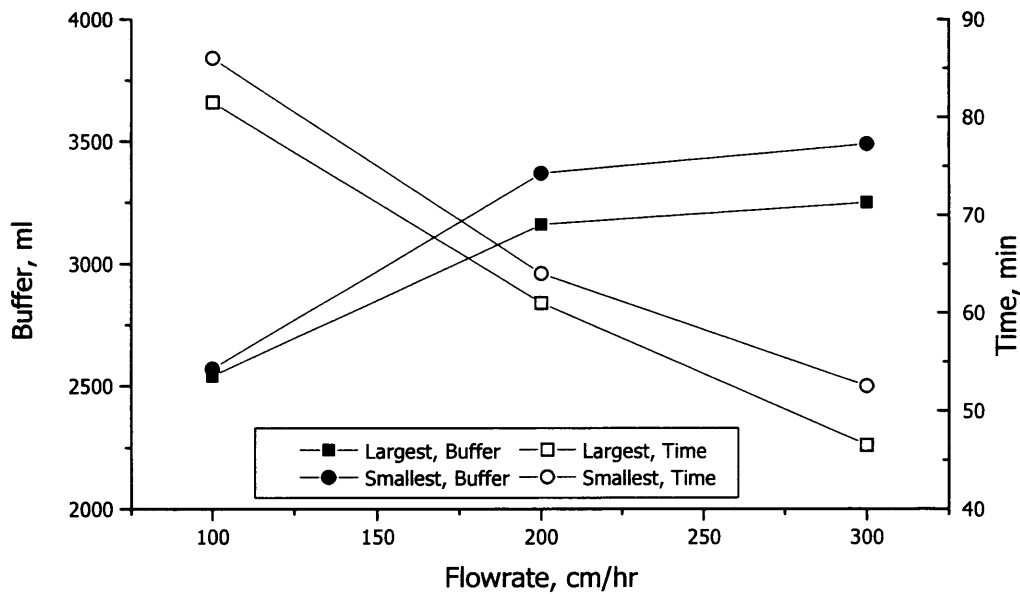


Figure 8.1: The trade off between buffer consumption (mL) and processing time (min) when varying the operating flowrate and matrix particle size.

Whilst Figure 8.1 clearly illustrates the trade off between buffer consumption and processing time, the most critical parameter is the quantity of product that is recovered in the elution for further processing. If we now consider this in terms of buffer consumption and processing time, Figure 8.2 is the resulting graph.

A useful way of considering the effect of both operating velocity and matrix particle size is the residence time concept introduced in Chapter 4. If we now consider the total ADH recovered as a function of the t_R , described in 2.6.7, defined in equation 2.4 and evaluated for the Yeast/ADH processes in Table 4.3, this yields Figure 8.3.

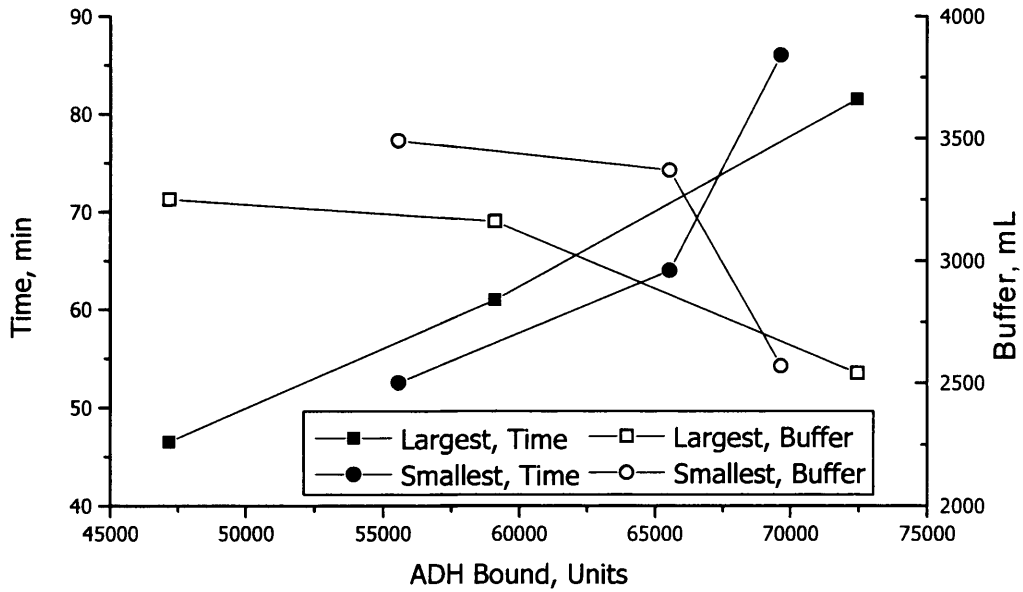


Figure 8.2: The trade off between buffer consumption and processing time in relation to the total ADH recovered in each process.

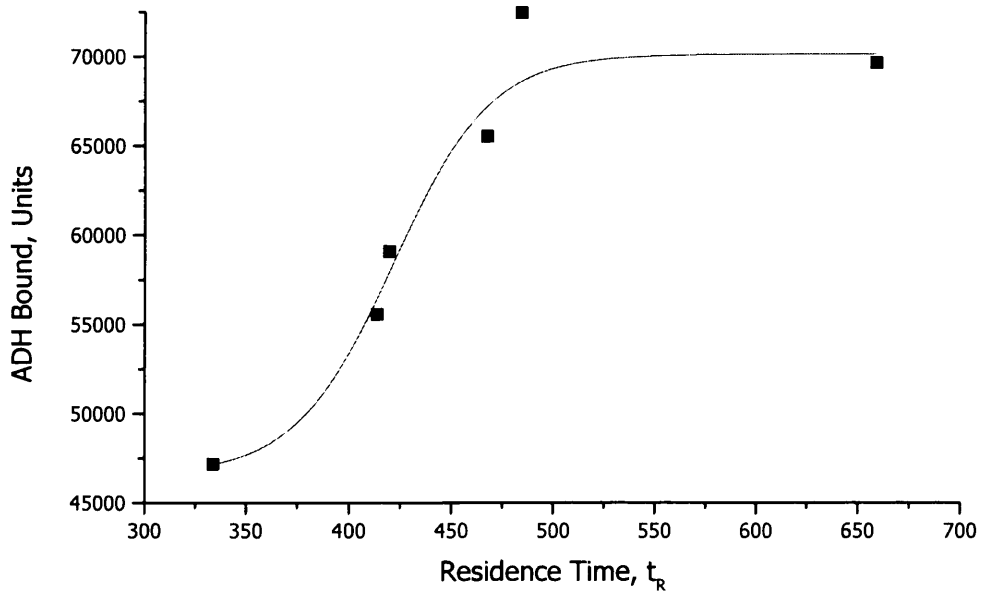


Figure 8.3: The effect of residence time, t_R , a measure of operating velocity and matrix particle size distribution on the total ADH recovered for each system set-up based on particle size and operating velocity.

Whilst the productivity may be defined as Units of ADH per mL buffer consumed per min processing time in order to compensate for the trade-off between buffer consumption and processing time, it is very much a process-specific definition. If we consider the buffer consumption, only processes that utilise the same buffers can be compared using this expression, as the cost and hence significance of buffer consumption will be directly related to the buffers utilised in the process.

However, if processing time can be reduced with the same quantity of product recovered, this would be a very attractive proposal. For example, if the downstream processing for product X can be reduced from 5 to 4 days whilst maintaining the same product quantity and quality, and if we assume that the processing plant is operational for 80% of the year, 73 batches of product can be produced for the 4 day process compared with 58 batches for the 5 day process - a 26% increase.

As the total product recovered per processing time is a simple yet meaningful and relevant measure of productivity, it will be used to evaluate the processes investigated in this thesis. This will be compared with the productivity calculated based on total product bound from integration of the breakthrough curves and the total product bound at 5% breakthrough for the Yeast/ADH processes.

It should be noted that such a productivity evaluation is limited to similar processes such that their costs are approximately equivalent - which is the case here. However, if the processes under comparison were different, for instance in the above example the total processing time may be reduced by employing alternative DSP, it would be advisable to assign costs to the various parameters of the process in order to better understand the benefit, or indeed possibly the loss, that the reduction in time may confer.

8.3 Productivity Evaluation of the ADH Process

The productivity of the Yeast/ADH process investigated in Chapter 4 is summarised in Table 8.1 detailing the total ADH recovered in each process (Units) and each of the process residence times (t_R , sec) and the corresponding total processing time, including the load, wash and elution time.

Process	t_R , sec	ADH recovered, Units	Processing Time, min	Productivity, Units ADH recovered/min
Large, 100cm/hr	485	72,458	82	889
Small, 100cm/hr	658	69,637	86	810
Large, 300cm/hr	333	47,170	47	1,014
Small, 300cm/hr	414	55,560	53	1,058

Table 8.1: The productivity defined as the total ADH recovered (Units) in the elution fraction per minute of processing time for each of the Yeast/ADH processes.

The breakthrough curves for the Yeast/ADH processes in Chapter 4, Figures 4.3 b and c were integrated to evaluate the total ADH bound to the matrix and then integrated to calculate the total ADH bound at 5% breakthrough and the productivity re-evaluated based on these. This is summarised in Tables 8.2 and 8.3 for the total ADH bound in the process and the total ADH bound at 5% breakthrough respectively.

Process	t_R sec	ADH bound, Units	Processing Time, min	Productivity, Units ADH bound/min
Large, 100cm/hr	485	76,132	82	934
Small, 100cm/hr	658	73,168	86	851
Large, 300cm/hr	333	77,161	47	1,659
Small, 300cm/hr	414	78,346	53	1,492

Table 8.2: The productivity defined as the total ADH bound (Units) based on breakthrough curve integration per minute of processing time for each of the Yeast/ADH processes.

Process	t_R sec	ADH bound (5%), Units	Processing Time, min	Productivity, Units ADH bound (5%)/min
Large, 100cm/hr	485	32,258	60	538
Small, 100cm/hr	658	55,628	73	762
Large, 300cm/hr	333	55,526	41	1,354
Small, 300cm/hr	414	58,852	48	1,239

Table 8.3: The productivity defined as the total ADH bound at 5% product breakthrough (Units) per minute of processing time for each of the Yeast/ADH processes.

8.4 Productivity Evaluation of the GST Process

For the *E. coli*/GST process various operating parameters were investigated; in Chapter 5, the effect of operating velocity was considered on the binding of GST and in Chapter 7 the effect of feed conductivity was considered.

Also, various matrix properties were considered in the investigations; in Chapter 5 the matrix particle size was considered and in Chapter 7 the ligand and base matrix was investigated.

The different processes have been summarised separately below.

8.4.1 Velocity and Particle Size Distribution Effects

The productivity of the *E. coli*/GST process investigated in Chapter 5 is summarised in Table 8.4 detailing the total GST recovered in each process (mg) and each of the process residence times (t_R , sec) and the corresponding total processing time, including the load, wash and elution time.

Process	t_R sec	Total GST recovered, mg	Processing Time, min	Productivity, mg GST/min
Large, 100cm/hr	583	77	169	0.46
Small, 100cm/hr	615	77	180	0.43
Large, 300cm/hr	344	58	71	0.81
Small, 300cm/hr	385	68	78	0.87

Table 8.4: The productivity defined as the total GST recovered (mg) per minute of processing time for each of the *E. coli*/GST processes where the effect of operating velocity and particle size distribution was investigated.

8.4.2 Conductivity Effects

The productivity of the *E. coli*/GST process investigated in Chapter 7 is summarised in Table 8.5 detailing the total GST recovered in each process (mg) and each of the process residence time (t_R , sec) and the corresponding total processing time, including the load, wash and elution time.

Cond. mS/cm	Matrix	tR, sec	Total GST recovered, mg	Processing Time, min	Productivity, mg GST/min
20	SL Direct DAB	180	482	30	15.85
	SL Direct DEAE	185	140	37	3.75
	SL DEAE	570	328	126	2.6
10	SL Direct DAB	180	516	46	11.17
	SL Direct DEAE	185	461	46	9.99
	SL DEAE	570	541	170	3.18
2.5	SL Direct DAB	180	495	129	3.84
	SL Direct DEAE	185	431	129	3.34
	SL DEAE	570	562	285	1.97

Table 8.5: The productivity defined as the total GST recovered (mg) per minute of processing time for each of the *E. coli*/GST processes investigated in terms of conductivity effects.

8.5 Discussion

There are a variety of ways of defining and calculating process productivity. This chapter set out to evaluate various options using the Yeast/ADH process developed in Chapter 4 as an example. Productivity is ultimately related to cost. As such, those parts of the process that cost money were initially evaluated; these were the processing time and buffer consumption. The effect of increasing velocity and varying matrix particle size distribution on the buffer consumed and the processing time is shown in Figure 8.1. As can be seen in this Figure, increasing the operating velocity leads to shorter processing times but increases the buffer utilised in the process. At each flowrate, the large particles required less processing time and buffer than the small particles. This is due to the small particles expanding more than the large particles at a given flowrate and thus should be expected and is predictable.

If we further examine this graph and choose the point at which the buffer consumption and processing time are both at a minimum, this would lead to the conclusion that the large particles operated at a velocity of around 160cm/hr would be the most productive option.

However whilst this choice may minimise processing costs in terms of buffer consumption and processing time, the quantity of revenue generating product, in this case the ADH, has not been considered. If we now examine Figure 8.2 which illustrates the effect of increasing the ADH recovered on buffer consumption and processing time, it can be seen that at the maximum quantity of ADH recovered, buffer consumption is at its minimum, but processing time is close to the maximum. As relative costs have not been associated with the buffer consumption, processing time and ADH, it is difficult to conclude whether this would be the most productive and as such this would be an area of further work. With such data it would be possible to determine the precise optimum point of operation for any set of relative operational parameters.

An alternative method that indirectly considers both the buffer consumption and processing time is to examine the effect of t_R on the total ADH recovered. As the buffer consumption and processing time are directly affected by the matrix particle size distribution and operating velocity, as illustrated in Figure 8.1, utilising the t_R concept introduced in Chapter 4 allows us to consider these effects on the ADH recovered. This can be seen in Figure 8.3 where it is clear that increasing the residence time by lowering the flowrate leads to benefits in total ADH bound up until a t_R of ~480secs at which point there is no improvement in the recovery. Taking this into consideration, a possible interesting area of study would be to modify the operating velocity and particle size distribution such that the residence time is 480secs and then attempt to optimise the process in terms of buffer consumption and processing time.

As outlined above, no costs have been associated with the buffer consumption, processing time and product. Without these for each of the processes, it is difficult to evaluate accurately and compare the productivity. This is especially true if buffer costs are low in relation to product value and processing time. As all production companies understand processing time, its use in a productivity expression defined as the total product recovered per minute of processing time provides a simple yet meaningful measure of process productivity. As such, the productivity for each process investigated in this thesis was calculated and results are shown in Tables 8.1 - 8.5.

If we consider the results in Table 8.1 for the ADH process, it can be seen that the most productive option is to utilise the small particles at a flowrate of 300cm/hr; the least productive option is the small particles at 100cm/hr. At the low flowrate, for both of the matrix particle sizes the whole process takes much longer than at the high flowrate. This is increased even further for the small particles due to the increase in expansion experienced with this particle size at the same flowrate. This is coupled with the increase in residence time offering no advantage in terms of ADH recovered.

At the high flowrate, the small particles are more productive than the large particles. Whilst the overall processing time is longer for the small particles due to the increased bed expansion, this increase in expansion provides a longer residence time and hence more time for product binding. Therefore the increase in processing time is compensated for by the increase in overall ADH recovered leading to a more productive process.

If we now consider the productivity of these processes based on the total ADH bound, calculated from the breakthrough curves (Table 8.2) it can be seen that the most productive process is the large particles operated at 300cm/hr. The least productive is the small particles operated at

100cm/hr. The small particles at the low velocity is the least productive for the same reasons discussed above when considering the productivity based on the total ADH recovered. However, the most productive option is to use large particles and to operate at the highest flowrate. This contrasts to the results based on ADH recovered where the choice is to use small particles at the high flowrate. This is due to the similarity in levels of ADH bound for both particle sizes at the higher flowrate, as expected based on the breakthrough curves. The large particles require a shorter processing time based on their lower expansion characteristics. The resulting large particle productivity is higher compared to that for the small particles.

In this thesis, for each process, the performance of each matrix was compared when challenged with the same total quantity of product. This was due to the difficulty in controlling the load volume for a specific breakthrough level. In an industrial process it would be unlikely that product would be loaded to more than 5-10% breakthrough dependent on its value, as this would lead to unacceptable product losses. To mimic this, the breakthrough curves for the Yeast/ADH processes were evaluated to calculate the ADH bound at 5% breakthrough, and the processing times noted at the point at which this quantity of feed was loaded. When the productivity is evaluated on this basis, the least productive option is to use the large particles at 100cm/hr and the most productive is the large particles at 300cm/hr.

Despite the smaller particles operated at the lower velocity taking longer to process a given feed volume than the large particles, their dynamic binding capacity at 5% is higher. This is due to the higher specific surface area offered by these particles, which leads to a higher productivity. This would be expected when comparing the breakthrough curves in Chapter 4 Figure 4.4b where it can be seen that the small particles have a much shallower breakthrough curve than the large particles.

At the higher velocity, where the large particles are more productive than the small particles, the result is most likely due to the large particles taking less time to process, coupled with the similarity in performance at the higher velocity due to mass transfer limitations. This is to be expected based on the breakthrough curves (Chapter 4 Figure 4.4c)

From these analyses it appears that the most realistic value to use in all the cases is the actual ADH recovered as it is the actual quantity of ADH obtained from the EBA stage that would be used in any further processing strategies. As such, the productivity evaluation for the remaining systems in this thesis are based on the product recovered in each of the processes.

The productivity of the *E. coli*/GST system when investigating the effects of particle size and operating velocity, follows similar trends to the Yeast/ADH system. The least productive option is the small particles at 100cm/hr and the most productive is the small particles at 300cm/hr. It can also be seen that increasing the residence time leads to an increase in the overall GST recovered up until a residence time of ~580secs. Whilst this is a higher residence time than that of the ADH process, it should be noted that the residence time for the GST system was based on more complete penetration of the matrix particles. For the ADH process it was based on surface area only. As such, a higher residence time should be expected for the GST system as compared with the ADH system.

Despite the difference in the GST and ADH systems in terms of the both the chromatographic method used and the size of the molecules (leading to surface binding and full penetration for the ADH and GST respectively) similar conclusions for both systems have been reached in terms of the effect of matrix particle size and operating flowrate on the performance and productivity indicating that the results from this work are transferable.

If we now consider the effect of conductivity on the productivity of three adsorbents, summarised in Table 8.3, it can be seen that overall, the most productive option is the STREAMLINE Direct DAB matrix at a conductivity of 20mS/cm; the least productive option is the STREAMLINE DEAE at 2.5mS/cm.

If we consider the three adsorbents in turn, it can be seen for the STREAMLINE Direct DAB that the productivity decreases as the conductivity decreases. This is to be expected as the total GST bound at each conductivity level was comparable and as such, a reduction in the conductivity led directly to a larger feed volume due to the required feed dilution and consequently this led to a longer processing time.

For the STREAMLINE Direct DEAE and the STREAMLINE DEAE, at the highest conductivity level (20mS/cm) the productivity is low due to the inability of the DEAE ligand to operate at high conductivity levels. When the conductivity is reduced to 10mS/cm the productivity improves as the ligand is able to function at this conductivity level. The productivity then drops as the conductivity is further reduced due to the larger feed volume leading to an increase in the processing time coupled with no improvement in the total GST bound. This result is an interesting example of the competitive processes that control overall behaviour.

The impact of the new densified base matrix, STREAMLINE Direct, leads to improvements in the overall productivity. If we compare the STREAMLINE Direct DEAE with the STREAMLINE DEAE, it can be seen that despite the STREAMLINE DEAE binding more GST at each conductivity level, the productivity is lower due to the lower operating velocity.

If we then combine this base matrix with the prototype multi-modal DAB ligand that can operate at high conductivity levels, the productivity is further improved as the need to dilute the feed to reduce the conductivity is eliminated.

If we assume that the process of choice with the commercially available STREAMLINE DEAE ligand would be to run at 10mS/cm, the productivity in this scenario is 3.18 mg GST/min processing time. If we now assume that the process of choice if using the prototype STREAMLINE Direct DAB would be to run at 20mS/cm, the productivity for this process is 15.85 mg GST/min processing time - a 5 fold increase. This demonstrates that the use of the prototype STREAMLINE Direct DAB matrix offers significant benefits in terms of the productivity improvements available.

8.6 Conclusions

The analyses within this chapter have led to the use of process productivity being defined as total product recovered per min of processing time. This is a simple yet meaningful definition of productivity that can be applied to any process and is not limited to EBA.

If we consider the EBA processes investigated in this thesis, the impact of increasing the operating flowrate leads to improvements in productivity when defined as above as this leads to shorter processing times.

If the impact of matrix particle size is also considered, the most productive for both the ADH and GST systems is the use of small particles at the higher flowrate.

Conversely, the least productive is also the use of small particles at low flowrates. It has been observed that increasing the overall residence time will only offer improvements in total product bound up to a point, beyond which the additional time is not matched by a comparable rise in product bound.

When comparing the prototype high salt tolerant ligand coupled to a new densified base matrix with the commercially available STREAMLINE DEAE adsorbent, the productivity can be improved 5 fold.

The overall implications of the work in this thesis will be discussed in the next chapter and areas of further work will also be considered. The regulatory and commercial implication of EBA will then also be examined.

9 OVERVIEW AND CONCLUSIONS

The aims of this study were to investigate the effects of various matrix properties and operating parameters on the product breakthrough behaviour in an expanded bed adsorption column and to investigate the result of these effects on the productivity of the expanded bed. In particular, the studies were based upon complex feedstocks, such as homogenates, to provide realistic challenges to the EBA system.

The systems under investigation were the recovery of Alcohol dehydrogenase (ADH) from Yeast via hydrophobic interaction chromatography and Glutathione S-Transferase (GST) from *E. coli* via anion exchange chromatography. The effect of the matrix particle size and operating velocity was conducted comparing these systems using the commercially available matrices STREAMLINE Phenyl and STREAMLINE DEAE. The use of prototype second generation anion exchange expanded bed matrices designed to operate at high feed velocities (300–600cm/hr) and high conductivity levels (20mS/cm) were also examined using the *E. coli*/GST system.

Scale-up and development work on the *E. coli*/GST system led to a reproducible 5L fermentation producing 13mg/mL dry cell weight of *E. coli* with a corresponding GST concentration of 1.5mg/mL. The reaction time of the GST assay was successfully reduced from 5 to 1 minutes allowing quicker product analysis.

The effect of matrix particle size distribution and operating velocity on the recovery of ADH and GST using conventional EBA adsorbents was investigated. Conventional breakthrough curve analysis is not applicable to situations of variable particle size and operating velocity and in order to facilitate such studies a dimensionless experimental time group was developed based on the contact time in the column. This group allowed

direct comparison of breakthrough curves from systems run at different flowrates and consisting of matrices formed from differing particle size.

For both systems it was found that at low operating velocities (100cm/hr), beds formed from smaller particles exhibited shallower breakthroughs than beds formed from larger particles. At the higher velocity (300cm/hr) typically utilised in EBA, the behaviour of beds formed from either small or large particles was comparable in terms of breakthrough behaviour. This was despite both systems being applied to different types of chromatography and dominant mode of binding - HIC and surface area, and anion exchange and more complete bead penetration for ADH and GST respectively.

Various productivity definitions were assessed for their suitability in evaluating the processes investigated in this thesis, and was defined as the total product recovered per minute of processing time. It was found for both the ADH and GST systems that at the lower velocity of 100cm/hr the beds made up of larger particles were more productive than the beds made up of small particles. However, the most productive option overall was the use of beds made up of smaller particles and operated at the higher velocity.

The second generation of expanded bed base matrix, named STREAMLINE Direct, is based on smaller but much denser matrix particles that can operate at higher velocities and as such should improve process productivity. The work in this thesis evaluated a selection of prototype multi-modal ligands that were coupled to the new STREAMLINE Direct base matrix.

The multi-modal ligands are anion exchangers that can tolerate conditions of high conductivity typical of many fermentation broths thereby allowing processing of undiluted homogenates and leading to further productivity improvements. The ligands presented for study were examined for their binding of bovine serum albumin (BSA) from buffer

and GST from *E. coli*. Based on these studies, one ligand (DAB) was chosen to investigate the effect of conductivity on the binding of GST and to compare this performance with that of the commercially available STREAMLINE DEAE.

It was found that the STREAMLINE Direct DAB adsorbent performed consistently in the range of conductivity levels tested (3 - 20mS/cm) and its performance was comparable with that of STREAMLINE DEAE when operated at 10mS/cm. Productivity with the STREAMLINE Direct DAB could be increased 5-fold as compared with STREAMLINE DEAE with no loss of yield or purity.

The work presented in this thesis provides a new method of breakthrough curve analysis that allows comparisons across a broad range of situations and thereby provides insight into the competing mechanisms that govern the rates and levels of adsorption. The thesis presents an analysis of the relative productivity of a range of systems and highlights the gains in terms of productivity to be achieved with the development of second-generation EBA multi-modal adsorbents. The thesis concludes with a summary of the potential areas of further study and an analysis of the commercial and regulatory aspects of EBA.

10 FURTHER WORK

The work carried out in this thesis has presented many opportunities for further study. Areas to consider are listed below:

- The development of an improved elution protocol for both the Yeast/ADH and *E. coli*/GST systems in order to recover close to 100% of the bound product, as this would improve productivities.
- A more thorough and detailed understanding of the impact of residence time on binding. It was observed that product binding and recovery only improved with increasing residence time up to a point beyond which additional residence time was not matched by a comparable rise in product bound.
- Costing of buffers, time and product in order to base the productivity expression on strictly economic grounds.
- Investigation into the effect of pH on GST binding to the prototype STREAMLINE Direct DAB. The purification of GST using this matrix was based on the protocol developed for STREAMLINE DEAE, however the effect of pH was not investigated and as such the purification of GST may be improved by such an investigation, thereby leading to gains in productivity.
- Integration of upstream and downstream processing. As observed in this work, the binding of GST on STREAMLINE Direct DAB was prevented by some competitive entity, most likely some component of the fermentation media, in particular the yeast extract. By integrating fermentation development with that of the expanded bed step problems such as this could be avoided and provide a more complete analysis of the integrated process behaviour.

- The increased understanding of binding kinetics based on particle size and operating velocity provided in this thesis may be of use in the field of expanded bed modelling.

The above considerations all relate directly to the work carried out in this thesis. More generally, with the trend towards MAb/FAb products, development work utilising EBA and these types of products should be encouraged. Of particular interest would be to investigate whether expensive affinity processes utilising ProteinA matrix should be used early on in the downstream processing as is often practised, or whether it would be more beneficial to utilise an ion exchange EBA step followed by an affinity step of reduced size and hence costs. The productivity analysis methods developed in this work would provide a useful framework to commence such a study.

11 BIOPROCESS PROJECT MANAGEMENT

11.1 Introduction

In an increasingly competitive environment, process economy is a key issue in the management of bioprocesses. Reducing the number of processing steps can lead to savings in operational cost and processing time and will improve the overall process yield.

Amersham Biosciences (now part of GE Healthcare) is a market leader in the production of expanded bed adsorption (EBA) matrices and columns, a unit operation that was designed to meet the above challenges. However, in order to remain in such a position, it is important that their products for this unit operation are able to keep up with advances in the field and customer requirements.

The work carried out in this chapter was part of an 8 month secondment to Amersham Biosciences during the Engineering Doctorate (EngD) and focussed on the research and development (R&D) project for a new generation of EBA matrices. For reasons of commercial sensitivity the specifics of the project are not considered, instead the structure and management of a general R&D project including descriptions of the various project phases are presented.

11.2 Project Phase Definition

All Amersham Biosciences R&D projects consist of 6 phases which allow the project to be defined and developed with new products being launched based on proven technology, strategic relevance and potential profitability. Each phase of the project has various aims and objectives to be met and entry into the next phase must be approved by the Business Area Head.

11.2.1 Phase 0: Objectives

Aims: "To describe and initiate consideration of a product opportunity and to agree the resources needed to prepare a more detailed development proposal during Phase 1."

During this phase, marketing needs as proposed by the marketing department are described in a "project definition request" (PDR) document. This document outlines ideas for new projects that may be based on customer feedback or general industry developments.

11.2.2 Phase 1: Definition

Aims: "For the Core Team first to confirm the business opportunities and available technology (if requested), to define the key requirements of the product, and then to prepare project plans. These will be detailed enough to make commitments on delivery, and for the Business Area to evaluate consistency with strategic goals and profitability, in order for the Business Area Head to give their approval to continue."

An extensive business opportunity study provides forecasts and trends for the future, highlighting areas for potential growth and development that will complement the PDR from Phase 0. In addition the study will provide details around the specifics for the project in terms of deliverables. These will have been established from detailed customer surveys and from the business opportunity study. The available technology study will identify any possible complementary R&D projects and existing products that may be used in the project. As with all product launches, time to market is a key factor in maintaining market share and so at the outset of the project a realistic project timeline is established.

11.2.3 Phase 2: Detailed Planning

Aims: "To build the complete project team, to clearly define the product specification and high level design, validate product implementation plans, and to prepare detailed project planning to confirm project commitments."

The detailed planning phase will generally be based on the extensive studies carried out in Phase 1 and as such these 2 phases may be run concurrently as the deliverables defined in Phase 1 may be detailed enough for Phase 2. If not, then the deliverables will be defined in this Phase such that the next phase may be entered. It is also critical that the product does not impinge on any existing and current patents not belonging to Amersham Biosciences.

11.2.4 Phase 3 Development

Aims: "Development and verification of the product, development of manufacturing processes and planning for availability and support."

Throughout this Phase (typically the longest), development of the product and any manufacturing processes will be completed. Dependant on the specific project this may range in time from 1 year to 5 years. Decisions on the product in this Phase will be based on a number of criteria that will have been specified in the detailed planning but will include economics.

11.2.5 Phase 4: Market Readiness Preparation

Aim: "Preparing for availability, verification and validation of the product at the manufacturing scale and validation of the manufacturing processes. Continuation of activities, started in 3, preparing for launch, product support and servicing."

The market readiness phase will typically be run concurrently to the development phase. The launch team, generally consisting of a number of departments including marketing, R&D, regional representatives and the project manager will begin to make preparations for the launch of the final product.

A number of different areas such as pricing, marketing tools, name, in-house training etc have to be considered and as the project develops and the final product design comes closer to becoming a reality, there is a need to finalise decisions in order to be ready for product launch. It is also imperative that any literature that is prepared for marketing tools be approved by legal and regional departments.

Products typically have to be registered and so names must be carefully chosen such that they convey all aspects and selling points.

Product performance must be verified and validated. Application notes explaining when and how the product can be used in real life examples and situations are prepared. In order to produce consistent quality the production manufacturing process must also verified and validated.

Launch preparation discussions revolve around a number of areas. The product price is a crucial decision; too high and it would not be an attractive option to customers and too low and the company would stand to make losses if there were any problems for example with production. It is also important to be able to justify prices to customers by use of economic appraisals. Forecasts for post launch also have an impact on pricing decisions. It is imperative that these forecasts be as realistic as possible as ultimately, deviations from these forecasts could lead to changes in profit and loss (P&L) and could also lead to bad pricing decisions. Product marketing must also be considered.

11.2.6 Phase 5: Launch

Aim: "To support market introduction and volume manufacturing capability as well as evaluating the project performance and recommending follow up activities."

Once all the previous Phases have been exited and the product officially launched, it is necessary to measure the success of the launch. Various success criteria are defined and the launch is measured against these.

Achieving these goals would deem the project a success, however, if and when these goals are achieved, the launch phase is not over. This phase of the project is ongoing and should be viewed as a process that is continually reviewed and not as an end point or single activity.

11.3 Discussion

Getting a product to market does not necessarily ensure its success or that of the company. The product may fail for a number of reasons such as poor design, lack of resource for continued support, no market need for the product, bad marketing etc. By clearly defining the various project phases for a new product development, risks to the firm can be minimised as projects can be terminated at early stages if they are not viewed as potential successes. Careful structuring of a project leads to successful products as all areas are considered before the product “hits the shelves”.

The guidelines for an R&D project lead to higher chances of success as the structure ensures a team approach which leads to efficient communication between relevant departments, decisions being made in a timely manner and a final robust product. Overall, this should ensure that Amersham Biosciences maintain their dominant market position and reputation as a leading provider of bioseparation tools.

12 VALIDATION

12.1 Introduction

Validation is a process that industry must face in order to get products to market. Often, in the rush to market, validation may be sacrificed as it is seen as a costly and time consuming process. However it should be viewed as an opportunity to review comprehensively equipment and processes leading to an in-depth understanding of the process, thereby reducing product failures and variability. By planning validation into the process development, it is possible to design a robust process.

Validation is defined by the US Food and Drug Administration (FDA) as “Establishing documented evidence which provides a high degree of assurance that a specific process will consistently produce a product meeting its pre-determined specifications and quality attributes.” (US FDA) Put simply, this means providing evidence that a process does what it should.

This chapter summarises the validation issues surrounding an expanded bed chromatography column and will consider how this should be validated as a unit operation in a whole process.

12.2 General considerations

Whole process validation requires a careful consideration of many factors, such as raw materials, purchasing, facility design, air and water quality, equipment, change control, personnel training, maintenance programs and documentation requirements, amongst others.

The formulation of a Validation Master Plan (VMP) to cover all of the factors is to be encouraged. The VMP should consist of plans for execution of facility and equipment validation, covering installation, operational and performance qualification. The VMP should cover at

which point in process development various tasks should be undertaken. For example, full validation of equipment and processes may not be done until Phase III and a graded approach is generally accepted by regulatory agencies although product equivalence must be demonstrated from one phase to the next.

It is important to note that any process changes, including increases in batch size (i.e. scale-up) requires validation of the change.

12.3 Expanded Bed Adsorption Validation

To validate an EBA step in a process, there are a number of factors to consider. The equipment should be qualified, acceptance criteria for the raw materials and chromatography media should be defined, the process should be qualified and cleaning, sanitization and storage conditions validated.

12.3.1 Equipment Qualification

Equipment qualification consists of installation qualification (IQ) and operational qualification (OQ). IQ at its most basic definition ensures equipment is installed according to manufacturer's recommendations. The OQ tests that that column functions properly by running the equipment with a sample.

For an EBA column, the IQ and OQ confirm that each component of the system meets design criteria, including any valves and pumps associated with the column. For packed beds, the OQ would involve testing the symmetry of the packed bed column (Sofer and Hagel, 1997), however this is not applicable to an EBA unit. As such the OQ would utilise a tracer molecule, such as acetone, to test for residence time and to measure bed expansion (Sofer, 1999).

If the system is automated then IQ and OQ should also be performed for both hardware and software.

12.3.2 Raw Materials

For those raw materials that are purchased, such as buffer ingredients and chromatography media, vendors should be audited and certified in order to reduce the chance of variability. For chromatography media, vendors will typically supply certificates of analysis and regulatory support files (RSF). Whilst this type of file reduces the quantity of testing performed by the end user, it is imperative that acceptance criteria are defined such as identity testing (usually visual inspection of the media and packing/label inspection) and small scale function testing related to the application.

Another key criteria particularly for chromatographic media is the issue of leachables. All chromatography media leak and therefore it is necessary to determine where in the process leakage occurs and to specify what level of leakage is acceptable. Particularly for new media such as the second generation matrices investigated in this thesis where little data is available, leakage studies would be absolutely crucial. In order to test leakage, exposure of the media to extreme pH values followed by identification of any leakage products and quantification of these leakage products in the eluate would be advisable.

For those raw materials that are not purchased, such as feedstream, acceptance criteria would typically be defined to include a range of parameters such as total protein, total product, viscosity and conductivity. As demonstrated in this thesis, when employing ion exchange chromatography, conductivity is a key parameter. Viscosity in expanded beds is also crucial as it affects the overall degree of expansion which can lead to variability in the residence time, also a key factor in product binding.

12.3.3 Process Qualification

Process qualification is aimed at ensuring process consistency. Process performance can be defined in terms of a number of parameters, such as yield and purity of product which must be reproducible within a defined range. Generally parameters that are validated during the process performance qualification are defined within broad ranges during the development stages of a process. As understanding of the process is gained through experience, the ranges are narrowed.

To prove the process is consistent, consecutive batches at full or pilot scale are run. In the USA, this is typically a minimum of three batches; in Europe five batches are required.

12.3.4 Cleaning, Sanitization and Storage

Cleaning validation is a critical issue in validation. Whilst it is the case that media is utilised for one product, the equipment may be used for multiple products and therefore it is essential that any cleaning validation can demonstrate the absence of carry-over through the use of product specific assays and general assays such as total organic carbon (TOC) and total protein.

EBA columns can be completely dismantled and therefore thorough cleaning and sanitization is possible, however, standard operating procedures (SOP's) must be developed that are easy to follow and removal of cleaning agents and detergents must be demonstrated.

Cleaning of the chromatography media is also crucial, especially due to the nature of the matrix in the sense that its porous structure may lead to potential contaminants that are difficult to detect. When carrying out cleaning studies for media it is common that the media lifetime is investigated concurrently. This is preferably carried out using actual product feedstream but standard proteins such as lysozyme or BSA may

also be used to investigate the effect of clean-in-place (CIP) procedures on the dynamic capacity after multiple cycles.

Storage of media and columns must be able to demonstrate that storage solutions prevent microbial growth and can be fully removed. Labelling of “clean” and “dirty” columns and media also form part of the storage validation.

12.4 Conclusions

Validation is a necessary part of product development and it builds consumer confidence as it provides documented evidence that a process does what it should. Validation that is carried out early on in the development highlights potential failures thereby allowing the development of preventative measures and building a robust process.

Although products cannot be released without approval from regulatory bodies, validation should not cease once a product is on the market as regulatory bodies expect bioprocessing firms to remain up to date with new technology and guidelines.

REFERENCES

Barnfield-Frej AK, Hjorth R, Hammarstrom A. 1994. Pilot scale recovery of recombinant annexin V from unclarified *Escherichia coli* homogenate using expanded bed adsorption. *Biotechnol. Bioeng.* 44:922-929.

Bergmeyer HO. 1979. *Methods of Enzymic Analysis*. Verlag Chemie Weinheim.

Bradford M. 1976. A rapid sensitive method for the qualification of microgram quantities of protein utilizing the principle of protein-dye binding. *Anal. Biochem.* 72:248.

Bruce LJ, Chase HA. 1999. Evaluation of the effect of in-bed sampling on expanded bed adsorption. *Bioseparation* 8 (1-5):77-83.

Bruce LJ, Chase HA. 2001. Hydrodynamics and adsorption behaviour within an expanded bed adsorption column studied using in-bed sampling. *Chem Eng Sci* 56 (10):3149-3162.

Bruce LJ, Chase HA. 2002. The combined use of in-bed monitoring and an adsorption model to anticipate breakthrough during expanded bed adsorption. *Chem Eng Sci* 57 (15):3085-3093.

Bruce LJ, Clemmitt RH, Nash DC, Chase HA. 1999(a). Monitoring of adsorbate breakthrough curves within an expanded bed adsorption column. *J Chem Technol Biotechnol* 78:264-269.

Bruce LJ, Ghose S, Chase HA. 1999(b). The effect of column verticality on separation efficiency in expanded bed adsorption. *Bioseparation* 8:69-75.

Buijs A, Wesselingh JA. 1980. Batch fluidized ion-exchange column for stream containing suspended particles. *J Chromatog* 201:319-327.

Calado CRC, Cabral JMS, Fonseca LP. 2002. Effect of *Saccharomyces cerevisiae* fermentation conditions on expanded bed adsorption of heterologous culture. *J Chem Technol Biotechnol* 77:1231-1237.

Chang YK, Chase HA. 1996 Development of operating conditions for protein purification using expanded bed techniques: The effect of the degree of expansion on adsorption performance. *Biotechnol Bioeng* 49:512-526.

Chang YK, McCreath GE, Draeger NM, Chase HA. 1993. Novel technologies for direct extraction of proteins. *TranslChemE* 71 Part B:299-303.

Chase HA. 1994. Purification of proteins by adsorption chromatography in expanded beds. *Trends in Biotech.* 12:296-303.

Chase HA, Nash DC, Bruce LJ. 1999. On-line monitoring of breakthrough curves within an expanded bed adsorber. *Bioprocess Eng* 20:223-229.

Chetty AS, Burns MA. 1991. Continuous protein separations in a magnetically stabilized fluidized bed using nonmagnetic support. *Biotechnol Bioeng* 38:9 963-97.

Clemmitt, RH, Chase HA. 2002. Direct Recovery of Glutathione S-Transferase by Expanded Bed Adsorption: Anion Exchange as an Alternative to Metal Affinity Fusions. *Biotechnol Bioeng* 77:7 776-785.

Creighton TE. 1984. *Proteins, structure and molecular properties*. W.E. Freeman, New York.

Data File STREAMLINE Direct 24 and 95 columns. Code No 18-1177-63 AA. Amersham Biosciences.

Data File STREAMLINE Direct CST I. Code No 18-1177-65 AA. Amersham Biosciences.

Data File STREAMLINE SP/STREAMLINE DEAE. Code No 18-1111-73 AB. Amersham Biosciences.

DeLuca L, Hellenbroich D, Titchener-Hooker NJ, and Chase HA. 1994. A study of the expansion characteristics and transient behaviour of expanded beds of adsorbent particles suitable for bioseparations. *Bioseparation* 4: 311-318.

Draeger NM, Chase HA. 1991. Liquid fluidized bed adsorption of proteins in the presence of cells. *Bioseparation* 2:67-80.

Expanded Bed Adsorption Handbook. Code No 18-1124-26 AB. Amersham Biosciences.

Feuser J, Walter J, Kula MR, Thommes J. 1999. Cell/adsorbent interactions in expanded bed adsorption of proteins. *Bioseparation* 8:99-109.

Ghose S, Chase HA, Titchener-Hooker N. 2000. Bed height monitoring and control for expanded bed chromatography. *Bioprocess Eng* 23:701-708.

Gondkar S, Manudhane K, Amritkar N, Pai A, Lali A. 2001. Effect of adsorbent porosity on performance of expanded bed chromatography of proteins. *Biotechnol Progr* 17 (3):522-529.

Habib GB, Holwill I, Hoare M. 1997. Rapid piloting of a selective flocculation process for product purification. *J Biotechnol.* 59 No.1-2:91-101.

Habig WH, Pabst MJ, Jakoby WB. 1974. Glutathione S-Transferases. The first enzymatic step in mercapturic acid formation. *J Biol Chem* 249:7130-7139.

Halperin G, Breitenback M, Tauber-Finkelstein M, Shaltiel S. 1981. Hydrophobic chromatography on homologous series on alkyl agaroses. A comparison of charged and electrically neutral column materials. *J Chromatog* 215:211-228.

Hjerten S, Rosengren J, Pahlman S. 1974. Hydrophobic interaction chromatography. The synthesis and the use of some alkyl and aryl derivatives of agarose. *J Chromatog* 101:281-288.

Hjorth R, Kampe S, Carlsson M. 1995. Analysis of some operating parameters of novel adsorbents for recovery of proteins in expanded beds. *Bioseparation* 5, 217-223.

Hjorth R. 1997. Expanded-bed adsorption in industrial bioprocessing: recent developments. *Trends in Biotechnol* 15:230-235.

Hjorth R. 1999. Expanded bed adsorption: elution in expanded mode. *Bioseparation* 8:1-9.

Ion Exchange Chromatography Principles and Methods Handbook. Code No 18-1114-21 AA. Amersham Biosciences.

Kaplan W, Husler P, Klump H, Erhardt J, Sluis-Cremer N, Dirr H. 1997. Conformational stability of pGEX-expressed *Schistosoma japonicum* glutathione S-transferase: a detoxification enzyme and fusion-protein affinity tag. *Prot Sci* 6:399-406.

Karau A, Benken J, Thommes J, Kula M-R. 1997. The Influence of Particle Size Distribution and Operating Conditions on the Adsorption Performance in Fluidized Beds. *Biotechnol Bioeng* 55:1 54-64.

Khan AR, Richardson JF. 1989. Fluid-particle interactions and flow characteristics of fluidized-beds and settling suspensions of spherical particles. *Chem. Eng. Comm.* 78:111-130.

Korz DJ, Rinas U, Hellmuth K, Sanders EA, Deckwer W-D. 1995. Simple fed-batch technique for high cell density cultivation of *Escherichia coli*. *J Biotechnol* 39:59-65.

Laemmli U. 1970. Cleavage of structural proteins during the assembly of the head of bacteriophage T4. *Nature* 227:680-685.

Lihme A, Zafirakos E, Hansne M, Olander M. 1999. Simplified and more robust EBA processes by elution in expanded mode. *Bioseparation* 8:93-97.

Linden T, Ljunglof A, Kula M-R, Thommes J. 1999. Visualising Two-Component Protein Diffusion in Porous Adsorbents by Confocal Scanning Laser Microscopy. *Biotechnol Bioeng* 65:6 622-630.

Lutkemeyer D, Ameskamp N, Tebbe H, Wittler J. 1999. Estimation of Cell Damage in Bench- and Pilot-Scale Affinity Expanded-Bed Chromatography for the Purification of Monoclonal Antibodies. *Biotechnol Bioeng* 65:1 114-119.

Pahlman S, Rosengren J, Hjerten S. 1977. Hydrophobic interaction chromatography on uncharged Sepharose derivatives. Effects of neutral salts on the adsorption of proteins. *J Chromatog* 131:99-108.

Porath J, Sundberg L, Fornstedt N, Olson I. 1973. Salting-out in amphiphilic gels as a new approach to hydrophobic adsorption. *Nature* 245:465-466.

Protein Purification Handbook. Code No 18-1132-29 AB. Amersham Biosciences.

Richardson JF, Zaki WN. 1954. Sedimentation and fluidisation: part 1. *Trans Instn Chem Engrs* 32:35-53.

Richardson P, Ravenhall R, Flanagan MT, Holwill I, Malloy J, Hoare M, Dunill P. 1996. Monitoring and optimisation of fractional protein precipitation by Flow Injection Analysis. *Process Control and Quality* 8 No.2-3:91-101.

Scopes RK. 1994. *Protein Purification: Principles and Practice*, 3rd Edition. Springer-Verlag, New York.

Skidmore GL, Chase HA. 1990. Two component protein adsorption to the cation exchanger S Sepharose FF. *J.Chromatog* 505:329-347.

Smith MP, Bulmer MA, Hjorth R, Titchener-Hooker NJ. 2002. Hydrophobic interaction ligand selection and scale-up of an expanded bed separation of an intracellular enzyme from *Saccharomyces cerevisiae*. *J.Chromatog A* 968(1-2):121-128.

Sofer G. 1999. Validation issues related to expanded bed technology. *Bioseparation* 8:111-114.

Sofer G, Hagel L. 1997. *Handbook of Process Chromatography: A Guide to Optimization, Scale-up, and Validation*. Academic Press.

Tanfor C. 1973. *The hydrophobic effect: formation of micelles and biological membranes*. John Wiley & sons, New York.

Terranova BE, Burns MA. 1991. Continuous cell suspension processing using magnetically stabilized fluidized beds. *Biotechnol Bioeng.* 37:2 110-120.

Thelen TV, Ramirez WF. 1999. Monitoring, modelling, and control strategies for expanded-bed adsorption process. *Bioseparation* 8:11-31.

US FDA. *Guidelines on General Principles of Process Validation*. Center for Drugs and Biologics, Center for Devices and Radiological Health, FDA, Rockville (1987).

Wen CY, Yu YH. 1966. *Mechanics of Fluidisation*. Chem. Eng. Prog. Symp. Ser. 62:100-110.

Wilhelm RH, Kwauk M. 1948. Fluidization of solid particles. *Chem. Engng. Progr.* 44:201.

Willoughby NA, Hjorth R, Titchener-Hooker NJ. 2000(a). Experimental measurement of particle size distribution and voidage in an expanded bed adsorption system. *Biotechnol Bioeng* 69(6) 648-653.

Willoughby NA, Habib G, Hoare M, Hjorth R, Titchener-Hooker NJ. 2000(b). The use of rapid on-line monitoring of products and contaminants from within an expanded bed to control separations exhibiting fast breakthrough characteristics and maximise productivity. *Biotechnol Bioeng* 70(3) 254-261.

Zafirakos E, Lihme A. 1999. EBA columns with a distribution system based on local stirring. *Bioseparation* 8:85-91.

APPENDIX I – FLUIDISATION THEORY

Introduction

Fluidisation is the process whereby a continuous stream of fluid (gas or liquid) is allowed to pass through a bed of solid particles, with the separation of the particles caused by the fluid flow itself. Fluidised reactors and beds have been used in many applications in the chemical industry for well over half a century, and their use is well documented in such applications as catalytic cracking (where a stream of hydrocarbon gas is allowed to contact a solid catalyst to force a splitting reaction creating smaller molecules). This is one example of gas-solid fluidisation. However, the less common (at least in the chemical industry) process of liquid-solid fluidisation is the basis of this research. In the field of Biotechnology, chromatographic separations have been successfully carried out using expanded beds, and a dedicated series of chromatography columns and matrices are available from Amersham Biosciences (STREAMLINE components) solely for expanded bed operations.

Fluidisation theory for liquid-solid systems

Liquid can flow either up or down through a bed packed with solid particles. In term of fluidisation, flow downward through a bed is of little interest since the bed cannot become fluidised in this state. However flow downwards in the bed is important for other reasons and will be discussed elsewhere.

When liquid flows upwards through the bed, pressure drop from along the length of the bed will be directly proportional to the flowrate of the liquid at low flowrates, and the bed remains in a “packed” configuration. However as flowrate increases, and the apparent weight of the particles becomes equal to the frictional drag exerted on them by the fluid flow

(the apparent weight is the actual weight of the particle minus the buoyancy of the particle in the liquid concerned) then the particles begin to move and rearrange themselves so as to offer less resistance to liquid flow - the bed is beginning to expand. This point is known as the fluidising point. This process continues with increasing liquid flowrate until the particles reach the state where they are offering the least possible resistance to fluid flow. This is the situation where the pressure drop is highest, since further increases in liquid flow result in the particles becoming further separated, but since the resistance to flow remains approximately the same so does the pressure drop. At this stage the bed is said to be fluidised.

In the fluidisation of a particulate bed, it is vital that the fluidisation is as good as possible (free of channelling, regions of backmixing, etc.). This is achieved with plug flow of liquid through the bed. This is very difficult with a bed of solid particles, especially if they are of irregular shapes, or if they aggregate easily. Hence the study of flow patterns is important to achieve good fluidisation.

By plotting $\log \Delta P$ (pressure drop along column) against $\log U$ (superficial liquid velocity) as shown in figure AI.1 the effects described above are shown graphically. $\log \Delta P$ increases linearly until the point A (the fluidising point). The pressure drop continues to increase until it reaches a maximum (point B) before falling slightly and becoming independent of superficial velocity and hence independent of flowrate (region CD). Note that if velocity were reduced again the pressure drop would remain constant until the particles were just touching one another (point E - the point of maximum stable porosity for a fixed bed). The bed would in theory remain in this state as flowrate was further lowered but in practice any external vibrations would cause particle rearrangement and a return to the line OA rather than the theoretical line EF, with lower pressure drop for a given superficial velocity.

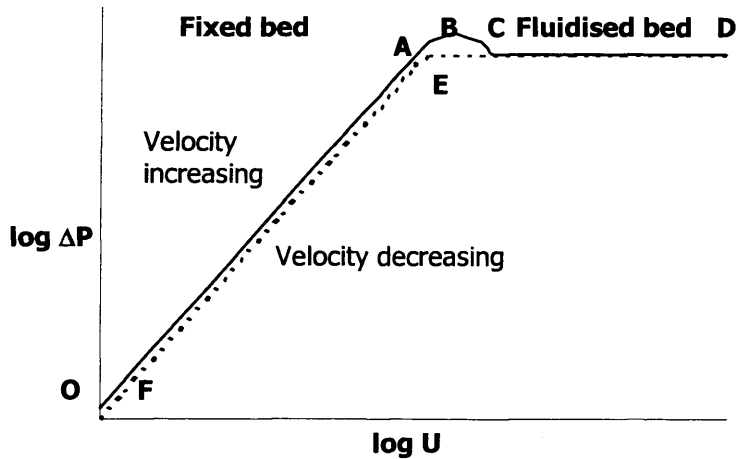


Figure AI.1: Illustration of different stages of particle fluidisation.

In order to relate the pressure drop to the difference in density of the solid and liquid phases, it is necessary to perform an unsteady state momentum balance. Given that a fluidised bed can be assumed to be a two phase closed system, bounded by the bottom of the bed vessel (plane b) and the upper surface of the particles (plane t) then a momentum balance, after converting vectors to scalars for simplicity, yields:

$$\frac{\partial}{\partial t} P_{tot} = \rho_{f_b} (u_b^2) S - \rho_{f_t} (u_t^2) S + p_b S - p_t S - F - mg \quad (\text{AI.1})$$

In the above expression, P_{tot} is the total momentum of the system, S is the cross sectional area of the column and u is the local velocity at any given point. The terms on the right hand side of the system represent, respectively, the rate of momentum into the system by bulk motion, the rate of momentum leaving the system by bulk motion and the pressure forces exerted on the system by the bottom and top planes. F is the force exerted by the surfaces of the solid in the system on the liquid and mg is the force on the liquid due to gravity. Since in an expanded bed of solid particles, the surface area of particles is generally much greater than the internal surface area of the containing column then the latter can be neglected hence F is the force exerted by the surface area of the entrained particles only, and is therefore equal to the weight of these particles.

$$F = (1 - e)SH\rho_s g \quad (\text{AI.2})$$

Where H is the height of the bed and e is the voidage, or the fraction of liquid contained in the bed. At steady state $\partial / \partial t(P_{tot}) = 0$

Assuming constant velocity profiles across the bed, and that the liquid in the system is effectively incompressible, $\rho_{f_b} = \rho_{f_t}$ and $(u_b^2) = (u_t^2)$

The force acting on the fluid due to gravity, mg , can be converted to a more manageable form by replacing the mass term thus $mg = e\rho_f SHg$

If all these terms are substituted into the fundamental momentum balance it becomes

$$(e - 1)H\rho_s g - e\rho_f Hg = p_t - p_b \quad (\text{AI.3})$$

Now defining $P = p - \rho_f gh$ where h is distance to any plane (so if h is distance to plane t then $(H-h)$ is distance to plane b) then by substitution and rearrangement,

$$-\Delta P = P_b - P_t = (1 - e)(\rho_s - \rho_f)Hg \quad (\text{AI.4})$$

This expression holds while the bed is in the fluidised regime.

Minimum fluidisation velocity

As the upward flow of liquid through a packed bed of uniformly shaped particles increases, a certain point is reached when the particles are just freely supported in the liquid. This is known as the point of incipient fluidisation. At this point a corresponding minimum fluidisation velocity u_{mf} can be calculated based on the Carman-Kozeny equation for the voidage in a fixed bed. This equation is only valid given STREAMLINE flow in a bed packed with uniform spheres of diameter d , but these are the conditions that apply in a well-packed expanded bed utilising a standard beaded matrix. The Carman-Kozeny equation is based on the theory that the pressure drop in a fixed bed is equal to the buoyant

weight of the solid particles supported in it. This holds until the transition to fluidisation.

The equation below is obtained when the voidage at the point of incipient fluidisation (e_{mf}) is substituted into the Carman-Kozeny equation:

$$u_{mf} = 0.0055 \frac{e_{mf}^3}{1 - e_{mf}} \frac{d^2 (\rho_s - \rho_f) g}{\mu} \quad (\text{AI.5})$$

Although the voidage at the point of incipient fluidisation depends a great deal on the particle size, shape and even density, for uniform spherical particles it would be assumed to be about 0.4. Thus substituting this into the above equation:

$$(u_{mf})_{e_{mf}=0.4} = 0.00059 \frac{d^2 (\rho_s - \rho_f) g}{\mu} \quad (\text{AI.6})$$

Under some conditions, such as when the particles are too large for STREAMLINE flow to take place at the point of fluidisation, a more general equation based on the pressure gradient in the bed (for example the Ergun equation):

$$\frac{-\Delta P}{l} = 150 \frac{(1 - e^2)}{e^3} \frac{\mu u_{mf}}{d^2} + 1.75 \frac{(1 - e)}{e^3} \frac{\rho_f u_{mf}^2}{d} \quad (\text{AI.7})$$

Thus by substituting $e = e_{mf}$ at the point of incipient fluidisation and $-\Delta P$ from equation (AI.4) the equation can be expressed in terms of u_{mf} :

$$(1 - e_{mf})(\rho_s - \rho_f)g = 150 \frac{(1 - e_{mf})^2}{e_{mf}^3} \frac{\mu u_{mf}}{d^2} + 1.75 \frac{(1 - e_{mf})}{e_{mf}^3} \frac{\rho_f u_{mf}^2}{d} \quad (\text{AI.8})$$

Then by multiplying both sides by $\frac{\rho_f d^3}{\mu^2 (1 - e_{mf})}$ to express the equation in

terms of dimensionless numbers:

$$\frac{\rho_f (\rho_s - \rho_f) g d^3}{\mu^2} = 150 \frac{1 - e_{mf}}{e_{mf}^3} \frac{u_{mf} d \rho_f}{\mu} + \frac{1.75}{e_{mf}^3} \left(\frac{u_{mf} d \rho_f}{\mu} \right)^2 \quad (\text{AI.9})$$

In this equation several dimensionless numbers can be inserted for ease of expression. For instance, $\frac{d^3 \rho_f (\rho_s - \rho_f) g}{\mu^2}$ is the Galileo number Ga , and $\frac{u_{mf} d \rho_f}{\mu}$ is a modified form of the Reynolds number and in this case will be designated the Reynolds number at minimum fluidisation velocity or Re_{mf} .

This allows equation (AI.9) above to be simplified to:

$$Ga = 150 \frac{1 - e_{mf}}{e_{mf}^3} Re_{mf} + \frac{1.75}{e_{mf}^3} Re_{mf}^2 \quad (\text{AI.10})$$

Since by definition $u_{mf} = \frac{\mu}{d \rho_f} Re_{mf}$, and the voidage at minimum fluidisation can be predicted or measured, then the minimum fluidising velocity for a given system can be obtained.

Models for describing bed expansion

It is important to consider the behaviour of the individual particles within an expanded bed as a route to predicting the behaviour of the whole bed. To this aim, this section introduces published mathematical models for describing bed behaviour.

There are two main methods for describing the behaviour of a bed of particles during fluidisation. In general liquid-solid fluidised systems are characterised by the regular expansion of the bed as velocity increases above the minimum fluidising velocity (but below terminal particle falling velocity). The general relationship between liquid linear velocity and voidage is very similar to the relationship between sedimentation velocity and particle volumetric concentration in a solid-liquid suspension. This is perhaps not too surprising as the systems are hydrodynamically very similar, with the "stationary" phase being the solid particles in the case of an expanded bed and the liquid in the case of

a suspension. The utilisation of this fact in a model to predict behaviour was first postulated by Wilhelm and Kwauk (1948) and further developed by Richardson and Zaki (1954) and was dubbed “the cell model” as it treats one particle as being limited to movement within a fixed cell. The cell is taken to consist of two concentric spheres, the radius of the inner being that of the particle. It was noted by these workers that:

$$\frac{u_c}{u_i} = e^n \quad (\text{AI.11})$$

Where u_c is the fluidisation velocity, u_i is the corresponding velocity at infinite dilution, e is the voidage and n is an index. This was seen by plotting particle Reynolds number against bed voidage over a range of conditions during fluidisation. Values of n were found to range from 2.4 to 4.8 and can be found for known Galileo number Ga given the expression

$$\frac{4.8 - n}{n - 2.4} = 0.043 Ga^{0.57} \left[1 - 1.24 \left(\frac{d}{d_t} \right)^{0.27} \right] \quad (\text{AI.12})$$

Although the conditions are similar for both sedimentation and fluidisation, Richardson and Zaki found that while u_i and u_o (free settling velocity of a particle in infinite medium) are very similar for sedimentation they were found to vary in fluidisation and proposed the following equation:

$$\log_{10} u_o = \log_{10} u_i + \frac{d}{d_t} \quad (\text{AI.13})$$

Since d/d_t is the ratio of particle diameter to tank diameter, it would in all probability be very small in a sedimentation tank but may be significant in a fluidised column. This is believed to account for the difference noted by Richardson and Zaki. More recently modifications of the above correlation have been developed (Khan and Richardson (1989)) to allow for the influence of the walls of the vessel during fluidisation. When

voidage is plotted against superficial liquid velocity on logarithmic coordinates, the voidage remains constant at low flowrates (fixed bed regime) and then increases in a linear fashion with velocity (fluidised regime).

The second and more widely used model is based on viewing the bed as a series of bundles of tangled tubes for fluid flow. If these tubes could be viewed as individual straight tubes, then the bed could be modelled based on this. Based on a derivation of the Hagen-Poiseulle equation but replacing the mean tube velocity u in the equation with the interstitial velocity u/e and the tube diameter with the hydraulic diameter D_H gives the following modified version of the Hagen-Poiseulle equation:

$$\Delta P = \frac{2(36)\mu u H(1-e)^2}{d^2 e^3} \quad (\text{AI.14})$$

This model is however flawed slightly as it would be erroneous to assume that the bed consists of straight-pathed tubes as modelled by the above equation. In order to take account of this the value 2 at the start of the equation is replaced with the value 25/6. This results in the Blake-Kozeny equation. The modification of the value 2 is known as the tortuosity factor τ where:

$$\tau = \frac{\text{average path length}}{\text{bed height}} \quad (\text{AI.15})$$

This model can be used to predict the behaviours of both fluidised and fixed beds, but it must be noted that the tortuosity varies for fluidised beds but remains constant for fixed beds. A completely fluidised bed will have a tortuosity value of approaching unity.

Effect of particle size distribution on fluidisation velocity

In general it can be assumed that, if the particles being fluidised have a uniform size then the transition between fixed and fluidised bed will be

categorised by a discrete step on the pressure drop-liquid velocity curve (Figure AI.1). However as the distribution of particle sizes becomes more spread, the transition tends more towards a smooth curve, thus creating three discrete regions on the pressure drop-fluidisation curve; the fixed bed region, the fully fluidised region and a transition region separating the two. In this case there is no specific minimum fluidising velocity, but a small range of velocities from the velocity at the onset of fluidisation (often known as u_{bf}) and the velocity at which the bed is totally fluidised (known as u_{ff}). In this case the value for minimum fluidisation velocity must be approximated, and can be obtained from equations such as (AI.14) using a mean particle diameter value (often approximated to diameter at 50% total frequency on a particle diameter vs. frequency plot) so long as the value for the voidage at minimum fluidisation velocity is known. This can usually be approximated to $e_{mf} = 0.4$ although Wen and Yu (1966) found that $e_{mf} = 0.42$ gave improved bed stability.

Effect of particle size distribution on voidage

In a fluidised bed with uniform sized particles, uniform voidage would also be expected. However in the case of a bed with a size distribution, the particles will segregate according to their terminal falling velocity in the fluid, and as such the voidage will vary along the length of the bed as the particles are segregated. This presents problems with respect to system modelling since the void fraction is variable with height in the bed.

This problem has been considered by Wen and Yu (1966) who studied binary systems and stated that, if the ratio $\frac{\text{largest particlesize}}{\text{smallest particlesize}} \leq 1.3$ then

all particles would form a single layer in the system. Thus the expansion characteristics of the bed could be defined by equation (AI.16) below where the particle diameter is replaced by an equivalent:

$$e^{4.7} \frac{dg(\rho_s - \rho_f)\rho_f}{\mu^2} = 18 \text{Re} + 2.7 \text{Re}^{1.687} \quad (\text{AI.16})$$

Under the conditions $0.01 \leq \text{Re} \leq 1000$ for the system studied (water) and where $d = d_e$ as defined:

$$d_e = \left(\sum_{i=1}^n \frac{x_i}{d_i} \right)^{-1} \quad (\text{AI.17})$$

Where x_i is the fraction of the total weight of the particles of all particles with diameter d_i . In the case of particle size distributions larger than those covered by the above equations, the particles were seen to segregate and the voidage could be determined by summing the voidage of individual layers of the system.

APPENDIX II - PUBLICATIONS

Printed overleaf:

Gardner PJ, Willoughby N, Hjorth R, Lacki K, Titchener-Hooker NJ. 2004. Use of dimensionless residence time to study variations in breakthrough behaviour in expanded beds formed from varied particle size distributions. *Biotechnol Bioeng* 87:3 347-353.

Use of Dimensionless Residence Time to Study Variations in Breakthrough Behaviour in Expanded Beds Formed From Varied Particle Size Distributions

P.J. Gardner,¹ N. Willoughby,² R. Hjorth,³ K. Lacki,³ N.J. Titchener-Hooker¹

